The Glaciolacustrine Sediment Record of Cariboo Lake, BC: Implications for Holocene Fluvial and Glacial Watershed Dynamics

By

Alexander Charles Cebulski

A thesis submitted in conformity with the requirements

for the degree of Master of Science

Department of Geography and Planning

University of Toronto

The glaciolacustrine sediment record of Cariboo Lake, BC: Implications for Holocene fluvial and glacial watershed dynamics.

Alexander Charles Cebulski

Master of Science

Department of Geography

University of Toronto

2018

Abstract

Cariboo Lake is a glacier-fed lake located in the Cariboo Mountains of eastern-central British Columbia. Fine clastic sediments produced in the glaciated headwaters of the Cariboo Lake watershed provide the main source of sediment to the lake. Sediment delivery into Cariboo Lake is primarily governed by overflow currents of suspended clastic sediments from the main Cariboo River. Sediments deposited in deep basins over 30 m deep are characterized by couplets of coarse grained laminae, followed by fine grained sediments and are inferred to be annually laminated varves. Inflow of clastic sediments to Cariboo Lake has remained high enough to produce annual varves for the past two millennia. Down-core trends in varve thickness, grain size, and percent organics from Cariboo Lake sediment archives reveal changes that corresponded to climate fluctuations over the past two millennia.

Acknowledgements

Several generous contributions have made this research possible. First, I would like to thank my advisor Dr. Joe Desloges for his inspiring expertise which has guided me through my studies at the University of Toronto. Our field work in the Cariboo Lake watershed would not have been possible without assistance from Michael Allchin, Laszlo Enyedy, and Caitlin Langford at the Quesnel River Research Centre. Generous landowners at Cariboo Lake also provided vital moorage for our research vessel *W.H. Matthews*. Thanks to Anna Soleski for training me on the many sediment analysis required for this project, and her continual support along the way. I would also like to acknowledge Selina Amaral, for her excellent organisational skills which were very helpful in the many tedious lab analyses in this project. Instruction from Mike Gorton, George Kretschmann, and Yanan Liu on the use and maintenance of various lab instruments is also greatly appreciated. Special thanks to the Toronto climbing community for initiating research breaks on the Niagara Escarpment. Finally, I would like to thank my friends and family, without their support this thesis would not have been possible.

Table of Contents

List of Figures

List of Appendices

1.0 INTRODUCTION

1.1 Background

Researchers have been working to understand how glaciated watersheds across western Canada have responded to past changes in climate (Gilbert, 1975; Desloges & Gilbert, 1994b; Souch, 1994; Menounos, 2002; Menounos, Clague, Gilbert, & Slaymaker, 2005; Hodder, Desloges, & Gilbert, 2006). Anthropogenic climate change is predicted to reduce glacier extent to near depletion in the Interior and Rocky Mountains of western Canada by 2100 (Clarke, Jarosch, Anslow, Radić, & Menounos, 2015). Thus, there is a need to determine how alpine watersheds have responded to past warming events in order to prepare for the implications of future climate change. To document the effects of past climate fluctuations on alpine watersheds, studies have utilized two primary techniques: 1) documenting glacier advances through dating of terrestrial material, such as terminal glacier moraines and woody debris from glacier forefields, and 2) down-core analysis of sediment cores from glacier-fed lakes. Records from terrestrial material are generally limited to providing dates of glacier advances and thus have produced a long-term, but discontinuous, record of glacial activity across western Canada (Menounos, Osborn, Clague, & Luckman, 2009). However, sediment cores from glacier-fed lakes can provide a more continuous record of glacier activity through preservation of glacially derived sediments (Karlen, 1981; Leonard & Reasoner, 1999; Heideman, Menounos, & Clague, 2017). Moreover, sediment records from glacier-fed lakes are related to watershed-wide activity, and thus represent an integrated record of catchment activity related to fluctuations in climate (Desloges & Gilbert, 1994b, 1994a; Hodder, Gilbert, & Desloges, 2007; Heideman et al., 2017).

Glaciolacustrine sediment records have indicated that the production, connection, and transport of sediment in glaciated watersheds is correlated with changes in glacier extent,

temperature and precipitation patterns (Desloges & Gilbert, 1994a; Hodder et al., 2006; Striberger, Björck, Holmgren, & Hamerlík, 2012; Erik Schiefer et al., 2018). When considered in three dimensions, annually laminated sediment records from glacier-fed lakes provide an estimation of annual settlement yield (Heideman et al., 2017). Annually laminated sediments, also known as varves, are formed by a coarse-grained layer of sediment deposited in the spring melt season, followed by a fine-grained layer deposited in the winter (Zolitschka, Francus, Ojala, & Schimmelmann, 2015). Similar to tree-rings, varves can be counted and measured down-core to provide a trend in how sediment delivery has changed over time (Desloges & Gilbert, 1995; Leonard & Reasoner, 1999; Menounos et al., 2005; Hodder et al., 2007; Zolitschka et al., 2015; Erik Schiefer et al., 2018). By analyzing down-core trends in laminae thickness, grain size, and organic content, these studies have observed how sediment production and transport has changed during past climate changes.

Studies on glacier-fed lake sediment records have primarily focused on lakes proximal to glacier activity in the Coastal Mountains in British Columbia and Rocky Mountains in Alberta (Hodder et al., 2006; Menounos et al., 2009). Thus, more research is needed in different environments to understand how changes in the glaciated headwaters affect down-valley environments. Additional studies are also needed for climate regimes other than the Coastal and Rocky Mountains such as the warmer and dryer Cariboo Mountains to indicate regional differences in climate change responses. By increasing the body of knowledge of how alpine environments responded to past climate changes, we can better outline the anomalous nature of current anthropogenic climate change and also prepare for future implications.

1.2 Objectives

The purpose of this study is to determine Holocene glacier activity and watershed dynamics using recent and long-term sediment archives from glacier-fed Cariboo Lake in eastern central British Columbia. The primary research objectives of this study are:

1) To establish an understanding of the fluvial geomorphology of the watershed which controls sediment connectivity between Cariboo Lake and the primary sediment production zone in the glaciated headwaters of the Cariboo Lake watershed.
2) Determine the primary physical characteristics of Cariboo Lake and the surrounding watershed that govern sediment deposition such as: temporal and spatial variability of sediment flux, key sediment sources, and lake morphology.
3) Analyze whether long-term sediment archives from Cariboo Lake reflect fluctuations in glacier extent and sediment dynamics throughout the Holocene.
4) Compare fluctuations in the Cariboo Lake sediment record to other glaciolacustrine lake sediment studies, glacier advances and climatic records across western Canada.

2.0 LITERATURE REVIEW

2.1 Process Domains of a Glaciated Watershed

The processes and interactions occurring within a glaciated watershed can be simplified into three main process domains: i) the zone of erosion in the headwaters, ii) the zone of transportation, and iii) the zone of deposition (Fig. 2.1, Wohl, 2014). Although these processes occur contiguously throughout the watershed, these process domains outline the dominant process occurring in a given catchment area. The following section includes a generalized description of these three process domains.

2.1.1 Zone of Erosion

The region of a watershed where the production of sediment is the dominant process is called the zone of erosion (Fig. 2.1; Wohl, 2014). Generally, the dominant source of sediment in glaciated watersheds is derived from glacially eroded bedrock in the headwaters of the watershed (Leonard, 1986; Desloges & Gilbert, 1994a). Glaciated watersheds are often characterized by steep terrain, which also results in other sediment sources through mass movements of sediment such as slumps, debris flows, and debris avalanches leading to additional sediment production (Benn & Evans, 2010). However, research by Hooke & Elverhøi, (1996) and Hiemstra & Rijsdijk, (2003) demonstrate that upwards of 80% sediment delivered down-valley is from glacier activity in glaciated watersheds with over 5% permanent ice cover. Fine silt and clay sediments derived from sub-glacial erosion are often well connected to down-valley environments as they are easily suspended and transported through suspended load in meltwater streams (Cavalli, Trevisani, Comiti, & Marchi, 2013). Coarser grained sediments derived from mass movements are not as easily transported and remain stored in alluvial fans for longer time periods resulting in lower contributions to down-valley sediment yields (Wohl, 2017)

2.1.2 Zone of Transportation

Down-valley of the erosional zone, the transport of sediment through river channels becomes the dominant process (Fig. 2.1, Wohl, 2014). The transport efficiency of sediment derived in the production zone to down-valley stream networks depends on the connectivity of the headwaters (Wohl, Magilligan, & Rathburn, 2017). In the headwaters of glaciated catchments, the steep gradient, persistent water supply, and abundant supply of fine sediment often results in a well-connected environment leading to the transfer of glacially derived sediment into the stream network (Carrivick & Tweed, 2013).

The mobilization of eroded sediments within a river bed depends on the boundary shear stress level, which takes into account the stream velocity and sediment grain diameter (Smith & Ashley, 1985). If the shear stress exerted by the river is enough to entrain the particle it will be transported down-valley by one of three different mechanisms: dissolved load, suspended load and bedload. Dissolved load occurs when sediment is carried in solution within a river, however this process is often insignificant in glaciated environments (Wohl, 2014).

Suspended sediment transport occurs when grains are transported downstream without contact with the river bed (Smith & Ashley, 1985). Grains in stagnant water will fall to the bed under gravity in proportion to their diameter. Thus, for grains to maintain suspension the settling velocity must be balanced by a vertical velocity attributed to flowing water (Wohl, 2014). In turbulent flow, some of the flow velocity is directed upwards, which can support the suspension of grains. Sediments derived in glaciated catchments are often very fine silt and clay grains which easily remain in suspension due to their small mass and can be transported long distances (Gurnell, 1982). In glacial-fed streams, research by Gurnell, (1982) has demonstrated that concentrations of suspended sediment are often higher before peak flows. This occurs when

stores of sediment in the headwaters and upper channel beds are depleted from the glacier and channel bed before peak flow is reached.

Bedload is the third mechanism of sediment transportation, and occurs through the movement of sediment along the channel bed (Allen, 1982). Bedload movement can be divided into three types: sliding, rolling, and saltation. Sliding occurs at lower discharges as sediment grains remain in continuous contact with the river bed, and experience little or no rotation. At slightly higher discharges, grains begin to roll remaining in continuous contact with the bed surface. Saltation occurs at the highest discharge levels as grains experience periods of suspension where the particle is only in contact with the channel bed for short intervals. While all three bedload processes can occur concurrently in a stream reach, usually there is one transport mechanism that dominates depending on the river planform and flow velocities.

The transport of sediment down-valley is often interrupted by intermittent areas of storage marked by decreases in river velocity (Carrivick & Heckmann, 2017). The decrease in energy results in intermittent deposition of sediment and reduces connectivity to downstream environments. The degree of storage along the transportation zones can often be inferred by river planform classifications. Rivers are generally classified into planform types based on their two-dimensional planform, bank stability and downstream slope gradient (Wohl, 2014). In glaciated catchments the two most common types of river planforms are meandering and braided channels (Smith & Ashley, 1985). Meandering channels generally form in regions with low slope gradients and are characterized by a single channel with regular bends that have a sinuosity of over 1.5 (Wohl, 2014). The meanders of these channels mitigate stream power by dispersing energy into the outer bank of the bend creating a zone of erosion leading to the formation of a cut bank. Along the inner bank, flows are reduced leading to a zone of deposition of sediment and

formation of a point bar reducing the sediment transport capacity (Fig. 2.1). In meandering channels, during peak flows erosion is limited as water spills into the floodplain, reducing the energy within the channel. Generally, during normal flow levels the dominant sediment transport mechanism in meandering channels is suspended load, however, bedload transport can also occur during bankfull discharge (Wohl, 2014).

Braided rivers are multi-thread channels, where individual channels are separated by bars (Wohl, 2014). Generally, braided rivers are formed from higher flow velocities than meandering channels and promote movement of substantial clay, silt, and sand sediments through bedload and suspended load transport (Wohl, 2014). The banks of braided rivers are less confining and are more erodible than meandering rivers. This facilitates channel widening in braided rivers and the formation of multiple wide-shallow channels leading to a higher sediment transport capacity. Due to the steep gradient of the headwaters in glaciated catchments, stream flow velocity in is generally high which leads to the formation of braided river planforms (Smith & Ashley, 1985). The high sediment load capacity of braided channels facilitates increased sediment connectivity between the headwaters and downstream environments (Cavalli et al., 2013). As the slope decreases down-valley and bank stability increases due to increases in vegetation, stream planforms often transition into a meandering channel resulting in an increase of sediment storage of coarser grained sediments. However, fine grained silt and clays generally remain in suspension and are transported downstream.

2.1.3 Zone of Deposition

The transition into the zone of deposition occurs as the process of sediment deposition outweighs the process of sediment transport (Fig. 2.1, Wohl, 2014). The transition to this zone is often characterized by a reduction in river velocity resulting in the formation of a river delta. In

the Cariboo Lake watershed, there are two types of deltas, river deltas and fan deltas. The main river delta in Cariboo Lake is an elongated river delta comprised of primarily silt and clay sediments located at the eastern end of the lake, at the terminus of the Cariboo River. Further down lake are two fan deltas, Keithley Creek and Frank Creek. Fan deltas are different than river deltas in that they are dominated by alluvial fan processes such as steep, coarse-grained conical cross-sectional shape with a distinct apex that terminates in the lake (Wohl, 2014).

In watersheds that have a deltaic depositional zone the delivery of sediment into the lake depends on river flow levels, and the difference in density, temperature, and suspended load concentrations between the river inflow and lake environments (Wright, 1977; Morehead & Syvitski, 1999). Depending on the density differences between the river and lake, inflow can occur as stratified or homopycnal flow (Smith & Ashley, 1985). Homopycnal inflow occurs when river inflow is of equal density to the lake water, and the lake is not stratified, and the inflow can spread freely in three-dimensions throughout the lake (Fig. 2.2c). Stratified inflow occurs when there is a large density gradient between the river and lake. In proglacial lakes, stratified inflow is common due to the cool temperature of glacier-fed river inflow which has a higher density than the warmer lake water (Smith & Ashley, 1985). The type of inflow into the lacustrine environment largely controls the delivery of sediment and thus the formation of lake bottom sediment deposits.

There are three types of stratified inflow: overflow, interflow and underflow (Fig. 2.2a, Benn & Evans, 2010). Overflow occurs when the river inflow is less dense then the surface water, and the inflow travels along the epilimnion (Fig. 2.2a). Suspended sediment transported by overflow currents will be transported across the top of the lake and eventually settles to the lake bed. Some fine fraction sediments can also be transported out of the lake with sufficient

flow velocity and if the density difference is large. If the density of the river inflow is greater than the epilimnion but less than the hypolimnion, interflow will occur, and the river inflow travels along the metalimnion (Fig. 2.2). An underflow forms when river inflow is denser than the lake water, as a result the incoming water will travel along the lake bed (Fig. 2.2a). Often one type of stratified inflow will dominate in the deltaic environment in a proglacial lake which greatly controls the formation of lake sediment deposits (Smith & Ashley, 1985). Sediment inflow through overflow and interflow currents develop the most well-preserved sediment records, as sediment drape uniformly over the lake bed surface. However, when underflow currents dominate down-lake, turbidity currents along the lake bed can disturb the formation of laminated sediment layers (e.g. Leonard & Reasoner, 1999; Hodder, Desloges, & Gilbert, 2006).

The deposition of sediment is controlled by the diameter of sediments and the velocity of inflow currents (Ben & Evans, 2010). Stokes law explains that the settling velocity (v) for a particle in fresh water varies with the diameter (d) of the particle and the density contrast between the sediment (ρ_s) and the water (ρ_w):

$$(1) \qquad v = \frac{(\rho_s - \rho_w) g d}{\eta}$$

v = velocity (m/s)
ρ = density
η = dynamic viscosity
g = gravitational force
d = particle diameter

Stokes equation calculates the velocity of a spherical particle that is falling through a lake column of infinite size filled with a Newtonian fluid of lower density. Settling velocity increases with particle size and with larger differences in sediment and water density, and decreases with increased viscosity. Settling velocities predicted by Stokes law and experimental results are

shown in Fig. 2.3 and exhibit a power function relationship. The settling velocities range from < 0.1 mm/s for small silt sediments (0.01 mm in diameter) and 1000 mm/s for larger gravel grain sizes (10 mm in diameter). As a result of this relationship, often there is an exponential decrease in grain size diameter of lake bed sediments with distance from the main river delta (Ben & Evans, 2010).

The settling of sediment deposits in lacustrine environments is also affected by the Coriolis force (Smith, 1978; Wells, 2009). In the Northern Hemisphere, the rotation of the Earth causes a deflection to the right of the direction of inflowing water (Fig. 2.4). This effect has been exhibited by several studies (e.g. Smith, 1978; Smith & Ashley, 1985; Atkinson, Lin, & Joshi, 1994). The strength of the Coriolis effect on sediment deposition depends on the velocity of inflow, the width of the receiving basin and latitude of the lake study site. This deflection of inflow has significant influence on the sedimentary record, and in the Northern Hemisphere results in a greater accumulation of sediment to the right of the direction of lake inflow and less accumulation to the left. However, the strength of the Coriolis effect depends on the energy of lake inflow currents (Desloges & Gilbert, 1991).

2.2 Processes of Lake Mixing

The following section describes how water interacts with sediments to form lacustrine deposits. Understanding the physical processes that govern sediment dynamics within lakes is necessary to make interpretations about the lacustrine sediment record (Desloges & Gilbert, 1994). This will involve discussing lake stratification of the water column and other vertical mixing processes in glacier fed-lakes.

2.2.1 Lake Stratification

The stability of the water column in lake environments is controlled by density differences in the water column (Smol, 2009). Water reaches its highest density at 3.98 ˚C under standard atmospheric pressure of ($1.013x10^5$ Pa) above and below this temperature the density of water decreases (Fig. 2.5a). Salinity and suspended sediment concentration (SSC) also influence the density of water within lakes. However, salinity is not of importance for stratification in continental proglacial lakes due to their high fresh water content (Ben & Evans, 2010). Glaciers upstream of proglacial lakes produce high amounts of fine sediments which increases the density of river inflow and can control lake stratification (Ben & Evans, 2010). Studies by Smith and Ashley (1985) have shown that SSC increases with depth which can influence lake stratification and is termed *sediment stratification*.

The vertical stratification of a lake water column resulting from density differences between the epilimnion, metalimnion, and hypolimnion is a common phenomenon in proglacial lakes (Fig. 2.5b, Ben & Evans, 2010). The general seasonal stratification of a lake that experiences warm summers and cool winters is exhibited in Fig. 2.5. The thermal stratification of the water column changes throughout the year due to seasonal changes in energy balance (Fig. 2.5c). In midsummer, an increase in solar radiation which increases the temperature and reduces the density of the epilimnion creating a strong contrast between the cooler and denser metalimnion and hypolimnion below leading to thermal stratification (Fig. 2.5c, v). When solar radiation decreases in the fall, surface water cools reducing the density difference in the water column (Fig. 2.5c, iii, iv). Continual cooling into late fall and early winter eventually destabilizes the thermal stratification which can bring the epilimnion and hypolimnion to equal temperatures. This process is called overturning and results in an isothermal water column (Fig. 2.5c, ii). When

the surface waters reach 0 ˚C, the epilimnion becomes less dense creating thermal stratification and reduces mixing between the epilimnion and hypolimnion (Fig. 2.5c, i, Benn & Evans, 2010).

Vertical mixing of the water column in lacustrine environments is important for the formation of lake sediment deposits, as well as other processes, and therefore lakes are often classified depending on the number of overturns per year (Smol, 2009). Dimictic lakes overturn once during fall and once during spring, monomictic lakes experience one overturn event per year, and polymictic lakes experience more than two overturn events per year. Lake overturning has implications for sedimentation as when lakes are stratified, some fine suspended sediments are not able to transfer between the epilimnion and hypolimnion layers (Fig. 2.5b). Thus, when lakes overturn suspended sediments can travel freely through the water column and can disturb the lake bottom sediments (Smith & Ashley, 1985). In some lake environments, lake stratification can lead to the formation of distinct annual sediment laminations due to the different sediment delivery processes that occur during the cycle of seasonal stratification (Zolitschka et al., 2015). The processes that lead to the formation of annual sediment laminations will be discussed in further detail in (Section 2.5).

2.2.2 Other Mixing Processes in the Water Column

Water within a lacustrine system is in constant interaction with forces that promote and limit movement of fluid (Smith & Ashley, 1985). Rarely are lakes in perfect balance between these two forces and are often dominated by factors that promote movement which can change sediment deposition processes and modify the form of deposited sediments (Fig. 2.6).

Mixing in the lake water column resulting from density instabilities can occur in two different ways: mixing of water with equal density is called isopycnal mixing and mixing occurring in water with unequal density is called diapycnal mixing (Imboden & Wüest, 1995).

With diapycnal mixing, a large density difference can prevent mixing between the layers. However, instability between these layers can be generated due to the large density gradient creating shear which can generate waves between the two layers (Imboden & Wüest, 1995). The resulting waves are also called Kelvin-Helmholtz instabilities which can cause turbulent eddies with a high enough density gradient, leading to some mixing between stratified water column layers (Fig. 2.6). With the absence of a thermal water column stratification, isopycnal mixing can occur. This mixing may begin by wind or river inflow which creates enough shear velocity to mix the water parcel (Imboden & Wüest, 1995).

Wind is an important factor that promotes mixing within lakes (Csanaday, 1978). Wind introduces energy to the lake system in the form of shear stress exerted on the lake surface. The level of shear stress exerted on the surface is directly dependent on the wind speed and fetch. High enough shear stress on the lake surface can result in the development of turbulent flow below the surface, which decreases in velocity with depth (Csanady, 1978). At a larger scale, the lake surface can be altered by consistent wind stress. This effectively increases the depth of water at the downwind end of the lake and decreases depth at the upwind end of the lake (Gloor, Wüest, & Münnich, 1994). Lake systems respond to this depth disparity by a deep return flow, where water at the deepest end flows down to the lake bottom and to the shallow end of the lake. This deep return flow can cause large scale mixing within, and if wind shear extends from weeks to months the return flow can reduce density induced stratification (Gloor et al., 1994).

Mixing in lakes can also be generated due to convective energy transfer with the lake surface resulting from evaporation (Green, 1987). The process of evaporation changes the density of water by cooling and/or increasing the concentration of solutes of surface water. As the surface water parcels begin to sink due to increased density, they are replaced by low-density

parcels creating a convective process (Green, 1987). However, in stratified lakes, the mixing induced by convection is limited to the epilimnion layer (Smol, 2009).

2.3 Sedimentary Processes

Within the lake system there are many processes that control the formation of lake bottom sediment deposits (Smith & Ashley, 1985). These processes include gravitational mass movements, turbidity currents, flocculation, focusing and diagenesis. The following section presents a generalized description of these processes in the context of a glacier-fed lake environment.

2.3.1 Gravitational Mass Movements

The release of sub-aqueous sediment from basin side slopes can affect the formation of lake bottom sediment deposits through disturbing sediment stratification and redepositing of old sediments (Smith & Ashley, 1985). These mass movements result from either a reduction in strength or a stress induced on a hillslope. There are three main types of movement which are differentiated based on the level of deformation, they include: slides, slumps, and flows (Smith & Ashley, 1985). Slides result when a block of sediment moves downslope along a plane and remains mostly intact. A slump occurs when a coherent mass of sediment moves down a slope and breaks into smaller pieces, modifying the original sediment structure before settling. Flows create the most deformation as sediment is completely reworked and mixed throughout its downslope movement (Smith & Ashley, 1985). Terzhagi (1955) predicted the shear strength (τ_s) of *sub aqueous* sediment using this equation:

τ_s = shear strength
c = cohesion (kg m^{-2})
z_s = depth of failure (m)
y = relative density of sediment in water at 5 ˚C
p_s = pore water pressure (kg m^{-1} s^{-2})
θ = friction angle

$$\tau_s = c + (yz_s - p_s) \tan \theta \quad (2)$$

This shear strength equation reveals that the strength of submerged sediments is highest at low angles, high cohesion, and low pore water pressure.

2.3.2 Turbidity Currents

Turbidity currents occur as an episodic underflow which transfers sediment along the lake bed (Leeder, 2009). There are two types of turbidity currents: i) semi-continuous currents originating from rivers with high sediment concentrations and ii) episodic surge currents resulting from slope failure in unstable sediments. The surge deposits occur over a much shorter time scale (minutes) and can occur randomly, while semi-continuous currents can occur over longer time scales (days). With either type, the sinking plume of sediment follows the bathymetry of the lake basin, and factors as bed friction and density loss due to sediment deposition can reduce the velocity of the turbidity current. In a study by Gilbert, (1975) on glacial-fed Lillooet Lake, fine sand was found to be carried over 6 km by turbidity currents.

The sediment deposits, also called turbidites, created by the two types of turbidity currents are quite similar in their forms (Smith & Ashley, 1985). Common features between the two are flutes or tool marking at their base which results from the turbulent scour and large clasts. With high flow conditions the deposition of turbidites results in parallel-layered sand deposits. In lower flow turbidity currents, sediment deposits form rippled beds. Evidence of discontinuous settling can differentiate between surge and semi-continuous turbidite deposits. An upward fining of sediments in the deposits often results from surge-type turbidity currents as they form over a shorter time period and have less time to mix. While semi-continuous turbidites result in an interbedded mixture of sand and silt (Smith & Ashley, 1985).

2.3.3 Flocculation

The process of flocculation occurs as bonds are created between individual clay grains while being transported in suspension (Smith & Ashley, 1985; Hodder & Gilbert, 2007). Subsequently, the grains aggregate creating a group of grains, called a floc. The floc has a greater mass than the individual grains which increases the rate at which sediment grains settle to the lake bottom. Sediment flocculation can be caused by electrostatic charges between the water and individual sediment grains and/or biological activity. A study by Smith, Venol, & Kennedy (1982) in proglacial Bow Lake, Alberta demonstrated that sediment ingesting zooplankton promoted biological flocculation by creating clay flocs through their digestive process. In their study they found 60% of sediments in a lake bottom trap consisted of ovoid-shaped fecal pellets of 100 to 350 µm in length. Therefore, in some lakes flocculation can have a significant influence on increasing the transfer of sediment from the epilimnion to the lake bottom (Hodder & Gilbert, 2007).

2.3.4 Form of Lacustrine Sediment Deposits

The form of sediment deposits in lacustrine systems can be affected by processes such as sediment focussing and diagenesis (Imboden & Wüest, 1995). Focussing occurs when there is non-uniform deposition of sediments into the lake, which results in greater accumulation of sediment in some areas of the lake bed (Smith & Ashley, 1985). Factors that can contribute to sediment focussing include: spatial distribution of river deltas, lake bathymetry, Coriolis forces, and reworking of existing sediments through mass movements. Sediment focusing is often split into two types: predictable and unpredictable. Predictable focusing is where the difference in sediment accumulation is attributed to factors such as the height of the water column above the

basin floor and proximity to river inlets (Smith & Ashley, 1985). Deeper water depths result in a larger volume of water which has the capacity to carry more sediment and results in increased sediment deposition. With shallower water depths, the reduction in water volume leads to less sediment carrying capacity and reduced sediment thickness in the lake bottom below. Unpredictable focusing results from stochastic processes such as hillslope failures, turbidity currents, and other sediment deposition events which induce local sedimentation within the lake (Smith & Ashley, 1985).

After sediments have settled in the lake bed any modification to the sediment morphology is called early diagenesis (Imboden & Wüest, 1995). These changes include chemical, physical and biological alterations to the sediment following to deposition. Chemical precipitation occurs when dissolved salts are deposited from solution, although this is uncommon in proglacial lake sediments (Håkanson & Jansson, 1983). Physical diagenesis occurs from sediment compaction resulting from the decrease in overall volume as individual grains are brought closer, thus together reducing porosity. This process is most effective in the early stages of sediment deposition when porosity is highest. Other factors that control compaction include grain size, sorting, grain shape, and water content (Menounos, 1997; Smol, 2009). Bioturbation is the mixing and dispersion of bed sediments caused by microfauna (bacteria, fungi), mesofauna (insect larvae, molluscs), and macro fauna (shell fish, reptiles and amphibians). The movement of these organisms can alter the stratigraphy of lake bottom sediments. The level of bioturbation depends on many different factors such as their spatial position within the lake, environmental conditions, lake stratification, and sunlight.

2.4 Sediment Archives as an Environmental Proxy

Sediment deposits from glacier-fed lakes reflect changes in catchment-wide activity often related to fluctuations in climate (Desloges & Gilbert, 1994a; Hodder et al., 2006). Studies across western Canada have shown glacier-fed lakes are ideal candidates for proxy analyses to do their large packages of glacially derived sediment (Karlen, 1981; Menounos et al., 2009). Several fjord-like basins are found across western Canada, characterized by high sediment trap efficiencies due to their high length-to-width ratio (Nasmith, 1962). The trenches that are now occupied by lakes across the interior of British Columbia, once acted as passageways for glaciers flowing down-valley during the Last Glacial Maximum deepening the fjord-valleys (Sugden, 1978; Harbor, 1993). The peak of the last glacier maximum lead to the formation of the extensive Cordilleran Ice Sheet around 29 000 yr BP which covered most of British Columbia (Clague, 1989). The downwasting of the Cordilleran Ice Sheet around 11 000 yr BP, exposed abundant sediment stores in upland areas leading to a large transfer of sediment to down-valley lacustrine environments (Fulton, Ryder, & Tsang, 2004). Over the last 11 000 yr BP, alpine lakes across western Canada have continued to receive sediment from the glaciated headwaters. The flux of sediment delivered to lakes during this time period has been shown to be dependent on climate fluctuations over the Holocene (Hodder et al., 2007; Menounos et al., 2009).

Therefore, due to the rich sedimentological history of alpine lakes across western Canada, several studies have analyzed these sediment archives to gain an understanding of past environments since the Last Glacial Maximum (Karlen, 1981; Leonard & Reasoner, 1999; Heideman et al., 2017). The following sections describes the various techniques used to analyze glaciolacustrine sediment deposits.

2.4.1 Geophysics of Lake Sediment Deposits

To reveal the history of sediment infill of various lake environments many researchers have utilized acoustic remote sensing techniques (Desloges & Gilbert, 1994a; van Rensbergen, de Batist, Beck, & Chapron, 1999; Gilbert & Desloges, 2012). Since deep drilling is often expensive and infeasible, researchers have turned to seismic reflection techniques which work by generating and detecting sound waves. A sub-bottom acoustic survey in lacustrine environments is generally conducted by running transects across the surface of the lake with an acoustic transducer onboard a research vessel (LeBlanc, Mayer, Rufino, Schock, & King, 1992). The results from these surveys reveals acoustic facies in the sediment stratigraphy that are characterized by varying impedance of sound wave propagation through different layers of sediment. Sediment characteristics that dictate the impedance of soundwaves include particle size, distribution, composition, and water content (LeBlanc et al., 1992). The depth and resolution of the sediment stratigraphy produced by an acoustic survey depends on the frequency of the transducer used (Hodder et al., 2006). A transducer with a lower frequency (3.5 khz) better penetrates to deeper depths and through thick reflective layers but results in a lower resolution. A transducer with a higher frequency (10 khz), has lower energy and thus will not penetrate through a reflective layer, such as coarse sediments near a river delta, but will provide higher resolution in acoustically transparent layers such as fine silts and clays.

These acoustic survey methods have been used to reveal the sediment stratigraphy in lakes across the Canadian Cordillera (Desloges & Gilbert, 1994; Hodder et al., 2006; Gilbert & Desloges, 2012). A study by Hodder et al., (2006) illustrate the pattern and timing of sediment infill to the glacier-fed Mud Lake (Fig 2.7). An acoustic survey paired with sediment core evidence revealed three main sedimentary facies (Fig. 2.7): in the lower facies (A) they observed

parallel-stratified acoustic reflectors characteristic of a glacial-proximal or ice-contact environment, potentially derived from high energetic turbidity underflows. Above facies (A), facies (B) did not exhibit significant acoustic reflectors, which was confirmed by low sediment accumulation rates in sediment cores at the same depth. This sedimentary unit is interpreted to be formed by a lower energy environment during reduced glacial activity. The top facies (C) indicates a return to more variable and higher discharge in the watershed leading to an increase in acoustic reflectors observed in the record likely a result of more frequent high energy turbidite underflows consisting of sand grained sediments. Areas proximal to the river delta in Mud Lake exhibit high acoustic reflection on the sub-bottom surface and is attributed to coarser grained sediments brought in by high energy underflows by the main river delta (Hodder et al., 2006).

Outside of Canada, a study by Rensbergen et al., (1999) implemented acoustic surveys to study post-glacial sediment stratigraphy in the French Alps. Five acoustic facies are described in that study which transition from high energy watershed activity during the early deglacial period, to more recent low energy sediment accumulation in recent times. Strong signaled acoustic reflectors are also interpreted as sandy deposits derived from turbidity currents, as in Hodder et al., (2006).

2.4.2 Varves and Suspended Sediment Yield

When present, the annual rhythmic lamination of sediment in glacier-fed lakes provides a high-resolution technique to study the stratigraphy of lake sediments over time (Hodder et al., 2007; Heideman, Menounos, & Clague, 2015; Zolitschka et al., 2015). Annual lamination of sediment often occurs in deep central locations in glacier-fed lakes where the deposition of clastic sediments is high and the disruption of the lake bed sediments is low (Desloges & Gilbert, 1994; Menounos & Clague, 2008; Zolitschka et al., 2015).

In alpine environments, glacier activity and low vegetation result in a high production of fine clastic sediments which often leads to the formation of varves in down-valley glaciated lakes when sediment production and transport are high enough (Zolitschka et al., 2015). The formation of clastic varves occurs when seasonal flows carry suspended sediments into a lake with a thermally stratified water column (Zolitschka et al., 2015). Depending on density differences between river inflow and the lake water column, suspended sediments will enter the lake as over, inter, or underflow as described in (Section 2.1.3). Larger sand grains will settle out immediately at the delta, while silt and clay sediments remain in suspension and are transported further down-lake (Zolitschka et al., 2015). Mid- and high-latitude glaciated watersheds often exhibit distinct hydrologic seasons, which results in variations in the velocity of river inflow, and thus sediments transported over the year (Zolitschka et al., 2015). This seasonality can result in the formation of a clastic varve couplet when sediment yields are high enough (Lamoureux, 2002; Hodder et al., 2007). A varve couplet in a glacier-fed lake generally consists of a coarse-grained layer deposited by seasonal high flows in the spring, followed by a fine-grained layer deposited when the lake freezes and flow velocity decrease (Zolitschka et al., 2015). In some lakes, multiple coarse-grained layers are observed in a single year resulting from cold spells interrupting snowmelt, or separate spring flow events (Cockburn & Lamoureux, 2008).

When considered in three dimensions, a single varve couplet provides an estimate of the total suspended sediment entering that basin in a given year relative to the watershed area, expressed as annual suspended sediment yield (SSY, $Mg \cdot km^{-2} \cdot a^{-1}$) (Onstad, 1984; E. Schiefer, Hassan, Menounos, Pelpola, & Slaymaker, 2010). Several studies across the Canadian Cordillera have used varved sediments to estimate SSY in glacier-fed lakes (Desloges & Gilbert, 1994a; Leonard & Reasoner, 1999; Menounos et al., 2005; Heideman et al., 2017). Studies have

compared SSY values in watersheds across the Canadian Cordillera revealing the varying importance of sediment sources, transport mechanisms, and storage across different basins. Examples of factors that control SSY include: glacier cover (Hodder et al., 2006), basin morphometry (Heideman et al., 2017), hydrology and climate (Lamoureux, 2002; Menounos, 2006a), land-use changes (O'Hara, Street-Perrott, & Burt, 1993; Zolitschka, 1998), landslides (Koi et al., 2008), and landscape connectivity (Wohl et al., 2017).

Examinations of varve thickness, and hence SSY, in sediment cores have revealed temporal trends related to past climate fluctuations (Hodder et al., 2006; Heideman et al., 2017). However, these interpretations come with two main complexities: 1) Evans & Church, (2000) note the importance of retrieving multiple cores from a lake basin in order to capture the cross-lake variability in sedimentation patterns. Their findings based on 10-12 cores from four alpine lakes in southwest British Columbia exhibit a 7 – 21% error range in sediment yield patterns between cores. 2) A process-network described by Hodder et al., (2007) outlines the complex relationship between climate and varve thickness in glaciolacustrine sediment. The process-network is comprised of six systems including: climate, glacier, fluvial, geomorphic, terrestrial biologic, and lacustrine systems which each interact to control the relationship between climate and varve thickness. Due to the multiple interactions between these systems and their varying degree of influence on varve thickness stratigraphy, the linkage between varve thickness and climate is weak at time scales of less than 10 years (Hodder et al., 2007; Menounos et al., 2008 Heideman et al., 2017). This is attributed to the fact that climate change effects often take longer than 10 years to propagate through a watershed. At longer time scales of over 100 years, trends in sedimentation rates are better correlated to climate fluctuations and glacier extents (Leonard & Reasoner, 1999; Osborn, Menounos, Koch, Clague, & Vallis, 2007; Heideman et al., 2017).

However, some short term events such as major floods and hillslope failures have been preserved in the varve record of glacier-fed lakes as these erosional processes can introduce large turbidites into the lake which are revealed in the sediment record (Desloges & Gilbert, 1994b; Menounos, 2006b).

2.4.3 Climate Controls on Lake Sedimentation

Sediment records from glacier-fed lakes have illustrated the potential to provide a proxy of past climate (Hodder et al., 2007; Menounos et al., 2009; Thomas & Briner, 2009; Glur, Stalder, Wirth, Gilli, & Anselmetti, 2015). The amount of sediment delivered to a glacier-fed lake in a given year is dependent on aspects of climate such as annual temperature, glacier extent, autumn precipitation, snowmelt runoff, and individual storm events (Gilbert & Desloges, 1994a; Hodder et al., 2007). These various aspects of climate act in concert to control the production and transport of sediment to down-valley lakes (Hodder et al., 2007). Analyses of down core sediment characteristics such as varve thickness, grain size, and percent organic content (%LOI) have been utilized to express past changes in the watershed related to fluctuations in climate (Desloges & Gilbert, 1994b; Hodder et al., 2006; Cockburn & Lamoureux, 2008).

In a glaciated watershed, the production of clastic sediment in the headwaters has been linked to percent ice cover; with an increase in glacier extent during cool periods leading to an increase in production of clastic sediment (Leonard, 1986; Desloges & Gilbert, 1994a; Hodder et al., 2007). During cool periods that persist at century time scales, a rise in sediment yield generally results in down-valley lakes which can lead to an increase in varve thickness, grain size, and %LOI in lake sediments (Hodder et al., 2006). An increase in varve thickness results from a rise in sediment production due to increased sub-glacial erosion in the glaciated headwaters which leads to higher amounts of fine clastic sediment transported into down-valley

lakes. This is further amplified by increases in spring flows which also increase the sediment transport capacity of streams (Zolitschka et al., 2015). An increase in grain size also results during cool periods due to increased snowpack and summer glacier melt which brings higher stream flows leading to the transport of larger sediment grains to down-valley lacustrine environments (Wohl, 2014). However, a decrease in organic content is observed as autochthonous biologic productivity within the lake is assumed to be constant, while allochthonous clastic material increases leading to the decrease in overall percent organics in lake bottom sediments (Smol, 2009). During periods of climate warming in glaciated watersheds, some lakes exhibit an initial increase in varve thickness and grain size; and a decrease in organic content in response to glacier retreat exposing sediment stores and higher flows resulting from ice melt (Menounos et al., 2005). However, shortly following this period of increased sediment yield, generally varve thickness and grain size decrease while %LOI increases in the glaciolacustrine sediment record as sediment production and sediment transport capacity is reduced (Menounos et al., 2005).

2.5 Holocene glacier history in the Southern Interior British Columbia

The Canadian Cordillera is a mountain range that spans from southern British Columbia and Alberta to the Arctic Ocean. It is comprised of the Western, Interior, and Eastern systems (Menounos et al., 2009). The western system includes the Insular, Cascade, Coast, and St. Elias mountains. The Interior System includes the southern Purcell, Selkirk, Cariboo, and Monashee mountains in the south and the northern Hazelton, Skeena, Cassiar, Omineca, and Ogilvie mountains. The Eastern System includes the southern Rocky Mountains and the northern Selwyn, Mackenzie, and Richardson mountains. Since the retreat of the Last Glacial Maximum (LGM) the Canadian Cordillera has experienced several fluctuations in glacier extent which have

greatly influenced the delivery of sediment into glacier-fed lakes across western Canada (Osborn & Luckman, 1988; Clague, 2000). The following section outlines the primary glacier advances that have occurred across the Canadian Cordillera throughout the Holocene.

2.5.1 Last Glacial Maximum

The Canadian Cordillera has experienced numerous periods of glaciation over the past hundred thousand years. The Last Glacial Maximum in western Canada resulted from the Fraser Glaciation of the Cordilleran Ice Sheet which was comprised of confluent glaciers and covered most of British Columbia (Fulton et al., 2004). The peak of the Last Glacial Maximum lead to the formation of the extensive Cordilleran Ice Sheet around 29 000 yr BP which covered most of British Columbia (Clague, 1989). The Cordilleran Ice Sheet had significant erosive power due to its large mass, which lead to the deepening of fjord valley lakes (Sugden, 1978; Harbor, 1993). The downwasting of the Cordilleran Ice Sheet around 11 000 yr BP, exposed large sediment stores in upland areas leading to a large transfer of sediment to down-valley environments (Fulton et al., 2004). The generalized timing of sedimentation in lakes across British Columbia that received mass amounts of sediment following the Last Glacial Maximum age is presented by Clague (2000). Sand and gravel were first deposited, followed by an upward grading sequence of silt and clay sediments which was deposited as erosive energy decreased and sediment stores are depleted. Studies by Desloges & Gilbert, (1994b), (1995); Gilbert, Crookshanks, Hodder, Spagnol, & Stull, (2006); Gilbert & Desloges, (2012) have exhibited similar Pleistocene sediment stratigraphy in various lakes in interior British Columbia. This period of glaciation began around 29 ka BP and reached maximum extents around 16.5 ka BP. Deglaciation began around 16.5 ka BP due to climate warming and eustatic sea-level rise (Clague, 2000). Regional

deglaciation of the Cordilleran Ice Sheet was complete around 11 ka BP marking the beginning of the Holocene (Menounos et al., 2009).

2.5.2 Early Holocene (11.0-7.5 ka)

During the Hypsithermal Interval, also known as the Holocene climate optimum, high-altitude glaciers and cirques across the Canadian Cordillera reached minimum extents starting around 11 ka BP (Menounos, Koch, Osborn, Clague, & Mazzucchi, 2004; Osborn et al., 2007; Koch, Osborn, & Clague, 2007). The extent of glaciers during this time are estimated to have been similar to current extents (Menounos et al., 2009). Evidence of reduced glacial extents in the southern Coast Mountains are supported by clastic-poor sediments in lacustrine sediment cores from Green Lake and detrital wood samples from glacier forefields in Garibaldi Park (Menounos et al., 2004; Koch et al., 2007; Osborn et al., 2007). In the Rocky Mountains, detrital wood was dated to 9.2 – 8.37 ka BP from the Athabasca glacier in the Canadian Rockies, meaning that the glacier was less extensive during when this tree was alive than when it was collected in 1993 (Luckman, 1988; Luckman, Holdsworth, & Osborn, 1993).

2.5.3 Early Neoglacial (7.5-5.0 ka)

The Neoglacial period is defined as the period of glacial regrowth following the Hypsithermal period where glaciers across the Canadian Cordillera began to expand from minimum extents (Porter & Denton, 1967). Evidence for a cooling phase around this time in the southern Coast Mountains is supported by detrital wood deposits dated from 6.95–5.62 ka BP (Ryder & Thomson, 1986; Smith & Desloges, 2000). Lake sediment cores in the southern Coast Mountains also indicate an increase in glacier extent during this time period through an increase in clastic sediment from 7.03–6.62 ka, 5.90–4.90 ka, and 6.95–5.62 ka (Souch, 1994; Osborn et al., 2007). Neoglacial advances in the Interior Cariboo Mountains and Rocky Mountains is

limited to detrital wood found in glacial forefields dated to 7.46-5.33 ka BP (Luckman & Wilson, 2005; Maurer et al., 2012). In general, across western Canada, evidence of glacier advances during the start of the Neoglacial time period generally coincide between 7.35–5.77 ka BP. This period of glacier advance is called the Garibaldi Phase in the Coast Mountains and the Crowfoot Advance in the Rocky Mountains (Menounos et al., 2009).

2.5.4 Early-Mid Neoglacial (5.0-3.5 ka BP)

In the middle of the Neoglacial period it is estimated that two main glacier advances occurred between 5.00 and 3.50 ka BP, supported by evidence of tree stumps and pro-glacial sediment cores across western Canada. In the Coastal Mountains, detrital wood from several different glacier forefields provide evidence of glacier advances between 5.04 and 3.93 ka BP (Koch et al., 2007; Osborn et al., 2007; Menounos et al., 2009). In the Rocky Mountains tree stumps in growth position in the Cariboo Mountains, Selkirk Mountains, and at Mount Athabasca also support advances between 4.85 and 3.95 ka BP. The lacustrine sediment based evidence includes a clastic interval occurring between 4.40-4.00 ka BP and at 4.90 ka BP in the Coastal Mountains, and 4.18, 4.40, 4.99 ka BP in the Rocky Mountains (Leonard & Reasoner, 1999; Menounos & Clague, 2008). The difference in timing of glacier advances between these two regions is suspected to be due to dating errors or climatic differences between the coastal and interior ranges (Menounos et al., 2009). A second, more recent increase in glacial activity around 3.5 ka BP was indicated by proglacial sediment cores from the Coastal and Interior Mountains. These cores exhibited that sedimentation rates around 3.50 ka BP were comparable to those of the Little Ice Age in the last millennium (Desloges, 1999; Hodder et al., 2006).

2.5.5 Middle-Late Neoglacial (3.5-1.0 ka)

During the Middle-Late Neoglacial period from 3.50-1.00 ka BP glaciers expanded to extents slightly less extensive than the LIA advance (Menounos et al., 2009). Multiple advances between 3.55 ka BP and 2.36 ka are indicated from detrital wood found in glacial forefields and increases in clastic sediment to glacier-fed lakes across the Canadian Cordillera (Ryder and Thomson, 1986; Koch et al., 2007; Osborn et al., 2007; Maurer et al., 2012). Several stumps and detrital wood from glacier forefields across the Coast Mountains have yielded dates between 3.50 – 2.37 ka BP (Menounos et al., 2009). Proglacial lake sediment records indicate extensive glacier extents in the southern Coast Mountains slightly earlier than terrestrial records with an increase in sedimentation rates beginning as early as 3.63 – 3.36 ka BP in Green Lake (Osborn et al., 2007). Sediment records from other lakes also exhibit an increase of clastic sediment around 3.0 ka BP in Diamond Lake (Minkus, 2006) and around 2.40 ka BP in Kokwaskeym, Kwoiek and Duffy Lakes (Souch, 1994; Menounos, 2002). These sediment records support the terrestrial records of many glacier advances during the start of the Middle-Late Neoglacial period and is named the Tiedemann Advance.

Studies from the Interior and Eastern Mountain Ranges also indicate glacier advances between 3.5-1.85 ka through corroborative evidence from detrital wood, stumps in growth positions, and proglacial sediment records (Luckman et al., 1993; Luckman, 2000; Maurer et al., 2012; Wood & Smith, 2013). Stumps sheared in their growth position from the Peyto and Saskatchewan glacier forefields dated between 3.07 and 2.78 ka BP provide the most relevant evidence of glacier advance during the Middle-Late Neoglacial (Menounos et al., 2009). Evidence from proglacial sediment records indicate two distinct periods of high sedimentation in Hector Lake in the Rocky Mountains around 3.00 ka BP and 1.85 ka BP (Leonard & Reasoner,

1999). Increased sedimentation rates at nearby lakes were observed at 3.46 and 2.33 ka BP in Chephren Lake and 3.10, 2.50, and 2.40-2.30 ka BP in Moose Lake (Dirszowsky and Desloges, 1997; Desloges, 1999). In the Cariboo Mountains, an increase in clastic sediment to On-Off Lake is observed between 2.73 and 2.49 ka BP (Maurer et al., 2012).

More recent glacier advances during the Middle-Late Neoglacial period, between 1.60-1.30 ka BP, have occurred in western Canada, Washington State, and Alaska and has been labelled the "First Millennium Advance" (Reyes et al., 2006). Numerous detrital wood samples and stumps in growth positions have been dated between 1.60 and 1.30 ka BP supporting the advancement of glaciers during this time (Reyes et al., 2006). Increase of sedimentation rates have also supported this advance at Green Lake between 1.92-1.63 ka BP and 1.30-1.09 ka BP, and at lower Joffre and Duffey Lakes at 1.50 ka BP (Menounos et al., 2009).

Evidence of the First Millennium Advance around 1.6 – 1.3 ka BP in the Eastern and Interior Mountain Ranges is supported by terrestrial dated material and sediment cores (Luckman, 1995; Dirszowsky and Desloges, 1997; Luckman, 2006; Maurer et al., 2012). In the Cariboo Mountains, Maurer et al., (2012) observe an increase in clastic sediment to On-Off Lake from 1.87-1.72 ka BP and 1.54-1.42 ka BP. In the Rocky Mountains, two samples of detrital wood material were dated to 1.81-1.42 and 1.55-1.32 ka BP at the Peyto Glacier (Luckman, 2006). Lacustrine sediment from Chephren Lake in the Rocky Mountains where a spike in inorganic sedimentation is noted at 1.47 ka BP (Dirszowsky and Desloges, 1997). Further north at Cavell Glacier in Jasper National Park, two detrital wood deposits were dated to 2.04-1.63 ka BP and 1.70-1.41 ka BP (Luckman, 1995).

2.5.6 Latest Neoglacial (1.0 ka BP to present)

The Latest Neoglacial period spans the last millennium and includes the little ice age (LIA) glacier advance which was the most extensive Holocene glacier advance for most of the Canadian Cordillera (Menounos et al., 2009). The timing of the LIA varies between glaciated watersheds across the Canadian Cordillera. However, in general most areas experienced an initial glacier advance around 12th and 13th century, reached maximum extents in the 17th and 18th century and had significant glacier retreats around the start of the 20th century (Desloges & Gilbert, 1995; Luckman & Kavanagh, 2000; Osborn et al., 2007).

In the Coast Mountains, dendrochronological evidence of the timing of the LIA from nine glacier forefields in Garibaldi Park indicate that glaciers reached maximum extents around AD 1690-1720 (Koch et al., 2007). Proglacial sediment records in the Coast Mountains observe peak sediment yield prior to dendrochronological evidence of glacier advances. Sediment yield peaked just after AD 1000 at Black Tusk and Green Lakes (Cashman, Clark, Clague, & Bilderback, 2002; Osborn et al., 2007), and AD 1250 at lower Joffre lake, Diamond Lake, and lakes in the Kwoiek Creek watershed (Souch, 1994; Minkus, 2006).

In the Interior and Rocky Mountains, evidence of the LIA is provided by dendrochronological evidence, proglacial sediment records, and photographic evidence (Luckman, 1988; Wood & Smith, 2004) and lichenometry (Reyes et al., 2006; Osborn et al., 2007). Luckman, (2000) collected 63 dates of LIA terminal moraines across the Interior and Rocky Mountains. Fifteen of these dates predate AD 1700, 27 are within the 18th century, and 21 are within the 19th century. As in the Coast Mountains, agreement of varved sediments and glacier activity is poor at time-scales less than 50-100 years (Menounos et al., 2009). Still, glaciolacustrine sediment records from Hector Lake and Moose Lake reveal increases in varve

thickness between AD 1200-1900 (Desloges & Gilbert, 1995; Desloges, 1999; Luckman, 2000). The most unequivocal evidence of glacier retreat during latest part of the Neoglacial period in the Interior and Rocky Mountains comes from aerial and ground photographs (Luckman & Kavanagh, 2000; Beedle, Menounos, & Wheate, 2015). Photographs from the early 1900s show glaciers close to their LIA maximum position and reveal rapid glacier recession shortly after (Gardner, 1972). Research by Beedle et al., (2015) on 120 glaciers in the Premier Range of the Cariboo Mountains exhibited a 25% loss in ice cover between the LIA maximum around AD 1800 and 1970.

2.5.7 Summary

Evidence from glacial forefields and lake sediments has demonstrated that glaciers have experienced numerous fluctuations in response to changes in climate over the past 11 ka. At the beginning of the Holocene, glaciers reached minimum extents around 9.2 – 8.37 ka BP across the Canadian Cordillera (Luckman, 1988; Luckman et al., 1993). Into the Neoglacial period of the Holocene, glaciers expanded as early as 7.03-6.62 ka BP in the southern Coastal Ranges and 7.46-5.33 ka BP in the Interior and Eastern Ranges. The Early-Middle Neoglacial period was characterized by two main increases in glacier extent at around 5.0 ka BP and 3.5 ka BP in the Western and Interior ranges and one increase between 5.0 – 4.18 ka BP in the Eastern Range (Koch et al., 2007; Osborn et al., 2007; Menounos et al., 2008). The Middle-Late Neoglacial period experienced increases in glacial extent around 3.63-2.36 ka BP and 1.60-1.30 ka BP in the south Coastal Mountains and 3.5-1.85 ka BP and 2.04-1.47 ka BP in the Interior and Eastern Ranges (Menounos et al., 2009). During the latest Neoglacial period, maximum glacier extents in the southern Coast Mountains date from AD 1690-1720s and in the Interior and Eastern Ranges from AD 1837-1845 (Koch et al., 2007). Regionally, the fluctuation of glaciers with climate

coincide at millennial time-scales between the Western Mountain Ranges, and the Interior and Eastern Mountain Ranges.

2.6 Discussion of Research Gaps

Holocene glacier fluctuations have been an important topic of study for several decades, however, gaps in the research still remain. Research on glacier fluctuations in western Canada has been proportionally focused on the southern Coast Mountains in British Columbia and the Rocky Mountains in Alberta (Menounos, et al., 2009). Fewer studies have focused on the northern Coastal Mountains and Interior Ranges of British Columbia. Increasing research in these regions characterized by different climates will allow for more robust understanding of how regional climate differences may affect glacial activity.

3.0 METHODS

3.1 Study Area

A field campaign was conducted in the summer of 2017 in Cariboo Lake, located in the foothills of the Cariboo Mountains, which lie within the northernmost range of the Columbia Mountains in eastern central British Columbia (Fig. 3.1). Cariboo Lake was chosen as our study site as it was expected to have a low annual sediment accumulation rate due to its distal location from glacier activity. The low sedimentation rate presents an opportunity to collect a longer temporal sediment record, compared to glacier-proximal lakes which have much higher sedimentation rates and require a longer core of sediment to retrieve the same temporal range. Moreover, studying a sediment record from a lake distal from glacier activity presents an integrated record of watershed wide processes.

The area of Cariboo Lake is approximately 11 km^2 and the length is 12.5 km. Cariboo Lake receives runoff from an area of 3242 km^2 (Fig. 3.2). The main Cariboo River delta is located on the eastern end of the lake and is elongated, and river dominated, providing inflow from the glaciated portion of the catchment 85 km to the northeast (Fig. 3.2). Smaller tributaries further down lake include Pine Creek, Kay Creek, and Keithley Creek on the north shore and Ladies Creek and Frank Creek on the south shore (Fig. 3.2). Six deep holes ranging from 30 – 58 m in water depth are observed along the lake bathymetry (Fig. 3.2). It is hypothesized that these deep holes were formed during glacial scouring during the glacial maximum (LGM) and have not filled in completely due to a low sedimentation rate within Cariboo Lake.

Sandy and Lanezi Lake are located 30 km up-valley of Cariboo Lake (Fig. 3.1). Sandy Lake has a shallow bathymetry with a maximum depth of 6 m. Lanezi Lake has a deep fjord like bathymetry with a maximum depth of 170 m. These up-valley lakes reduce the connectivity of

sediment transport down the Cariboo River from the glaciated headwaters to down-valley Cariboo Lake. The Cariboo Lake watershed has 80 km^2 of ice cover which covers 2.4% of the total watershed area permanently throughout the year. These glaciers are in four different areas adjacent to Mt. Kaza, Vixen Peak, Kristi Peak, and Mt. Lunn in the northeastern headwaters of the Cariboo Lake watershed (Fig. 3.1). The type of glaciers in the Cariboo Lake watershed include valley glaciers in the larger glacier area proximal to Mt. Lunn and smaller cirque and niche glaciers scattered around the alpine. The watershed relief ranges from 2600 m asl in the headwaters to 600 m asl at the Cariboo Lake outlet.

The Cariboo Lake watershed is comprised of two geologic terranes: the Barkerville terrane which is comprised of mainly sandstone, pelite, limestone and mafic volcaniclastics in the southern part of the watershed, and the Cariboo terrane comprised of mainly sandstone, pelite, and limestone in the northern part of the watershed (Struik, 1986). The meteorological record from the Barkerville station (MSC ID: 1090660) spans from 1888–2007 and lies 10 km northwest outside of the Cariboo Lake watershed (Fig. 3.3). The average annual precipitation from (1981-2010) is 1013 mm in the northern part of the watershed at an elevation of 1283 m near Barkerville, BC, and 692 mm in the southern part at an elevation of 723 m near Likely, BC, (Environment Canada, 2014).

Stream gauge records for this region are provided by the Cariboo River gauging station (1926-1994, 08KH003), which is 23 km downstream of the Cariboo Lake outlet (Fig 3.1). The streamflow regime of the Cariboo Lake watershed is nival-glacial, characterized by highest mean daily flow during the spring melt and also receives a small fraction of input from glacier melt. Peak mean daily flows of over 600 $m^3 s^{-1}$ are observed in late May and early June and then flows are reduced to below 400 $m^3 s^{-1}$ in July (Fig. 3.4). From late July to early August there is a

decline in mean daily flow which is followed by a slight increase from late August to late October, attributed to the onset of the fall storm season. Following the storm season, mean daily flows level out through November and stay below 100 $m^3 s^{-1}$ until March, as water is increasingly stored as snow or ice.

Human influences in the Cariboo Lake watershed began with hydraulic mining activity around 1860 during the Cariboo Gold Rush and continued until 1970. Clear cut logging in the Cariboo Lake watershed started in 1961 and continued until 2014. Both of these activities are expected to have significantly increased sediment delivery into Cariboo Lake after 1860.

3.2 Field Methods

To provide a record of the lake bottom sediment stratigraphy a sub-bottom acoustic survey was conducted using a StrataBox 3510 HD across Cariboo Lake following diagonal cross sections to the shore. The 10 kHz StrataBox 3510 HD transducer was deployed over the starboard side of the *W.H. Matthews* which put the transducer roughly 1 m below the surface and 1 m off the hull of the vessel. Thirty-four km of transects were run across Cariboo Lake (Fig. 3.5).

A Hydrolab Datasonde 4A was used to sample conductivity, turbidity, and temperature of the lake water column. The Hydrolab was deployed over the side of the *W.H. Matthews* at 15 locations following a longitudinal transect down Cariboo Lake (Fig. 3.6). Care was taken to deploy the Datasonde during calm conditions to avoid horizontal drift in the water column, however some horizontal drift is still expected (Fig. 3.6).

To determine the spatial and temporal distribution of sediment and the key mechanisms that govern sediment distribution in Cariboo Lake, lake bottom sediments were collected for lab analysis of various physical sediment characteristics. Twenty short cores (E1-E20) were

collected from Cariboo Lake using an Ekman dredge to a sediment depth of ~10 cm along a longitudinal transect (Fig. 3.7). The Ekman dredge collected an approximately 10 x 10 x 10 cm cube of sediment from the lake bottom. Each dredge sample was subsampled in the field producing a mini core, using PVC cylinders pushed into the block of sediment. The remaining sediment on the outside of the PVC cylinder was bagged and kept as a bulk sample.

Four sediment cores (V1-V4) were collected up to 4 m in length using a Rossfelder submersible vibrocorer from the four deepest basins in Cariboo Lake (Fig. 3.7). The Rossfelder vibrocorer consists of a gasoline generator connected to a hydraulic vibrator head. A 7 cm inside diameter by 6 m long aluminum pipe was attached to the chuck inside the vibrating head. To prevent sediments from coming out of the core, a metal '*core catcher'* with serrate teeth was curved inward and fitted to the bottom of the core. The coring apparatus was deployed over the stern of the *W.H. Matthews* using a gasoline powered winch. When the coring apparatus was near the lake bed the vibrating head was powered on and the aluminum pipe was lowered into the lake bottom sediment. To retrieve the core, the winch was powered on which lifted the coring apparatus out of the lake-bottom and up to the vessel. After retrieval, the 6 m core tube was brought to shore and sectioned into ~ 2 m sections for transport.

3.3 Laboratory Methods

Sediment cores were shipped from the Cariboo Lake to the Geomorphology Laboratory at the University of Toronto. The short (Ekman) cores and long (Rossfelder) vibra cores were split with one half preserved as an archive and the other as a working half. The face of the working half of the core was scraped width wise, parallel to the laminae of the core, to remove the disturbance from core splitting. After the disturbances were removed, the working half faces of the of the core were photographed. The working half photographs of the short cores (E1-E20)

and long cores (V1 and V2) were then digitally analyzed using ImageJ software to count and measure the thickness of sediment laminae. Due to the high amount of noise in the large number of long core varve thickness measurements, a 25-year moving average filter was applied.

Organic material for radiocarbon analysis was extracted from V1 and V2. One twig was extracted at 346 cm from V1. A twig was extracted from V2 at 220 cm and a second twig and pine needle were combined from V2 at a depth of 290 cm. This organic material was submitted to the André E. Lalonde AMS Laboratory at the University of Ottawa for radiocarbon dating analysis.

Loss-on-ignition (LOI) and grain size sediment analyses were conducted on E1-E20 bulk samples and V1 and V2 down-core subsamples. Ekman bulk samples were subsampled by using a 2 mm sieve and then separating into a working bag and archive bag using a sediment sorter. Cores V1 and V2 were subsampled at a 5 cm interval for LOI and grain size analysis, ~2 cm^3 cubes of sediment were extracted at each interval. Where rhythmic laminations were present, 6 laminae were included in the subsample. In heterogeneous sections of V1 and V2, the sampling interval resolution was increased to 2.5 cm to capture the variability. The subsampled sediment from V1 and V2 were then gently homogenised using a mortar and pestle.

The loss-on-ignition analysis followed methods outlined by Smith, (2003). Samples from E1-E20 and V1 and V2 were first weighed and then oven dried for 48 hours at 60 ˚C. Next, after oven drying sediment samples were weighed again and placed in and furnace for 2.5 hours at 550 ˚C and then weighed a third time.

Additional sample prep for grain size analysis on cores E1-E20 and V1 and V2 included the digestion of organic material following methods outlined by Gray, Pasternack, & Watson, (2010). The purpose of this step is to prevent a false increase in the fine fraction of the grain size

analysis by removing organic material from the sediment samples. Sediment subsamples were weighed out to 150 mg and bathed in a total of three 10 ml aliquots of 20% H_2O_2. The second and third aliquot of H_2O_2 were added to the bath when the previous aliquot stopped reacting. Following the organic digestion, the subsamples were dispersed in a 0.05% solution of Calgon for a minimum of 25 hours to prevent fluctuation of sediments. Lastly, the sediment bath was shaken until the solution of sediment was mixed thoroughly and then sampled using a pipette and placed in the Mastersizer Particle Size Analyzer 3000 for analysis.

4.0 RESULTS

This chapter has been divided into four main sections. Modern Processes (Section 4.1) includes findings from the hydrologic record, water column observations, and acoustic sedimentary record. Surficial Sediment Record (Section 4.2) includes results from Ekman cores. Temporal Record (Section 4.3) includes findings from the long-core sediment record. Suspended Sediment Yield (Section 4.4) includes results from the SSY calculation for the Cariboo Lake watershed.

4.1 Modern Processes

4.1.1 Hydrologic Record

The frequency and magnitude of hydrologic activity in the Cariboo Lake watershed is an important control of sediment delivery into Cariboo Lake. The hydrologic record from the Cariboo River gauging station (08KH003), 23 km downstream of Cariboo Lake illustrates the maximum mean-daily flows from 1926 - 1994 (Fig. 3.4). The watershed area of this gauging station is 3242 km^2. From 1926-1994, the highest maximum mean-daily flow occurs in June at ~271 $m^3 s^{-1}$. May and July experience the second highest maximum mean-daily flow at 187 $m^3 s^{-1}$ and 193 $m^3 s^{-1}$ respectively. The lowest maximum mean-daily flow measurements occur in winter, ranging from 23 $m^3 s^{-1}$ in January, 20 $m^3 s^{-1}$ February, and 20 $m^3 s^{-1}$ in March (Fig. 3.4). From June to September a falling limb of average monthly discharge is observed as snowpack is depleted reducing water availability. In the fall, there is a shift from snowpack dependent flows to shorter lived storm events, illustrated by peak daily discharge values from 1926-1994 (Fig. 3.4). However, in general throughout the year the hydrology of the Cariboo Lake watershed is most influenced by persistent snow and glacier ice melt rather than short term peak floods. Overall, the streamflow regime of the Cariboo Lake watershed is classified as nival-glacial. The

frequency of flood activity is illustrated by the flood frequency analysis of the Cariboo River gauge. The mean annual flood (Q_{maf}) for this watershed is 389 $m^3 s^{-1}$. The Q_2, Q_5, and Q_{10} are 507 $m^3 s^{-1}$, 554 $m^3 s^{-1}$, and 594 $m^3 s^{-1}$ respectively.

The discharge record from the Quesnel River gauging station (08KH006), 50 km downstream from the Cariboo River gauging station demonstrates how peak flows have changed over time from 1939-2013. Average monthly June discharge measurements exhibit more extreme peaks and minimum discharge values from 1964-2013 compared to much more stable conditions in previous years 1940-1963 (Fig. 4.1). A two-sample t-test assuming unequal variances was conducted to compare the mean June discharges between the two-time intervals. The discharge record also indicates discharge was significantly higher from 1964-2013 (M = 653.7, SD = 137.0) compared to 1940-1963 (M = 584.4, SD = 92.2); conditions ($t(67) = 2.59$, $p < 0.01$).

4.1.2 Water Column Characteristics

To demonstrate water column conditions in Cariboo Lake at the time of core sampling, 15 water column temperature and turbidity records were collected along a longitudinal section down lake (Fig. 3.6). Although limited to a single season, these records provide background information on the summer water column stratification which controls sediment inflow mechanisms. Results from CTD location B, 0.94 km from the Cariboo River delta at a depth of 20.6 m does not exhibit thermal stratification of the water column (Fig. 4.2, B). However, CTD location B is a shallow record and does not reach below 20.6 m where most stratification occurs down-lake. Temperature stratification remains weak 2.9 km from the Cariboo River delta at CTD location G, reaching a minimum temperature of 9.4 ˚C at a maximum depth of 38.4 m (Fig. 4.2, G). Turbidity profiles from CTD location B and G, near the Cariboo River delta, illustrate the

majority of sediment inflow enters the lake as overflow with up to 20 NTU registered above 2.4 m (Fig. 4.2, B & G).

Further down-lake, in the deepest two lake basins, CTD location H was retrieved from a basin 58 m deep and CTD location I from a basin 52 m deep. The temperature profile at both locations indicate strong stratification of the water column (Fig. 4.2, H & I). The deeper basin, CTD location H 3.75 km from the Cariboo River delta, has a thermocline between 4 m and 28 m. The minimum temperature reached is 4.4 ˚C at 35.5 m. CTD location I in the second deepest basin, 5.21 km from the Cariboo River delta, indicates a thermocline between 4 and 22 m. The minimum temperature reached is 4.7 ˚C at 32 m. The turbidity profile at both locations illustrate the highest turbidity values occur as overflow with over 20 NTU's above 4 m.

In the Frank Creek basin 8.02 km from the Cariboo River delta, CTD location M reaches a maximum depth of 30.5 m (Fig. 4.3, M). A minor cooling zone is observed at a depth of 2-5 m. The lake temperature profile at this location is stratified with a thermocline ending at 23 m, and a minimum temperature of 4.6 ˚C at 30.4 m. At this location, the highest turbidity of over 20 NTU's are registered at overflow depths of < 3 m. Concentrations increase slightly at ~ 30 m suggesting the presence of some underflow currents.

In the Keithley Creek basin, CTD locations N and O are 10.5 and 11.7 km from the Cariboo River delta and reach maximum depths of 25.7 and 28.4 m (Fig. 4.3, N & O). At both of these locations the temperatures are higher at around 15 ˚C and nearly isothermal with only slight warming at the surface to 17 ˚C. Location N reaches a minimum temperature of 12.5 ˚C at 25 m and location O reaches a minimum temperature of 12 ˚C at 28.5 m. The highest turbidity values are registered as overflow with over 20 NTU's above 2 m.

Since the Cariboo Lake CTD profiles were restricted to two sampling days in July 2017, the west basin of nearby Quesnel Lake is used to characterize typical seasonal water column profiles in fall, winter and spring. The Quesnel Lake west basin is expected to have similar seasonal water column characteristics due to its close proximity to Cariboo Lake and similar physical lake size and morphology. Field investigations by Petticrew et al., (2015) from 2002-2005 observed that the Quesnel Lake west basin is dimictic with lake turnovers occurring every spring and fall. It is expected Cariboo Lake is also dimictic with turnovers occurring in spring and fall. This hypothesis is supported by summer stratification in Cariboo Lake observed in the summer of 2017 and winter ice cover from observed from satellite imagery form 1990-2017.

4.1.3 Acoustic Sedimentary Record

To determine the nature of lake bottom sediments in Cariboo Lake, 34 km of sub-bottom acoustic records were collected using a Stratabox 10 khz sub-bottom profiler (Fig. 3.5). Results from the acoustic survey ranges from coarse impenetrable sediments near the Cariboo River delta, to packages of fine silt and clay sediments, observed starting 2.5 km down-lake and continue to the end of the lake. Where acoustic penetration is not limited by coarse deltaic sediments, the acoustic profiles are inferred to represent the Late Glacial Maximum to Holocene sediment record. Sediment packages range from 10-15 m thick in deep pockets of the Cariboo River and Frank Creek Basins and thickness decreases with distance down-lake. In the Keithley Creek basin, the observable maximum sediment thickness is 4 m. Generally, across the lake, packages of fine sediment drape conformably over the underlying till/bedrock substrate alternating between lighter more transparent layers and darker more reflective layers. The six transects A – F, observed in Fig. 3.5, will be interpreted in detail in the following section.

Transect A is 1.3 km down-lake from the Cariboo River delta, reaching a maximum water depth of 37 m. Along this transect there is limited acoustic penetration, indicating significant coarse sand-grained material (Fig. 4.4). This is expected proximal to the delta due to higher energy currents of Cariboo River which bring in coarse grained sand sediments. A multiple reflector is observed 20-40 m below the surface reflector also indicating a hard sediment water interface caused by course sediments.

Transect B is 3.4 km down-lake and traverses through the sidewall of the deepest basin in the lake and reaches a maximum water depth of 55 m (Fig. 4.5). A maximum observable sediment thickness of 15 m is reached at a water depth of 55 m, the thickest sediment package observed across the lake. The north sidewall of the transect exhibits very faint sediment layering 3-4 m thick. On the south sidewall, the sediment package is thicker with 8 – 10 m of sediment accumulation. The increased accumulation of sediment on the southern sidewall is attributed to its more gradual slope. Two sharp crested v-notch channels are observed beneath the conformable sediment cap (Fig. 4.5, i and ii). These are inferred to be scour channels formed by past glacial activity that predate the overlying sediment.

Transect C is 4.4 km down-lake from the Cariboo River delta, reaching a maximum water depth of 30.6 m and a maximum sediment thickness of 11 m (Fig. 4.6). The north shoulder holds 5 m of sediment while the south side of the transect has a sediment thickness of 9 m. The sediment conforms well to the south and north sidewalls due to their low gradient. The scour channels observed in transect B are also observed in this transect (Fig. 4.6, i & ii). In the north channel (i), the layered sediments are lighter and more conformable indicating finer sediments. In the south channel (ii), the sediment layering is darker and slightly less conformable to the bedrock/till layer below.

Transect D is 5.3 km from the Cariboo River delta, reaching a maximum water depth of 49.8 m and a maximum sediment thickness of 10.8 m (Fig. 4.7). The scour channels (i and ii) are less pronounced in this transect as they appear to be mostly filled in by sediment. An increase in sediment delivery to this area of the lake is likely due to the proximity to the Frank Creek Delta (Fig. 3.5). The north sidewall is steeper than the south sidewall however both hold a similar sized sediment package, at about 3.5 m thick. The south shoulder of this transect has a sediment thickness of 8 m. The south sidewall has a sediment thickness of 3.5 m and has evidence of slumping (Fig. 4.7, iii). The sediment layers are conformable across the transect.

Transect E in the Frank Creek Basin is 7.8 km from the Cariboo River delta, reaching a maximum water depth of 43 m and sediment thickness of 4 m (Fig. 4.8). In the north end of this transect some sediment layering is observed but is not present in the south end. The less pronounced sediment layering along this transect is due to the proximity to the Frank Creek delta which brings in coarse grained material into this basin and is not penetrable by the 10 khz transducer. The south and north sidewalls of transect E have accumulated 1-2 m of sediment.

Transect F is 10.8 km from the Cariboo River delta in the Keithley Creek basin reaching a maximum water depth of 37 m (Fig. 4.9). A maximum observable sediment thickness of 4 m is observed along the deepest part of this transect. The north and south shoulders of the basin hold 1-2 m of sediment. The steep south sidewall of the basin holds about 1 m of sediment, while the more gradual north sidewall holds up to 3 m of sediment.

A sediment thickness map was developed by interpreting the thickness of the sediment package across the entire 34 km of acoustic survey (Fig. 4.10). The thickest sediment packages of 12.5-15 m observed across Cariboo Lake are located in the deepest basin. Moving down-lake from the delta the sediment thickness is gradually reduced, with pockets ranging from 7.5-10 m

in the Frank Creek basin and 2.5-5.0 m in the Keithley Creek Basin. The sediment package observed down-lake in the acoustic records is expected to be late glacial to Holocene in origin (Desloges & Gilbert, 1994; Hodder et al., 2006; Gilbert & Desloges, 2012).

4.2 Surficial Sediment Record

Analysis of sediment characteristics on surficial sediment cores collected across Cariboo Lake provide evidence of the spatial variability sediment inflow to the lake. Twenty Ekman surficial cores (E1-E20) were retrieved from Cariboo Lake following a longitudinal transect starting in the Cariboo River Delta and finishing in the most distal basin of the lake, 11.7 km from the delta (Fig. 3.7). The core lengths range from 6-12 cm thick. Fifteen cores were retrieved from the Cariboo River Basin 0.29 – 6.4 km from the delta, two cores are from the Frank Creek Basin at 7.4 km and 7.9 km, and two cores are from the most distal Keithley Creek basin at 10.5 km and 11.7 km. These sediment cores were analyzed for laminae thickness, grain size, and organic content. Results from these analyses will be discussed in the following section.

4.2.1 Annual Laminations

Several studies have utilized the thickness of annual laminations in lake bottom sediments to estimate the annual flux of suspended sediment into glacial lakes (e.g. Menounos & Clague, 2008; Heideman, Menounos, & Clague, 2015; Zolitschka et al., 2015). Rhythmic lamination of sediment is common in glacier-fed lakes and generally occurs annually (Menounos & Clague, 2008; Heideman et al., 2015). Due to the 80 kilometers that separate Cariboo Lake from headwater glaciers it was uncertain whether fine sediment production in the watershed is high enough to produce annual laminations. However, in cores E9-E15 and E18-E20, distal from river deltas, a sequence of fine-grained dark layers followed by coarse-grained lighter layers is exhibited (Fig. 4.11, B & C). Seasonal variations in river discharge and lake stratification lead to

fluctuations in the grain size of sediments transported to deep lake basins, resulting in varve formation. In the winter, when lake ice cover reduces the velocity of lake currents, fine glacially derived sediments settle to the lake bottom comprising the darker winter laminae. In the spring, larger grained sediments are deposited by the higher energy discharges of spring nival floods and are typically lighter in colour. Furthermore, the deep bathymetry of Cariboo Lake and strong thermal stratification in the summer help preserve the lamination of lake bottom sediments through decreased turbulence (O'Sullivan, 1983). Based on these watershed and lake characteristics it is typical to expect Cariboo Lake sediment laminae to occur when sediment supply is large enough.

The thickness of sediment laminae couplets were measured to provide an estimate of the spatial variability of sediment flux across Cariboo Lake. Cores proximal to the Cariboo River delta are comprised of mostly of sand grained sediments (Fig. 4.11, A). Around 2.5 km further down-lake Ekman cores E9-E15 and E18-E20 consist of an increased proportion of silt and clay resulting in distinct laminae formations, similar to those exhibited in Fig. 4.11, B & C. A decrease in maximum laminae thickness is observed from 5.6 mm, 2.5 km from the delta to 3.2 mm, 6.4 km from the Cariboo River delta (Fig. 4.12). Mean and minimum laminae thickness decrease gradually, from an average of 3.60 mm and minimum of 2.2 mm, 2.5 km from the delta to an average of 2.3 mm and minimum of 1.3 mm 6.4 km from the delta (Fig. 4.12). The overall decrease in laminae thickness with distance from the delta is expected as sediment flux typically declines with distance from the primary sediment source (Imboden & Wüest, 1995).

Ekman cores from the Frank Creek basin have coarser grained sediments and higher organic content due to their close proximity to the Frank Creek tributary delta. As a result, these

cores did not exhibit regular laminae structures and were not included in the laminae thickness results.

Ekman cores from the Keithley Creek basin exhibit some of the most well-preserved laminae structures across the whole lake (Fig. 4.11, C). The maximum laminae thickness in the Keithley Creek basin is 9.7 mm, 10.48 km from the Cariboo River delta and reduces to 7.0 mm 11.74 km from the delta (Fig. 4.12). Average and minimum values follow a more gradual decreasing trend within the Keithley Creek basin from an average of 4.3 mm and minimum of 1.8, 10.5 km from the delta to an average of 3.4 mm and minimum of 1.1 mm 11.74 km from the delta. Overall, within the main Cariboo Lake basin a decreasing trend in varve thickness is observed with distance from the main Cariboo River delta. However, laminae thickness increases within the Keithley Creek basin relative to the Cariboo Lake basin and is attributed to the additional large contributions locally from Keithley Creek.

4.2.2 Organic Content

The percent of organic material in lacustrine sediments is often inversely related to levels of erosion in the surrounding watershed, and thus can be considered a proxy for sediment delivery (Smol, 2009). Across Cariboo Lake, the average percent organics (% LOI) in surficial Ekman core bulk samples is 4.7%. The values of %LOI range from a maximum of 5.4%, 1.3 km from the Cariboo River delta and a minimum of 3.7%, 10.5 km from the Cariboo River delta (Fig. 4.13). The longitudinal variation in %LOI values down Cariboo Lake does not exhibit a systematic pattern. However, higher %LOI values are observed close to the main Cariboo River delta, potentially due to the closer proximity to allochthonous organic material introduced by high flows from the Cariboo River. Fragments of twigs were also found in Ekman bulk samples E1-E20, suggesting allochthonous organic material has an influence across the lake. The

contribution of allochthonous material across the lake likely weakens the inverse relationship between %LOI and erosion. However, the lowest %LOI value is observed in the Keithley Creek basin, proximal to the Keithley Creek delta. This suggests that erosion in the Keithley Creek headwaters may be higher than upstream of other tributaries in the northeast end of the Lake. A larger area of clear cut logging is observed in the Keithley Creek headwaters which could explain an increase in erosion leading to higher sediment delivery in this basin. The steeper and more proximal location of Keithley Creek is also a factor in higher ratios of clastic to organic matter input.

4.2.3 Grain Size

The diameter of sediment grains was measured on Ekman core samples to estimate the energy of inflow currents across Cariboo Lake. The average grain size of Ekman core sediments collected across Cariboo Lake consists of silt grains 21 µm in size. Grain size decreases exponentially with distance from the Cariboo River delta (Fig. 4.14). The largest decrease in grain size occurs between 0.3-0.8 km from the Cariboo River delta, dropping from a D_{90} grain size of 250 µm to 87.1 µm. From 0.82 - 1.8 km, there is a small increase in grain size with D_{90}values ranging from 104 -106 µm. The increase in grain size in these cores is attributed to their proximity to the Pine Creek delta. From 2.5 to 6.4 km the grain size resumes an overall decreasing trend in D_{90} from 57 µm to 20.5 µm. Proximal to the Frank Creek delta, 7.4 km down-lake, the D_{90} increases to 119 µm. In the Keithley Creek basin, the D_{90} grain size increases to an average of 64 µm.

The sediment composition of surficial Ekman cores in Cariboo Lake is 6.9% clay, 77.6% silt, and 15.5% sand on average across the lake. Near the Cariboo River delta sediments are comprised of 61% sand sized grains and past 0.55 km from the delta cores are comprised of over

60% silt sized grains (Fig. 4.15). On average, the sediment composition in the Cariboo Lake sub-basin, at the head of the lake is 7.0% clay, 89.6% silt, and 16.9% sand. In the Frank Creek sub-basin sediments are comprised of 11.2 % clay, 76.1% silt, and 12.7% sand. In the Keithley Creek sub-basin sediments are comprised of an average of 4.0% clay, 85.8% silt, and 10.2% sand. Increases in sand composition occurs down-lake proximal to river deltas. Near the Frank Creek delta, 7.35 km down-lake sand composition increases to 23.2% and near the Keithley Creek delta, sand composition increases to 12.3%.

4.2.4 Spatial Variability of Sediment Delivery

The spatial variability in varve thickness and grain size from surficial sediments across Cariboo Lake illustrate the influence of the main Cariboo River and tributary inputs on sediment delivery. The presence of twig fragments in sediment samples across the lake suggests that significant allochthonous material is transported throughout the lake likely weakening the relationship between %LOI and erosion. The massive structure of sediments and large grain size of 250 µm near the main delta confirm that the main Cariboo River is the primary source of sediment delivery to Cariboo Lake. Further down-lake tributaries are observed to have some influence on sediment delivery to Cariboo Lake. Up-lake of the Pine Creek delta at E5 the D_{90} grain size diameter is 86 µm. Next to the Pine Creek delta D_{90} grain size diameter increases to 105 µm and 106 µm at E8 and E9 (Fig. 4.14). The laminae thickness statistics also confirm a slight increase in laminae thickness proximal to Pine Creek at E9 (Fig. 4.12). Therefore, it is expected that the Pine Creek tributary is active in bringing significant sediment loads into the Cariboo Lake basin. Field surveys completed in summer of 2017 revealed evidence of hydraulic gold mining that took place upstream of this delta contributing to increased availability of sediment and active erosion along this tributary likely leading to the increased grain size

proximal to this delta. At the Frank Creek delta, grain size increases from a D_{90} of 21.5 µm up-lake of the delta to 119 µm adjacent to the Frank Creek delta. This spike in grain size illustrates that the Frank Creek tributary also brings in significant sediment loads and it at least locally significant. The disturbed nature of surficial cores around the Frank Creek delta likely result from turbidity currents and coarser grained sediment gravity currents in this area. Finally, surficial core E18 most proximal to the Keithley Creek delta exhibits a D_{90} grain size of 71 µm and only decreases slightly moving down lake to E20 which has a D_{90} of 65 µm. The Keithley Creek tributary also brings in significantly large sediment loads that are more consistently distributed throughout the Keithley Creek basin. A consistently high influx of sediment across the Keithley Creek basin is also confirmed by the increase in laminae thickness in E18-20 (Fig. 4.12). Surficial sediments distal from river deltas consist of the lowest D_{90} values from 29 µm at E11 and decreasing to 22 µm at E14 (Fig. 4.14). Thus, these regions of the lake are the most sheltered from high energy turbidity currents and contain well preserved fine clay and silt sediments. An overall decrease in varve thickness down-lake in the main Cariboo Lake basin provides evidence that secondary tributaries do not provide sufficient silt and clay suspended sediment flows to increase varve thickness across the lake. Rather, glacially derived silt and clay sediments from the main Cariboo River provide the primary source of suspended sediments to areas of the lake distal from down-lake deltas.

4.3 Temporal Record

Four vibra cores (V1, V2, V3, and V4) were retrieved from the four deepest basins of Cariboo Lake to illustrate temporal changes in sediment characteristics (Fig. 3.7). Core V1 is 3.84 m long, 3.74 km from the Cariboo River delta at a water depth of 57 m. Core V2 is 3.01 m long, 5.45 km from the delta at a depth of 52 m. Both core V1 and V2 were extracted from the

Cariboo River basin (Fig. 3.2). Core V3 is 1.95 m long collected from the Frank Creek basin and core V4 was retrieved from the Keithley Creek basin at a length of 4.15 m.

4.3.1 Sedimentology

The tops of all cores exhibit varying depths of disturbed sediment. Core V1 has ~ 11 cm, core V2 has ~7 cm and V4 has ~55 cm of disturbed sediment at its top. Sediments in the bottom of V1, V2 and V4 provide the best representation of alternating dark and light layers similar to those found in Ekman short cores (Fig. 4.16). However, the entire length of V3 was disturbed during vibra coring and exhibits multiple perforations from degassing of sediments (Fig. 4.16). The laminae in V1 and V2 are comprised of darker and finer grained sediments compared to V4 which has lighter and coarser grains throughout (Fig. 4.16). Due to the deep basin bathymetry and distance from river deltas where V1-V4 were retrieved, only clay and silt grained sediments remain suspended long enough to reach their locations. There is evidence of bottom currents bringing some sand grained sediments to V1 and V2, however these are limited to event-based turbidites.

Long core sediment analyses in this study focus on V1 and V2 for three main reasons: 1) V1 and V2 were retrieved from the deepest water depths, 2) are distal from river deltas, and 3) are comparable due to their proximity to each other. The laminae observed in V1 and V2 exhibit fluctuations in thickness down-core. On average laminae from V1 are slightly larger than V2 possibly due to the closer proximity of V1 to the Cariboo River delta. Turbidites observed in V1 and V2 do not occur frequently, seven in V1 and nine in V2, throughout both cores (Fig. 4.17). The largest event-based laminae at V1 is 1.6 cm thick (Fig. 4.18). The sediment record from V2 exhibits a larger event-based turbidite bed ~ 5 cm thick (Fig. 4.18). The timing of the turbidite events is discussed in Section 4.3.3.

4.3.2 Chronology

To determine if sediment laminae are annual in nature and to provide a rate of sediment accumulation for V1 and V2, organic materials were submitted for AMS radiocarbon analysis. A small twig from V1 at 347 cm results in a date of 1899-1819 cal BP. A 4 cm long twig from V2 at 222 cm results in a date of 490-316 cal BP. Since the first date from V2 was much younger than expected, a second sample from V2 was analyzed by combining a small twig at 286 cm and pine needle at 294 cm. A date of 2045-1895 cal BP was determined.

As in the Ekman cores, the laminae observed in V1, V2, and V4 were initially assumed to be annual in nature. The physical composition and appearance of the sediment laminae in V1 and V2 are identical to those found in the Ekman cores. A description of their appearance is in Section 4.2.3.

To test the validity of laminae as annual varves, the chronology established from counting laminae in V1 and V2 were compared to the chronology from AMS radiocarbon dating. Laminae couplets counted down-core to AMS dates resulted in 1451 layers in core V1 and 1872 layers in V2. The organic material dated for V1 was extracted at a depth of 347 cm and resulted in an AMS date of 1899-1819 cal BP. Based on manual laminae counting it is estimated this material was deposited 1451 cal BP resulting in a 368-448 year difference between the two dates. Organic material dated at V2 was extracted at 290 cm and the AMS date was 2045-1895 cal BP. The estimated date using manual laminae counting is 1870 cal BP. An 89-239 year difference is observed between the varve counting and AMS radiocarbon dates. Based on the relatively close agreement between laminae counting and AMS radiocarbon dates the initial radiocarbon date of 490-316 cal BP at a core depth of 222 cm provided for V2 is assumed to be an error as the date it is significantly younger than expected based on the sediment stratigraphy. It also suggests a

sedimentation rate of 4.53-7.03 mm/yr which is too high for the largely filtered and distal Cariboo Lake. Due to the large size of the twig it is possible that this piece of material was pulled down during core splitting resulting in an abnormally young date.

In both cores, the laminae counting date is between 89-448 years younger than the calibrated average AMS radiocarbon date. Considering the range of error in the dating techniques, there is good agreement between the dates. Due to the close correspondence between the AMS radiocarbon and laminae counting dates at V1 and V2, sediment laminae are assumed to be annual in nature (i.e. varves).

4.3.3 Varve Interpretation

Sedimentation rates for Cariboo Lake were estimated from AD 440-2017 at V1, and AD 150-2017 at V2, using both AMS radiocarbon dates and calibrated varve depths. Sections of core that did not exhibit distinct layering due to disturbance resulted in areas without varve measurements, 127 cm at V1 and 75 cm at V2 were disturbed. Average sedimentation rates were used to interpolate the time elapsed in these disturbed layers. Event-based laminae comprised of light coarse-grained material with thicknesses greater than three standard deviations above the mean were removed from the varve thickness analysis (Fig. 4.17). This was done assuming these layers represent discrete events, rather than a seasonal long interval. Varve thickness was measured for V1 and V2 following the same protocol as for the Ekman cores described in (Section 4.2.3). The sedimentation rate for V1 is 2.1 ± 0.3 mm/yr and for V2 it is 1.5 ± 0.1 mm/yr. A somewhat higher sedimentation rate at V1 is expected due to its closer proximity to the Cariboo River delta at 3.74 km compared to V2 which is 5.45 km from the delta.

Trends in down-core varve thickness illustrate fluctuations in sediment yield to Cariboo Lake from AD 440-2017 at V1 and from AD 150-2017 at V2 (Fig. 4.19, 4.20). Varve thickness

values were standardized by calculating the number of standard deviations away from the mean to better compare varve thickness with other sediment proxies, such as grain size and percent organics. Following standardization, a 25-year moving average filter was used to smooth out the thousands of noisy data points and better illustrate trends at time-scales of decades to centuries. A one-way analysis of variance (ANOVA) was conducted at V1 and V2. For V1 varve thicknesses were averaged and compared between the following groups AD 150-750, 751-1250, 1251-1750, 1751-1950, 1951-2017 (Fig. 4.20). For V2 varve thicknesses were averaged and compared between AD 450-750, 751-1250, 1251-1750, 1751-1950, 1951-2017 (Fig. 4.21).

The V1 varve thickness ANOVA exhibited statistical significance with each group comparison. The full table for each ANOVA group comparison is provided in Table A.1. The comparison of each age group to the mean is reported in the following section using the standardized departure value and statistical significance from the ANOVA results. Varve thickness at V1 from AD 440-750, is 0.53 standard deviations above the mean ($p < 0.05$, n=230). After AD 750, varve thickness remains 0.22 standard deviations above the mean until AD 1250 ($p < 0.05$, n=343). From AD 1251-1750, varve thickness stays an average of 0.40 standard deviations below the mean ($p < 0.05$, n=386). From AD 1751 to 1970, varve thickness is 0.56 standard deviations below the mean ($p < 0.05$, n=86). Overall, varve thickness at V1 demonstrates a decreasing trend from AD 440-1970 with varve thickness significantly above the mean from AD 440-1250 and significantly below the mean from AD 1251-1970.

The V2 varve thickness ANOVA exhibits statistical significance between the core mean and; AD 150-750 and AD 751-1250 (Table A.2). At V2, varve thickness is 0.29 standard deviations above the mean from AD 150-750 ($p < 0.05$, n=479). From AD 751-1250, varve thickness drops an average of 0.33 standard deviations below the mean ($p < 0.05$, n=298), and

remains below average until 1750. From AD 1751-1950, varve thickness returns to average levels with 0.04 standard deviations above the mean (*n.s.*, n=182). Varve thickness increases 0.43 standard deviations above the mean from 1951-2017 (*n.s.*, n=20). The trend in varve thickness at V2 from AD 150-1970 demonstrates a more parabolic trend compared to V1 with a shorter period of above average varve thickness from AD 150-750, followed by below average levels from AD 751-1250, and a return to above average levels from AD 1951-2017.

Overall, the trend in varve thickness down-core at V1 is observed to be linear, while the trend at V2 is more parabolic (Fig. 4.19). The observation of a linear trend at V1 and parabolic trend at V2 may result from the more distal location of core V2 from the Cariboo River delta. However, coring disturbances in the top section of the core may also have contributed to these differences.

Seven anomalously thick event-based laminae/beds were removed from the V1 varve analysis ranging from 2.7 – 15.9 mm thick (Fig. 4.17). The largest event observed at V1 was 15.9 mm and occurred at a depth of 137 cm and is estimated to have occurred around AD 1400 (Fig. 4.17, 4.18). Nine event-based layers were observed in V2 ranging from 2.3 – 47.0 mm thick. The largest event observed at V2 was 47.0 mm thick and occurred at a depth of 230.5 cm and is estimated to be AD 403 (Fig. 4.17, 4.18). A graded fining up sequence is observed in the V2 event-based layer (Fig. 4.18). The timing of these turbidite layers is not observed to be correlated between cores V1 and V2. Therefore, it is inferred that these turbidite layers are formed by isolated events, local to a single core location such as adjacent hillslope failures, turbidite side-wall slumps and/or very local debris flows.

4.3.4 Grain Size

The diameter of sediment grains was measured down-core to estimate variability in the flux of sediment transported into Cariboo Lake over time. Grain size results from V1 and V2 are reported using dates interpolated from the varve chronology analysis. Standardized departures were calculated as in the varve thickness analysis, and an ANOVA was used to compare the overall mean core varve thickness to each date group (Fig. 4.20, 4.21). Event-based layers identified in the varve thickness analysis were removed from the grain size analysis for separate analysis. The composition of sediment grains within the event-based layers were all characterised by a single mode with less than 0.01% clay, over 98% silt and less than 1% sand.

Sediments from core V1 are comprised of an average of 86% silt, 13% clay and 0.8% sand sized particles. The average D_{90}, D_{50}, and D_{10} are 25.9 µm, 7.6 µm, and 1.3 µm, respectively. The V1 AD 1398 flood layer has a D_{90} grain size of 27.2 µm and is comprised of 98.8% silt and 1.1% clay sized particles. The down-core fluctuation in grain size diameter is illustrated in (Fig. 4.22). Results from the grain size standardized departure and ANOVA test of statistical significance between each core mean and date groups are summarized in Figure 4.20 and 4.21. The most persistent stretch of above average grain size occurs from AD 440-750 where the D_{50} grain size is 0.45 standard deviations above the mean (*n.s.*, n=10). Between AD 751-1750 overall grain size dips 0.3 standard deviations below the mean (*n.s.*, n=10). From AD 1751-1950 sediment grain size increases above average 0.31 standard deviations (n.s., n=5). Grain size increases further from AD 1951-2017 to 1.40 standard deviations above the mean (p <0.05, n=5).

The composition of sediments in core V2 is 81% silt, 18% clay, and 0.5% sand sized sediments. The average D_{90}, D_{50}, and D_{10} sediment diameters are 21 µm, is 6.4 µm, and 0.9 µm, respectively. The largest flood layer in V2 occurred around AD 490 and has a thickness of 4.7

cm and is 3.9 cm thicker than any other flood layer in V2. The bottom of this flood event has a D_{90} grain size of 91 µm and is comprised of 76.2% silt and 23.8% sand. The top of the AD 490 flood event has a D_{90} of 39.5 µm and is comprised of 96.8% silt and 3.2% sand. This is the only turbidite layer in either V1 or V2 that registered > 1% sand. The down-core trend of D_{50} sediment grain diameter in V2 is similar to the trend exhibited in core V1 with the most persistent increase in grain size occurring from AD 150-750 (*n.s.*, n=13, Fig. 4.22). D_{50} dips 0.84 standard deviations below average from AD 751-1250 (*n.s.*, n=11), and remains below the mean until 1950. From AD 1951-2017 the D_{50} returns to above average levels 0.83 standard deviations above the mean (*n.s.* n=5). At both V1 and V2 a slight parabolic curve in D_{50} is observed with above average values from AD 440-750, below average from around AD 751-1750, and above average after AD 1950.

4.3.5 Percent Organics

The percent organics from cores V1 and V2 illustrates the fluctuation in the amount of organic material that reaches the lake bed from allochthonous and autochthonous sources which can be related to levels of erosion in the surrounding watershed (Fig. 4.23). To illustrate down-core trends, percent organic standardized departures were calculated, and the global mean of percent organics were compared to the mean at each date range using a one-way ANOVA (Fig. 4.20, 4.21).

Core V1 has an overall average % LOI of 4.8% and a standard deviation of 0.27. The % LOI at V1 is above average from AD 440-1250 at 0.39 standard deviations. After AD 1250, %LOI remains mostly below average. Reaching a low of 1.59 standard deviations below the mean between 1951-2017 ($p < 0.05$, n=5). Core V2 has an average % LOI of 4.8% and a standard deviation of 0.34. At V2 %LOI is also above average from AD 150-1250 at 0.31

standard deviations above the mean. Between AD 1251-1750, %LOI dips below average 0.49 standard deviations (*n.s.*, n=26), and returns back to above average levels from 1751-1950. From 1951-2017, V2 also has a low of 0.86 standard deviations below the mean (*n.s.*, n=3). The overall trend %LOI between V1 and V2 exhibits a similar pattern with above average values from AD 440-1250 and generally below average values following AD 1250. At both V1 and V2 trends in %LOI exhibit parabolic patterns at shorter time intervals of ~ 250 years compared to the parabolic trends observed in varve thickness and grain size.

4.4 Suspended Sediment Yield

Studies on suspended sediment yield (SSY) from glacier-fed sediment records give insight on the sources, production, transport, and storage of sediment between different watersheds (Hodder et al., 2006; Heideman et al., 2017). Suspended sediment yield calculated from V1 and V2 illustrates the average volume of sediment that moves through the watershed and into Cariboo Lake per year. The SSY values were calculated for Cariboo Lake using a watershed area of 3242 km^2, a lake area of 10.26 km^2, an average bulk density of 1.2 g/cm^3, and a range of sediment accumulation rates. At V1 the range of accumulation rates is 1.83 – 1.91 mm/year from the AMS radiocarbon date and 2.40 mm/year from varve chronology. For V2 the sedimentation range is 1.42 – 1.53 mm/year from the AMS radiocarbon dating and 1.52 mm/year using the varve chronology. The bulk density value used was averaged from Ekman cores in each lake basin. The SSY value is estimated in each core by first calculating the average sediment accumulation rate (AR, in $kg \cdot m^{-2}\ a^{-1}$) which is the product of the bulk density (BD, in $g \cdot cm^{-3}$) and sedimentation rate (SR, in $m \cdot a^{-1}$).

(1) $AR = (SR)(BD)$

Sediment mass (M, in $kg \cdot a^{-1}$) is calculated by multiplying the accumulation rate by the lake area (Area, in m^2).

(2) M = (AR)(Area)

Lastly the suspended sediment yield (SSY, in $kg \cdot km^{-2} \cdot a^{-1}$) is calculated by dividing the sediment mass (M, kg a^{-1}) by the catchment area (CA, in km^2).

(3) SSY = M / CA

The average SSY at V1 is 6.95-7.25 $Mg \cdot km^{-2} \cdot a^{-1}$ utilizing the AMS sedimentation rates and 9.22 $Mg \cdot km^{-2} \cdot a^{-1}$ with the varve chronology sedimentation rate. The SSY at V2 1.75 km further down lake is 5.39-5.81 $Mg \cdot km^{-2} \cdot a^{-1}$ utilizing the AMS sedimentation rates and 5.95 $Mg \cdot km^{-2} \cdot a^{-1}$ from the varve chronology sedimentation rate. A decrease in SSY might be expected at V2 as it is farther from the Cariboo River delta, leading to less suspended sediment being transported to this location. To provide an average SSY rate for Cariboo Lake these values are combined to provide an average of 6.8 ± 1.4 $Mg \cdot km^{-2} \cdot a^{-1}$. Temporal trends in SSY follow the same trends as the varve thickness plots (Fig. 4.19).

5.0 DISCUSSION

5.1 The Cariboo Lake Watershed Sediment Cascade

Determining the watershed processes that govern the production, connection and transport of sediment into Cariboo Lake is key in linking patterns observed in the temporal sediment record to past changes in watershed dynamics (Hodder et al., 2007). The following section will discuss the fluvial geomorphology of the Cariboo Lake watershed that govern sediment dynamics from source to sink.

Although the percent glacier cover is low for this watershed at 2.4%, glaciers continue to produce a large amount of fine sediments in the headwaters which are transported down-valley to Cariboo Lake. Glaciers in the northeast headwaters of the Cariboo Lake watershed transfer fine clay and silt sediments directly into the proglacial upper reaches of the Cariboo River (Fig. 3.1). The upper Cariboo River, 85 km up-valley of Cariboo Lake has a steep gradient and is braided for roughly 4 km and then transitions into a lower gradient, irregular meandering stream planform from 60 to 80 km up-valley of Cariboo Lake. The transport of sediment through the meandering sections of the Cariboo River occurs mainly through suspended load transport of clay and silt sediments (Wohl, 2014). The reduced energy of the meandering sections slightly buffers sediment transport through storage in the lateral accretion of point bars. Additional storage of silts and fine sands occurs through vertical accretion of floodplains. However, in general floodplain storage is minimal and limited to periods of overbank flows (Wohl, 2014). In the meandering reaches of the Cariboo River, upstream of Lanezi Lake, erosion of the channel bed and sidewalls is limited during high flows as energy is dissipated through overbank flows. The high cohesion of fine sediments increases the flow velocity required for entrainment, also limiting the erosion of the channel bed and sidewalls (Wohl, 2014). Additional contribution of

sediment occurs from downstream tributaries and direct hillslope contributions to the floodplain and Cariboo River. Overall, the planform of the upper Cariboo River is conducive to transporting fine glacially derived clay and silts downriver. However, connectivity is mitigated by lateral accretion and the signal is suppressed slightly by downstream delivery of non-glacially derived sediment (Wohl, 2014).

Downstream of the upper Cariboo River, Lanezi Lake and Sandy Lake are located 30 km upstream of Cariboo Lake and mitigate the delivery of fine sediments into Cariboo Lake (Fig. 3.1). The deep fjord-like nature of Lanezi Lake reaches a maximum depth of 170 m and results in a high estimated sediment trap efficiency (> 95%) due to its large storage capacity of 1.34 km^3 and upstream watershed area of 1140 km^2 (Brune, 1953). The Lanezi Lake bathymetry is flat, suggesting deep pockets have been filled through high rates of sediment delivery during the Late Pleistocene and Holocene. Sandy Lake is connected to Lanezi Lake through a narrow channel and is characterized by a much shallower lake basin bathymetry reaching a maximum depth of 6 m. The smaller storage capacity of this basin 0.03 km^3, and small additional contributing watershed area of 140 km^2 results in a smaller estimated trap efficiency of ~ 45% (Brune, 1953). According to these high estimated trap efficiencies, a large percent of the sediment transported by the upper Cariboo River is stored in these lakes reducing connectivity to downstream environments. While large amounts of sediment are stored in these lakes, significant clay and silt sediment remain in suspension and are transported out of the lake in overflow currents down-valley to Cariboo Lake. The chalky-turquoise colour of Sandy and Lanezi Lake is indicative of high suspended sediment concentrations near the surface, confirming the suspended sediment load transport of some glacially derived clay and silt sediments to the Cariboo River downstream (Fig. 5.1).

Downstream of Lanezi Lake and Sandy Lake, the Cariboo River continues with a primarily irregular meandering planform, with some anabranching where the river is separated into multiple channels by vegetated islands (Fig. 5.1). Sediment transport mechanisms are similar to the upper Cariboo River with mainly suspended load transport. The overall gradient of this section of the Cariboo River is lower than the upper section contributing to a slight increase in storage of sediment through lateral and vertical accretion of the floodplain. The steepness of hillslopes along the lower Cariboo River is greatly reduced, lowering the influence of direct hillslope sediment contributions (Fig. 3.1). In the last 10 km of the river, immediately above Cariboo Lake, the gradient decreases further resulting in decreased wavelength and increased amplitude of meanders (Fig. 5.1). Scroll bars are observed in this section of the river indicating an increase in sediment storage through more rapid lateral accretion of point bars. The similar water colour of this section of the Cariboo River to the upper Sandy and Lanezi Lake confirm significant fine silts and clays remain in suspension and are transported down-valley to Cariboo Lake (Fig. 5.1).

The terminus of the lower Cariboo River is marked by a slow transition from meandering river planform into an alluvial delta characterized by increased sediment deposition (Fig. 5.1). The delta leading into Cariboo Lake is elongated and river-dominated. The Cariboo River delta is approximately 2.2 km long and 1.2 km wide and stores a significant quantity of sand in the distal margin with gravel in the upper delta channel. An increase in storage of coarse grained sediments occurs in this zone. However, clay and silt sediments that remain in suspension will enter Cariboo Lake and are transported down lake through overflow, interflow, and underflow currents depending on the seasonal stratification of the lake.

To summarize, the mechanisms in the cascade of sediments from source to sink in the Cariboo Lake watershed lead to a low overall sedimentation rate in Cariboo Lake with a slight reduction in connectivity to headwater sediment production. Significant sediment trapping by Sandy Lake and Lanezi Lake greatly reduces the amount of sediment delivered into Cariboo Lake. However, it is evident that significant amounts of fine glacially derived suspended sediment is transported into Cariboo Lake. The largely meandering planform of the Cariboo River is conducive to the transport of fine clay and silt sediments down-valley to Cariboo Lake. According to these watershed processes, changes in sediment delivery observed in Cariboo Lake are related to environmental changes in both the immediate upstream section for the coarse fraction and whole watershed for part of the fine fraction.

5.2 Patterns of Sediment Delivery into Cariboo Lake

Analysis of lake sediment deposits across Cariboo Lake indicate the spatial variability in sediment delivery to the lake. Findings from water column observations, sediment acoustic records, and analysis of surficial sediments confirm that deep basins (> 50 m deep) contain up to ~15 m of fine sediments, delivered throughout the late Pleistocene and Holocene. A decrease in the sediment package thickness, grain size, and varve thickness is observed with distance away from the main Cariboo River delta suggesting that the Cariboo River is the primary source of fine sediments to distal parts of Cariboo Lake. Sand makes up less than 1% of the composition sediments in deep lake basins proximal to surrounding tributaries, suggesting sediment delivery by down-lake Pine Creek, Frank Creek, and Keithley Creek deltas is limited to mostly gravel and sand lake-margin deltas (Fig. 3.1). Water column and acoustic observations indicate that proximal to the delta, sediments from the Cariboo River enter mainly as overflow and underflow currents. Further down-lake, overflow currents are the dominant source of sediment from the

main Cariboo River which settle out and conform well to the basin bathymetry. Deep pockets in the Cariboo Lake bathymetry have not been leveled out by high sediment accumulation rates throughout the late Pleistocene and entire Holocene which indicates that sedimentation into Cariboo Lake has been low during this time. According to these findings, it is expected that sediment accumulation in Cariboo Lake has been mainly been delivered from the Cariboo River by overflow currents throughout the Holocene.

5.3 Long Term Sediment Record

Studies on varved glaciolacustrine sediment cores from lakes distal to glacial activity sometimes demonstrate that temporal patterns in the sediment record relate to environmental changes at low temporal resolutions with very limited stratigraphic distinctions (Souch, 1994; Menounos et al., 2009). Sediment cores V1 and V2, from Cariboo Lake exhibit continual formation of varves throughout the past two millennia. Fluctuations in down-core sediment characteristics reveal distinct, but small, seasonal trends in varve thickness, grain size, and %LOI. The variation of these laminations is very noisy at annual timescales so to enhance the signal, trends were extracted from a moving average of 25 years from AD 250-2000 in Fig. 5.2, and a five-year filter for Fig. 5.3 to reveal more systematic fluctuations in sediment characteristics. Trends at 250-500 years are generally synchronous between cores V1 and V2 and between sediment yield metrics. From AD 250-750 at V1 and V2 an increase in sediment yield is observed through above average D_{50} and above average varve thickness. However, %LOI is above average indicating possibly reduced sediment yield, assuming constant organic input. From AD 750-1250, a slight decrease in sediment yield is observed with below average D_{50} at V1 and V2, average varve thickness at V1, below average varve thickness at V2, and above average %LOI at V1 and V2. From AD1250-1750, D_{50} increases to average levels at V1 and V2

indicating an increase in sediment yield, however %LOI and varve thickness at V1 and V2 exhibit less consistent trends during this time period. From AD 1750-1950 an increasing trend in D_{50} is observed at V1 and V2, varve thickness is below average at V1 and slightly above average at V2, and %LOI fluctuates around the mean at V1 and V2. Sediment metrics at V1 and V2 are less robust from AD 1950 to present due to the disturbed top sections of the cores (Fig. 5.3). This leads to a less robust sediment yield record during this time. Still, the sediment yield record from V1 and V2 indicates an increase in overall sediment delivery through increased D_{50}, varve thickness, and decreased %LOI from AD 1950 to present.

Overall, grain size and varve thickness present the most consistent record of sediment yield from AD 250-1750 (Fig. 5.2). During the same time period %LOI presents a less consistent record as occasional opposite trends in sediment yield are observed. The weak relationship between %LOI and sediment yield in Cariboo Lake may be due to low autochthonous organic production within the lake. Moreover, small allochthonous twig fragments were also observed in the V1 and V2 sediment samples which further reduces the relationship between %LOI and erosion. Other discrepancies observed in sediment yield metrics between V1 and V2 from AD 250-1750 could be attributed to differences in sediment delivery to the two coring locations. Sediment focussing outlined in section 2.3.3, and complexities in the relationship between lake sediments and watershed signals outlined in section 2.5, likely lead to slight differences in sediment delivery between these two locations. This translates into differences in sediment characteristics observed down-core. From AD 1750-1950 more inconsistencies are observed between grain size, varve thickness, and %LOI and is likely attributed to the increase in core disturbances in the top section of the cores caused during coring procedures (Fig. 5.3). The correlated increase in sediment yield through increased grain size and decreased %LOI observed

after AD 1950 in Fig. 5.3 could be attributed to an increase in sediment availability following the introduction of logging, mining activities, and anomalous glacier retreat after AD 1850 (Menounos et al., 2009).

Around AD 1850, the Cariboo Gold Rush introduced hydraulic mining activity into the Cariboo Lake watershed. Large landslides caused by this hydraulic mining activity introduced large amounts of sediment into Cariboo Lake at the Pine Creek delta (Fig. 3.2). Observations of tree stumps broken off at heights of 1-3 m from one large landslide were confirmed by field observations completed in summer of 2017 (Fig. 5.4). Significant deforestation also took place during this time period surrounding Cariboo Lake which may have also contributed to an increase in erosion increasing sediment yield in Cariboo Lake. Furthermore, in the headwaters of the watershed, significant stores of glacially derived sediment were uncovered during the retreat from maximum LIA glacier extents which also would have contributed to increased sediment yield from AD 1850 to present (Maurer et al., 2012).

These events occurring from AD 1850 to present, outline the increase in complexity of the sediment environment which contribute to the difficulty in attributing causes to climate driven sediment yield changes into Cariboo Lake during this time. In addition, the increasing trend of grain size and decreasing trend of %LOI observed in the Cariboo Lake sediment record from AD 1950-present is limited to four to five data points for both grain size and %LOI in each core (Fig. 5.3). Moreover, the more recent varve thickness record from AD 1950-1970 also does not indicate a robust record due to core disturbances in sections of V1 and V2 (Fig. 5.3). Therefore, the strongest evidence provided by the Cariboo Lake sediment record is from AD 250-1750 where fluctuations in the fine sediment cascade is more related to climate driven environmental changes and sediment metrics between V1 and V2 are better correlated (Fig. 5.2). In summary,

evidence from the Cariboo Lake temporal record indicates an increase in sediment yield from around ~AD 250-750. This is followed by a declining trend in sediment yield until around ~AD 1250, afterward sediment yield generally stabilizes back to average levels from ~AD 1250-1750. An increase in sediment yield is observed from ~AD 1750-present, however the evidence is less robust.

5.4 Comparison to Regional Glacier Records

The pattern and timing of trends in glaciolacustrine sediment records to fluctuations in climate and glacier activity have been compared in studies on glacial lakes across British Columbia and Alberta (e.g. Dirszowsky & Desloges, 1997; Menounos et al., 2008; Menounos et al., 2009; Maurer et al., 2012; Heideman et al., 2015; Solomina et al., 2016). Generally, studies illustrate an increase in clastic sediments during cool periods such as the First Millennial Advance around AD 200-700 and Little Ice Age Advance (LIA) around AD 1500-1900 (Menounous et al., 2009). Glaciers produce large amounts of fine sediment in alpine watersheds during times of maximum extent and during initial retreat (Harbor and Warburton, 1993; Desloges & Gilbert, 1994; Menounos et at., 2009). As a result, periods of high percent ice cover are often associated with high down-valley sedimentation rates due to increased area of subglacial erosion leading to a large production of finely ground sediments (Hodder et al., 2006; Heideman et al., 2017). However, the relationship between watershed dynamics and lake sedimentation rates is complex due to several external forces acting on the location, connection and transport of sediment (Hodder et al., 2007). Process-based interactions between various systems such as climate, glaciers, geomorphic setting, lacustrine, fluvial, and terrestrial biologic systems lead to this complexity. These systems have a varying degree of control on the location, connection, and transport of sediment, often resulting in an attenuated relationship between

expanded glacier extent and increased sediment yield (Hodder et al., 2007). Still, several studies on glacial lakes have exhibited similar response in the pattern and timing of sediment yield where periods of glacier retreat and rapid recession produce the highest load (Desloges & Gilbert, 1994; Hodder et al., 2007; Menounos et al, 2008; Maurer et al., 2012).

The earliest period of increased sediment yield in Cariboo Lake is indicated by an increase in grain size and varve thickness beginning around AD 250 and ending AD 750 (Fig. 5.2). An increase in sediment yield during this time is also supported by a rise in clastic sediments into On-Off Lake from AD 100-300 in the northeast headwaters of the Cariboo Lake watershed (Fig. 3.1, Maurer et al., 2012) and into Chephren Lake around AD 550 in the Rocky Mountains (Dirszowsky & Desloges, 1997). This time frame of increased sedimentation coincides to periods of glacier advance and subsequent recession following the First Millennial advance (Menounos et al., 2009). Evidence of this glacier advance in interior British Columbia and Alberta is provided by dated stumps from the Peyto Glacier moraine and Cavell Glacier dated to AD 30-440 (Luckman et al., 1993). After the First Millennial advance, evidence from On-Off Lake exhibits an increase in organic content and a decrease in extent of the Castle Creek Glacier from AD 300-500 (Fig. 5.2; Maurer et al., 2012). After the short period of decreased glacial activity, an expansion of the Castle Creek Glacier back into the Cariboo Lake watershed and rhythmically laminated silt and clay sediments in On-Off Lake begin around AD 500-600 (Maurer et al., 2012). The expansion and retraction of glaciers in the Cariboo Lake watershed from AD100-600 could explain why sediment yield remains high in the Cariboo Lake sediment record from AD 250-750. The response of On-Off Lake to the ice retreat from AD 300-500 warm period is indicative of ice proximal lakes showing a more direct connection with glacier activity. While

more distal lakes such as Cariboo Lake exhibit a watershed wide, regional, response and thus did not record, in detail, a strong decrease in sediment yield during this time.

A decrease in sediment yield from AD 750-1250 is observed in the Cariboo Lake sediment record (Fig. 5.2). However, findings from Maurer et al., (2012) in On-Off Lake exhibit rhythmically laminated silt and clay sediments that continue from AD 500 to present. Moreover, a tree trunk with intact roots dated to AD 1040-1160, located 230 m from the LIA moraine limit suggests that glaciers in the Cariboo Lake watershed remained near LIA extents from AD 500-present. Explanations as to why sediment yield in Cariboo Lake decreased around AD 750-1250 while glaciers remained near their LIA maximum extent could be indicative of a brief period of warming as indicated by Trouet et al., (2013) around the Medieval Warm Period AD 750-1100. This warming may have not reduced glacier extent enough to bring the high elevation Castle Creek Glacier behind the hydraulic divide thus limiting sediment supply to On-Off Lake. However, a small retreat of glaciers across the Cariboo Lake watershed may have occurred during the prolonged Medieval Warm Period leading to reduced sediment supply down-valley to Cariboo Lake from AD 750-1250. A decrease in glacier extent during this time is also supported by reduced sediment yield in Chephren Lake from AD 650-1400 also indicates decreased glacial activity in the nearby Rocky Mountains during the Medieval Warm Period (Dirszowsky & Desloges, 1997).

The return higher of sediment yield to Cariboo Lake back to average levels around AD 1750 coincides with the beginning of the LIA period (Menounos et al., 2009). Evidence of the beginning of the LIA is provided in the Rocky Mountains, where high sediment yield begins around AD 1450-1500 in Moose Lake (Desloges & Gilbert, 1995) and around AD 1465 at Chephren Lake (Dirszowsky & Desloges, 1997). Lakes in the Coastal Mountains exhibit an

earlier LIA sediment signal around AD 1090 (Osborn et al., 2007). Differences in the timing of sediment signals from the Coastal, Interior, and Rocky Mountain lakes are attributed to differences in regional temperature and precipitation and the timing of glacier expansion (Menounos et al., 2009). Additional evidence of the LIA period in the Cariboo Lake sediment record is provided by the estimated dates of turbidite event layers. The timing of turbidite layers were not found to be correlated between V1 and V2 however, the majority of the turbidites occur after the start of the LIA around AD 1200 (Fig. 4.17). An increase in turbidite events post AD 1200 is indicative of a more erosional environment expected during the LIA period (Menounos et al., 2009).

Evidence form the Cariboo Lake sediment record indicates that sediment yield remains around average from AD 1750-1950, and an increase in sediment yield is observed post AD 1950. Corroborated evidence from dendroglaciology and lichenometry show that glaciers reached maximum extents between AD 1840-1845 in the Rocky Mountains (Luckman et al., 1999) and AD 1880-1890 in the Cariboo Lake watershed (Maurer et al., 2012). Historical photographs also show glaciers near LIA maximum moraines during the first half of the 1900s in both the Rocky Mountains and Cariboo Lake watershed (Beedle et al., 2015). During the LIA, grain size is observed to be above average and %LOI is below average in Cariboo Lake which is indicative of higher sediment yield (Fig. 5.3). Reduction in glacier extents, starting around AD 1900 in this region would have exposed significant stores of fine sediments which could have contributed to the increase of sediment yield in Cariboo Lake after this time period (Heideman et al., 2017).

Overall, fluctuations in the sediment record from Cariboo Lake respond slowly to various periods of climate change. The response lag to the First Millennium and LIA advances is likely

attributed to the reduced connectivity of Cariboo Lake to headwater glacier activity leading to the low sedimentation rate in Cariboo Lakes. This leads to a buffered response to changes in watershed activity during warm and cool periods. In general, the Cariboo Lake sediment record provides evidence that sediment delivery to distal glacial-fed lakes responds less quickly, and over longer time periods compared to lakes proximal to headwater glacier activity.

5.5 Comparison to Regional Climate Records

Fluctuations in sediment yield in Cariboo Lake generally coincide with warm and cool periods represented in the regional climate record from the Interior and Rocky Mountains (Fig. 5.2). The increase in sediment yield between AD 250-750 and AD 1900 observed in Cariboo Lake in Fig. 5.2 coincides with periods of below average temperature in the reconstructed tree-ring and pollen climate record during the First Millennial advance (Luckman & Wilson, 2005; Viau, Ladd, & Gajewski, 2012; Trouet et al., 2013). The transition into a declining trend in sediment yield from AD 750-1250 could be attributed a warm period described in Trouet et al., (2013) occurring from AD 750-1000. A more recent climate proxy record from AD 1073-1983 is provided by Luckman & Wilson, (2005) based on a tree ring reconstruction of temperature anomalies in the Rocky Mountains. This record demonstrates that temperatures were mostly 1 ˚C below average during the past millennium. The increase in sediment yield in Cariboo Lake back to mostly average levels from AD 1250-1750 could be attributed to this cooling period (Luckman & Wilson, 2005; Trouet et al., 2013). The more general pattern of sediment yield in Cariboo Lake is likely also affected by factors other than glacier extent. Variations in snowpack during warm and cool periods largely influence discharge to Cariboo River and its tributaries which results in alterations in sediment delivery to Cariboo Lake. For example, during cool

periods an increase in snowfall would lead to greater snowpack accumulation leading to more intense spring runoff and hence higher discharge and SSY.

Effects of climate change often has immediate impacts on the glaciated headwaters, however implications for downstream environments are attenuated over longer time spans (Souch, 1994; Desloges & Gilbert, 1995; Leonard & Reasoner, 1999; Menounos, 2006a). While these changes occur over longer time scales, results from this study demonstrate effects of glacier retreat can have far reaching effects to down-valley environments.

5.6 Comparison to Regional Suspended Sediment Yield Records

Suspended sediment yield from the Cariboo Lake watershed is based on the glaciolacustrine sediment record in Cariboo Lake producing an average of 6.8 ± 1.4 $Mg \cdot km^{-2} \cdot a^{-1}$. The suspended sediment yield (SSY) value estimated for Cariboo Lake is lower compared to many glacier-fed lakes across British Columbia (Hodder et al., 2006; Menounos et al., 2006; Heideman et al., 2017). Observed SSY values in other glacier-fed lakes range from 33 to 220 $Mg \cdot km^{-2} \cdot a^{-1}$ in the Rocky Mountains and from 60 to 380 $Mg \cdot km^{-2} \cdot a^{-1}$ in the Coastal Mountains (Hodder et al., 2006). A lower SSY value in Cariboo Lake compared to other British Columbia glacial lakes is expected due to an overall low glacier cover and reduced connectivity to the sediment production zone in the headwaters. This leads to less sediment production and transport to Cariboo Lake. Several studies across British Columbia and Alberta have demonstrated that SSY increases with basin area (Hodder et al., 2006; Menounos et al., 2006; Heideman et al., 2017). Cariboo Lake fits well below the envelope curve of SSY which is explained in part by low ice cover and a dryer climate compared to the other sites in this study (Fig. 5.5). A trend between SSY and percent area of glacier cover has also been demonstrated in Hodder et al., (2006). The Cariboo Lake SSY value plots in the lowest range of data (Fig. 5.6). The low SSY

value observed in the Cariboo Lake Basin is attributed to three main factors that govern sediment production, transport and storage: 1) the sediment trapping of up-valley Lanezi and Sandy lakes 2) reduced glacier cover and a warmer and drier climate compared to the large number of Coastal Mountain and higher elevation Rocky Mountain sites in this comparison (Hodder et al., 2006) and 3) the true watershed area for Cariboo Lake is estimated to be smaller as the source of fine sediments to Cariboo Lake are primarily derived from a small area in the glaciated headwaters.

6.0 SUMMARY and CONCLUSION

6.1 Summary of Findings

This study presents a spatial and temporal exploration of the glaciolacustrine sediment record from Cariboo Lake, located in eastern central British Columbia. Numerous studies have looked at the correlation between sediment yield and previous climate changes (e.g. Dirszowsky & Desloges, 1997; Hodder et al., 2006; Menounos et al., 2009; Maurer et al., 2012; Heideman et al., 2017). However, these studies have largely focused on watersheds with high percent ice cover in the Coastal and Rocky Mountains. Findings from this study demonstrate that the distal glacier-fed Cariboo Lake, located in the Interior Mountains, provides an attenuated proxy of climatic and geomorphic change.

Analysis of the Cariboo Lake watershed fluvial geomorphology indicates sufficient connectivity is present between fine sediments derived in the glaciated headwaters and down-valley Cariboo Lake. Braided river channels in the steep headwaters provide efficient transfer of clay and silt sediments derived by headwater glaciers to down-valley meandering reaches where suspended load transport of clay and silt sediment remains high. Lanezi Lake and Sandy Lake also provide important sediment sinks. However, significant transfer of suspended sediments down-valley to Cariboo Lake occurs through overflow currents along the epilimnion of Lanezi and Sandy Lake. These up-valley fluvial and lacustrine sinks contribute to a filtered signal of climate change observed in the down-valley Cariboo Lake sediment record.

Findings from sub-bottom acoustic transects and analysis of surficial lake bottom sediments indicate that sediment supply to Cariboo Lake is primarily provided by suspended sediments from the main Cariboo River. Other sediment sources are also considered to be of some importance such as sidewall tributaries and hillslopes which introduce coarse grained

sediments, generally limited to the perimeter of the lake. Suspended clay and silt sediments that settle in bathymetric holes over 50 m in depth were found to be relatively undisturbed and consisted of the annual varve laminations. The formation of undisturbed varves is likely facilitated due to high production of silt and clay sediments in the glaciated headwaters, sediment connectivity to headwater sediment stores, the fjord like bathymetry of Cariboo Lake, and the annual stratification of the water column.

Analysis of grain size, varve thickness and %LOI on the Cariboo Lake sediment record exhibit patterns that coincide with fluctuations in the regional record of glacier extent and climate for the southern Interior and Rocky Mountains from AD 250-1750. Above average sediment yield is observed from AD 250-750 which corresponds with cooling during the First Millennial advance that led to increased glacier extent and winter snow pack increasing the production and transport of sediment to Cariboo Lake (Menounos et al., 2009; Maurer et al., 2012). A decline in sediment yield is observed from AD 750-1250 coinciding with the Medieval Warm Period, which reduced regional glacier extent and winter snowpack (Trouet et al., 2013). Following the Medieval Warm Period, the LIA brought below average temperatures along with regional glacier expansion from AD 1100-1900 which likely contributed to the rise in sediment yield in Cariboo Lake from AD 1250-1750 (Menounos et al., 2009; Trouet et al., 2013; Solomina et al., 2016). An increase in thick turbidite layers post AD 1200 in the Cariboo Lake sediment record also indicate an increase in sediment delivery to Cariboo Lake during this time. After AD 1900, sediment metrics from the Cariboo Lake record indicate an increase in sediment yield until present time. However, this evidence is not as robust due to core disturbance and complexity of the sedimentary environment due to human activity during this time.

Previous studies on glacial-fed lakes that focused on lakes proximal to glacier activity with higher sediment accumulation rates, indicate there is correlation between glacier activity and lake sediment yield (e.g. Desloges & Gilbert, 1994b; Menounos et al., 2005; Hodder et al., 2006, 2007; Heideman et al., 2017). The Cariboo Lake sediment record presented in this study demonstrates that distal glacier-fed lakes reveal trends in sediment yield related to catchment wide activity. These results support findings from Hodder et al., (2006) and Heideman et al., (2017) which demonstrate that distance from glacier sources, filtering, and the size and extent of glaciers control lake sediment sensitivity. The correlation of sediment yield in Cariboo Lake to the First Millennium Advance, Medieval Warm Period, and Little Ice Age reported in several other studies illustrates the sensitive nature of alpine watersheds to changes in regional climate and how these adjustments propagate to down-valley areas (Dirszowsky, 2004; Hodder et al., 2007; Menounos et al., 2009; Maurer et al., 2012; Heideman et al., 2017). Although 80 km from glacial activity, sediment delivery to Cariboo Lake over the past two millennia has remained high enough to form laminated varves. This indicates that sediment delivery from glaciers and other sources into Cariboo Lake watershed remained high enough to continue significant production of sediment over the late Neo-glacial period. Periods of reduced glacier extent during warm periods such as the Medieval Warm Period in the Cariboo Lake watershed may not have been long enough to fully deplete sediment stores throughout the watershed, resulting in the continual formation of laminations throughout. It would be expected that the formation of varves may have stopped in during longer periods of glacier recession such as during the early Hypsithermal period of the Holocene where glaciers retreated for longer millennial-scale time periods (Menounos, 2009).

Current climate change is projected to surpass previous temperature increases such as the Medieval Warm Period, leading to more extreme reductions in glacier extent and winter snowpack that has been observed in the past 11,000 years (IPCC, 2014). Over the past century, a large reduction in glacier extent and volume has been reported in the Cariboo Mountains in response to contemporary climate change (Menounos et al., 2009; Beedle et al., 2015; Mood & Smith, 2015). Projections of future glacier retreat is expected to continue with peak glacier recession occurring between 2020-2040 leading to few glaciers remaining in the Interior and Rocky Mountains by 2100 (Clarke et al., 2015). As glacially derived sediment stores are depleted in the Cariboo Lake watershed headwaters, following glacier retreat from 2050-2100, it is expected sediment yield to Cariboo Lake will drastically decline leading to the cessation of varve formation in Cariboo Lake. However, due to the filtering effects of the Cariboo Lake watershed presented in this study, these changes may take some time to be observed in distal glacial environments. Beyond the decline in sediment delivery to downstream environments, additional implications of glacier loss for the region of eastern central British Columbia include impacts on local aquatic ecosystems, agriculture, forestry, alpine tourism, water availability, and hydroelectric energy production (Matthews, Olaf Dahl, Nesje, Berrisford, & Andersson, 2000; Berthier, Schiefer, Clarke, Menounos, & Rémy, 2010; Clarke et al., 2015).

6.2 Possibilities for Future Work

Increasing pressure to understand how various environments respond to climate fluctuations has been brought on by the ramping up of climate change over the past half century. Several researchers have focused on understanding how glaciated watersheds respond to fluctuations in climate across the Coastal, Interior, and Rocky Mountains. However, some key tasks remain:

1. The up-valley Sandy and Lanezi lakes, which are less disturbed by human activity present an interesting opportunity to capture a more contemporary but higher resolution sediment record.
2. Additional investigations to retrieve better preserved sediment cores 25-50 cm in length would fill in the gap of the disturbed core captured in this study from AD 1850-present. A high-resolution record that overlaps the instrumental record may allow for development of transfer relations between current and past climates.
3. A paleo-climate record such as a tree-ring, ice core, or pollen analyses along the foothills of the Cariboo Mountains, would allow for the differences in temperature and precipitation patterns to be compared between the Coastal, Interior and Rocky Mountains.
4. Field investigations on glaciers currently active within the Cariboo Lake watershed have not been completed. These glacier forefields could provide additional dendrochronological material to provide a more definite timing of glacier extent in this region.
5. While the sediment record of Cariboo Lake is correlated to past climate anomalies, more research is needed on the process-based relationship outlined by Hodder et al., (2007) to attribute a direct causal relationship between distal glacier-fed sediment records and climate.

Figures

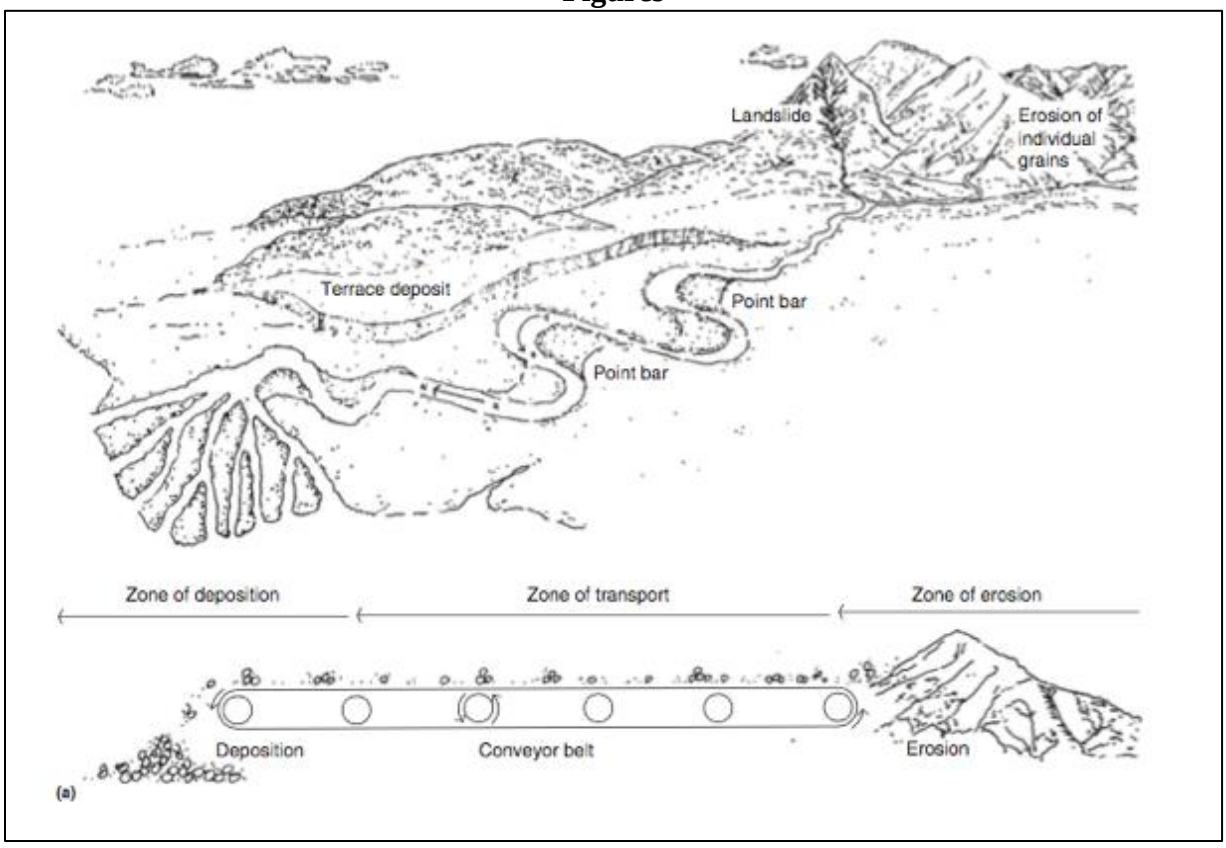

Figure 2.1: Watershed process domains and river morphology (Whol, 2014)

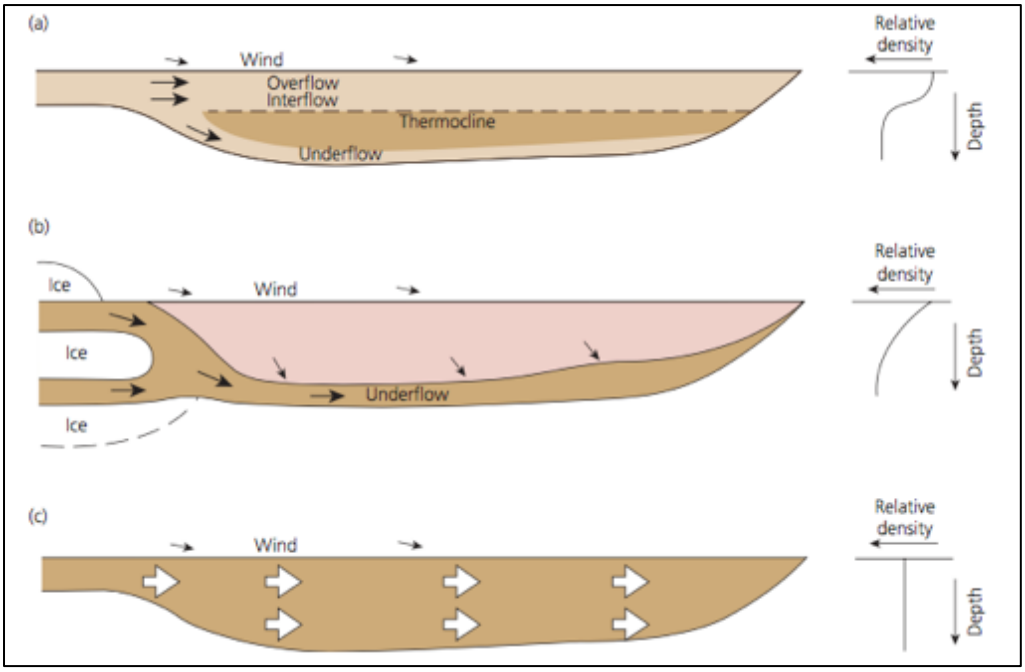

Figure 2.2: Inflow of meltwater and resulting height of flow depending on density of inflow and lake (Smith & Ashley, 1985). (A) River inflow into a stratified lake. (B) River inflow in an ice-contact lake with limited thermal stratification. (C) River inflow in an unstratified lake.

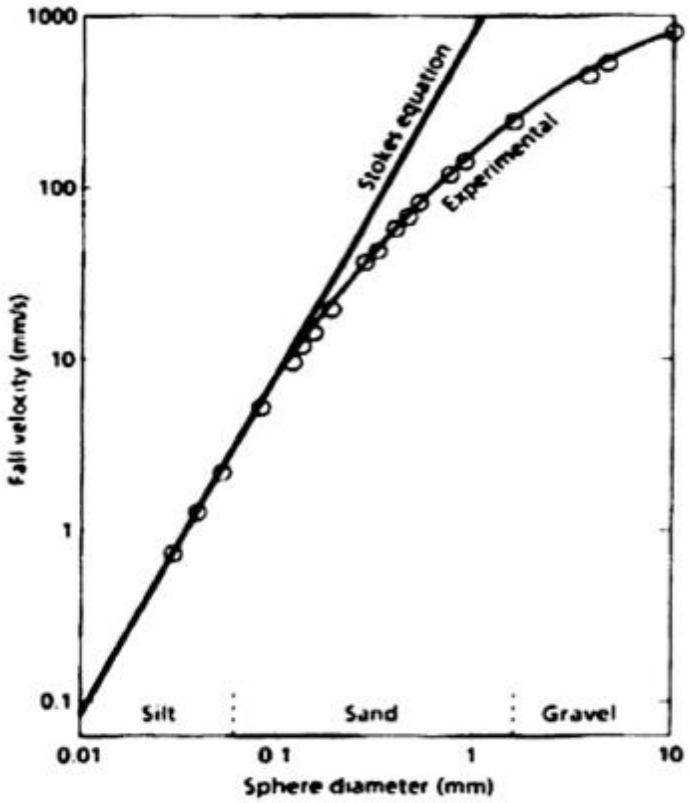

Figure 2.3: Relationship between fall velocity and sediment diameter predicted by Stokes law and experimental results in fresh water at 20˚ C (Leeder, 1999)

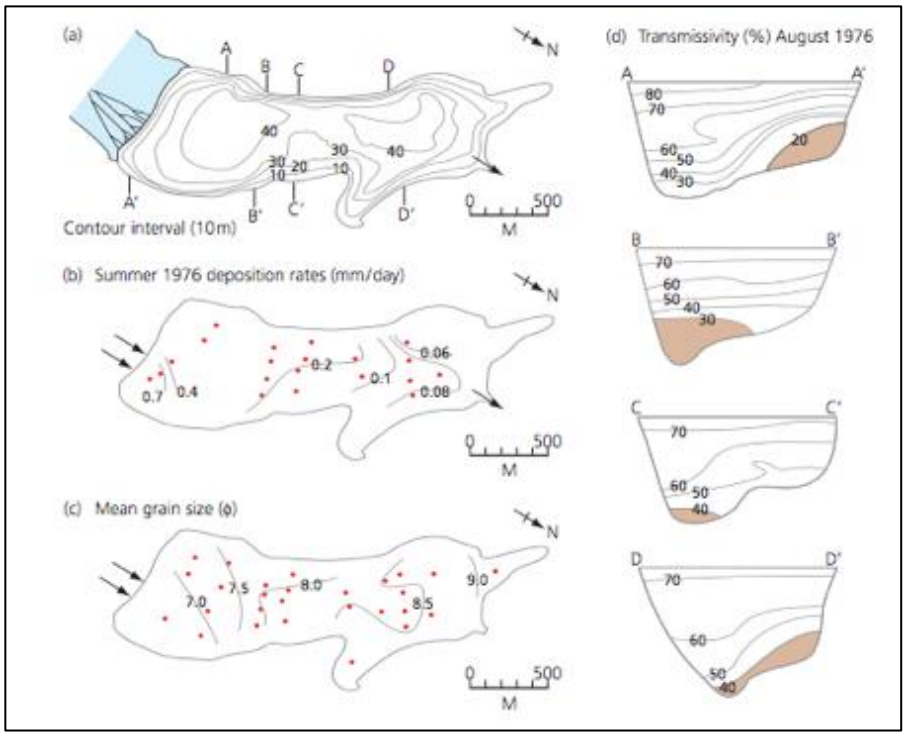

Figure 2.4: Transmissivity profile of Lake Louise, Alberta demonstrating the deflection of incoming currents to the right of forward motion. Transmissivity is a proxy measure of suspended sediment concentration (Smith & Ashley, 1985)

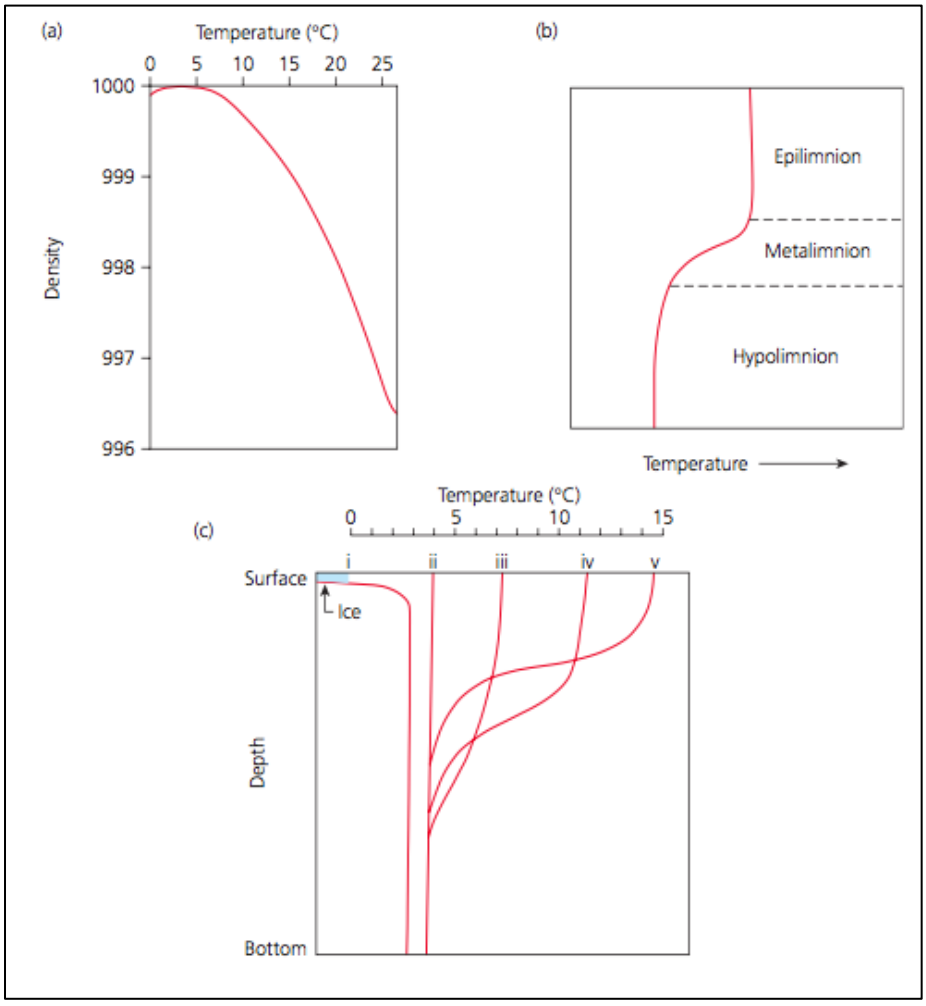

Figure 2.5: Temperature characteristics of lake water. (a) Relationship between temperature (˚C) and density (kg m^{-3}) for pure water. (b) Temperature profile resulting from surface heating and wind mixing. (c) Hypothetical evolution of the thermal structure of a deep lake between. (i) midsummer and (v) winter. Curve (iv) shows isothermal conditions resulting from lake overturn in autumn and spring (Ben & Evans, 2010).

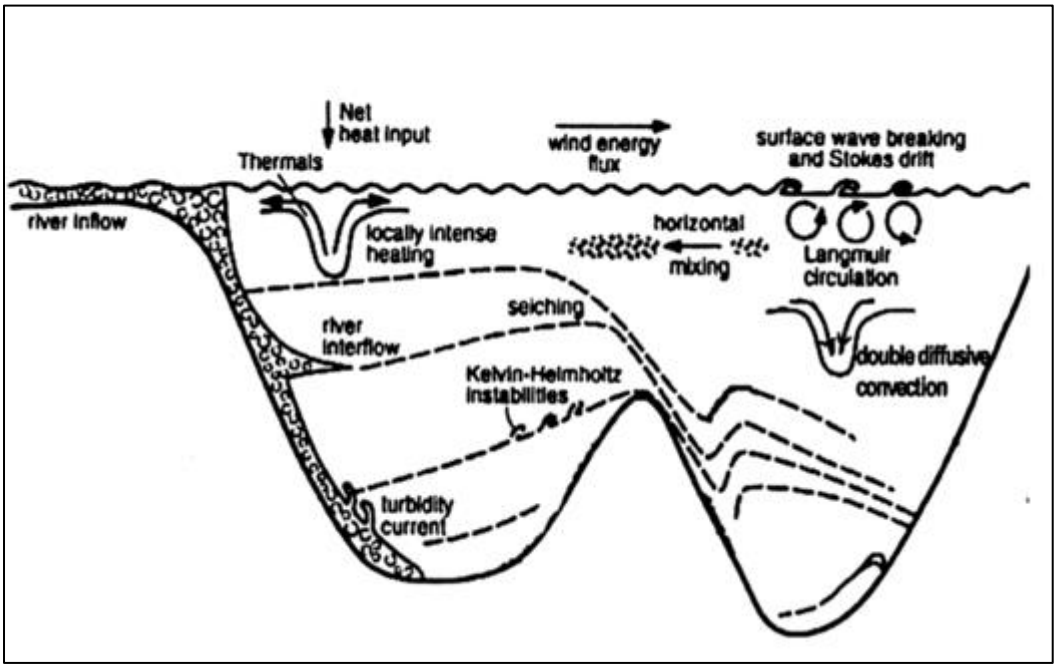

Figure 2.6: Overview of mixing processes in lakes (Imboden & Wuest, 1995)

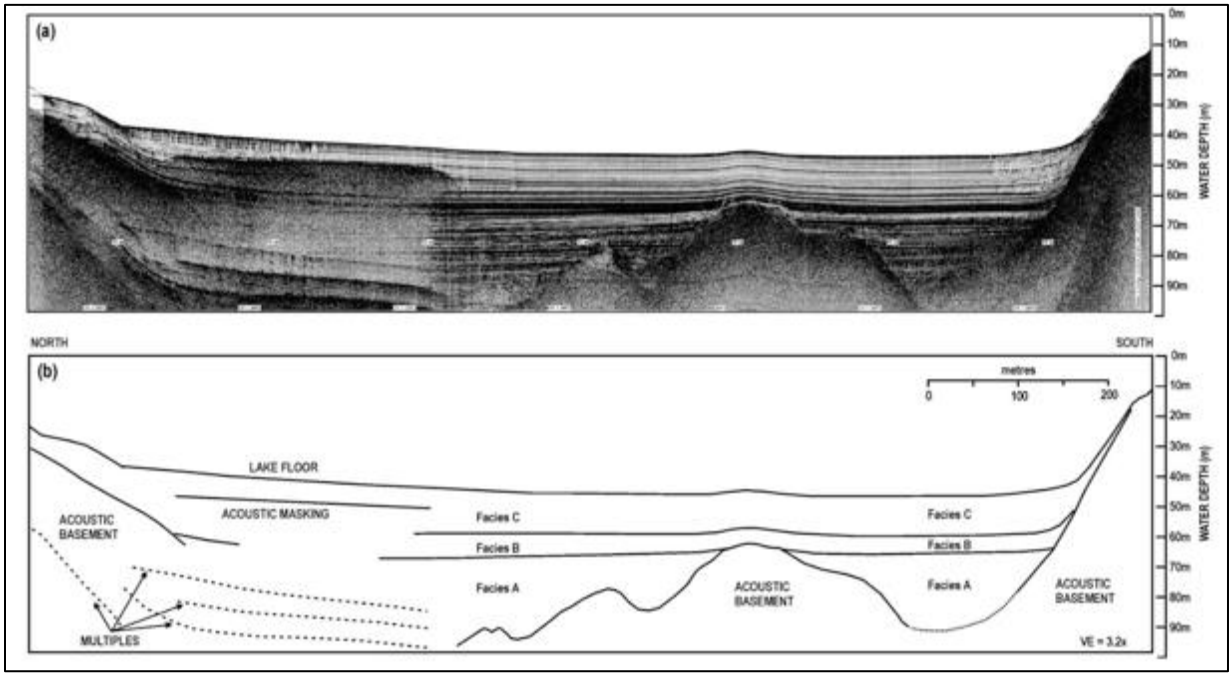

Figure 2.7: Mud Lake distal basin sub-bottom acoustic record from Hodder et al., (2006).

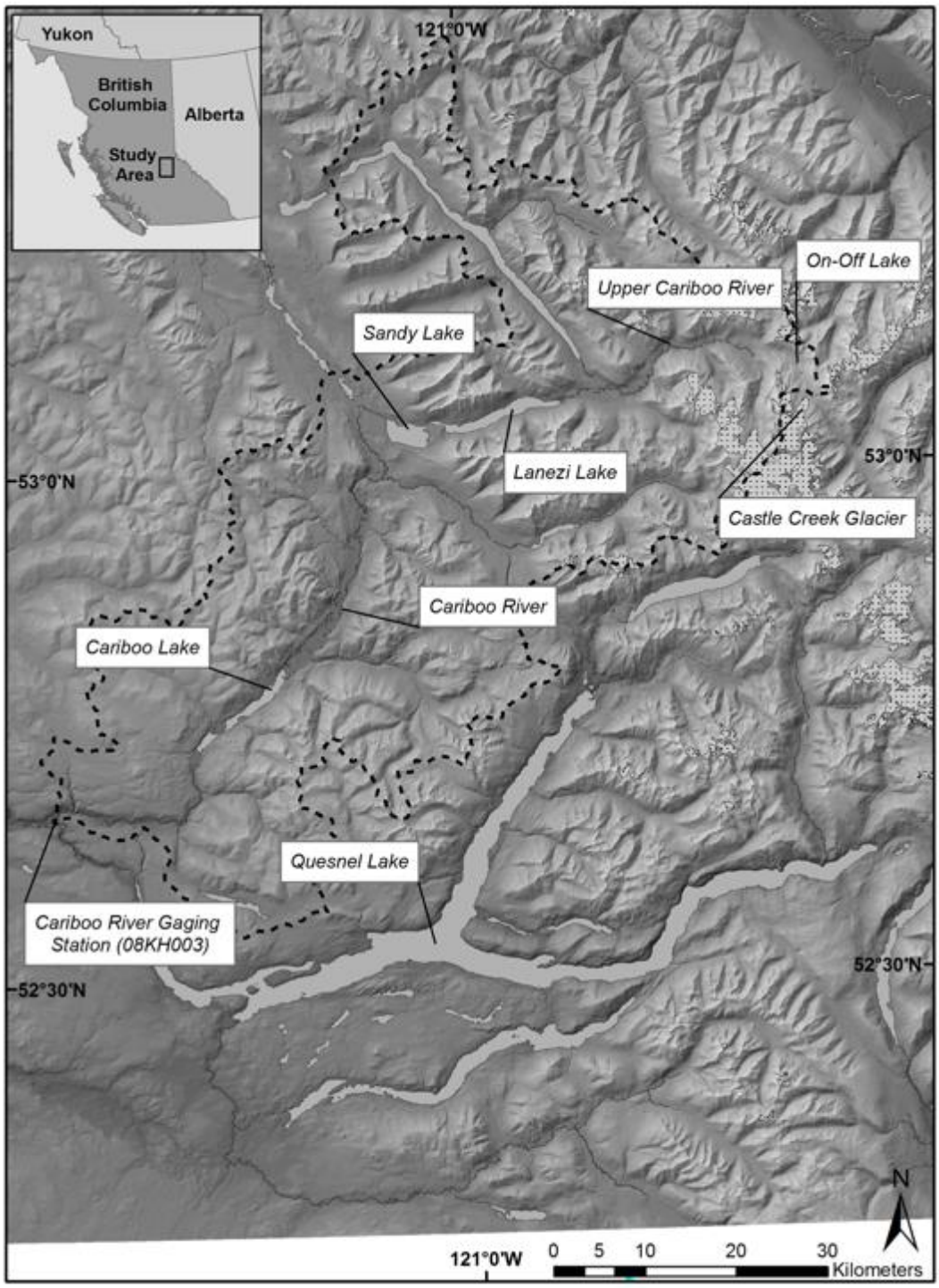

Figure 3.1: Cariboo Lake Watershed and surrounding area. Dotted polygons in the northeast corner are permanent ice cover.

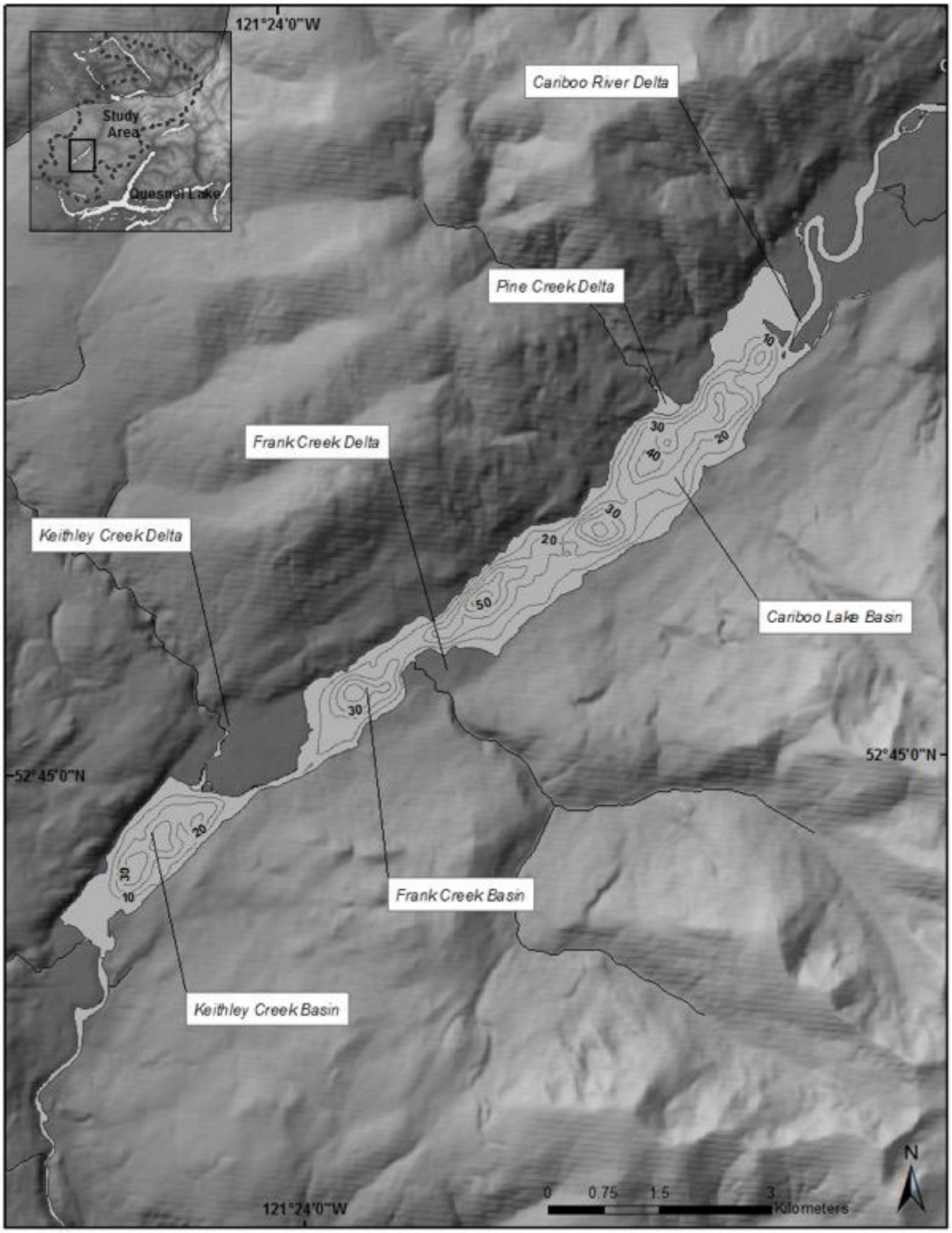

Figure 3.2: Cariboo Lake bathymetry map and location of surrounding delta. Contour interval is 10 m.

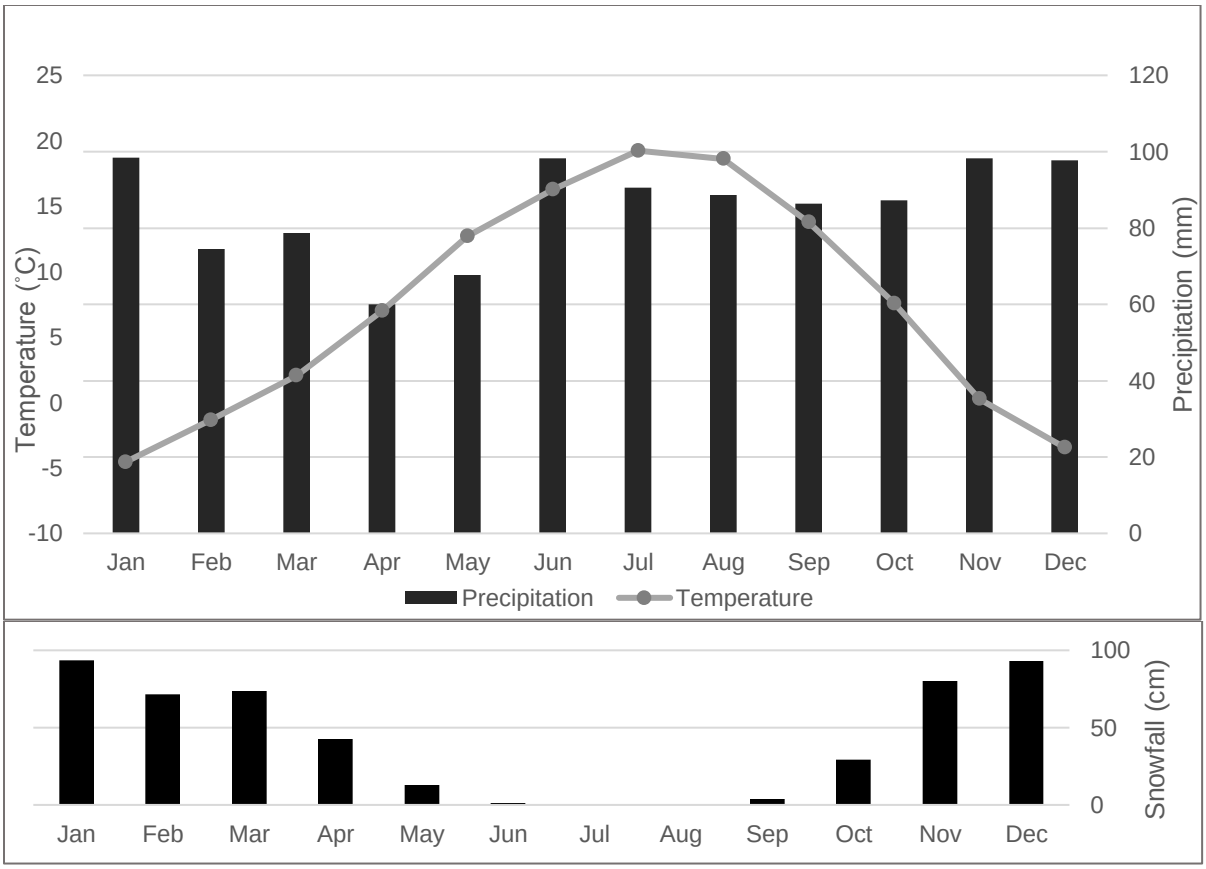

Figure 3.3: Climate data from Barkerville station (MSC ID: 1090660) dates 1888–2007. 10 km northwest of the Cariboo Lake

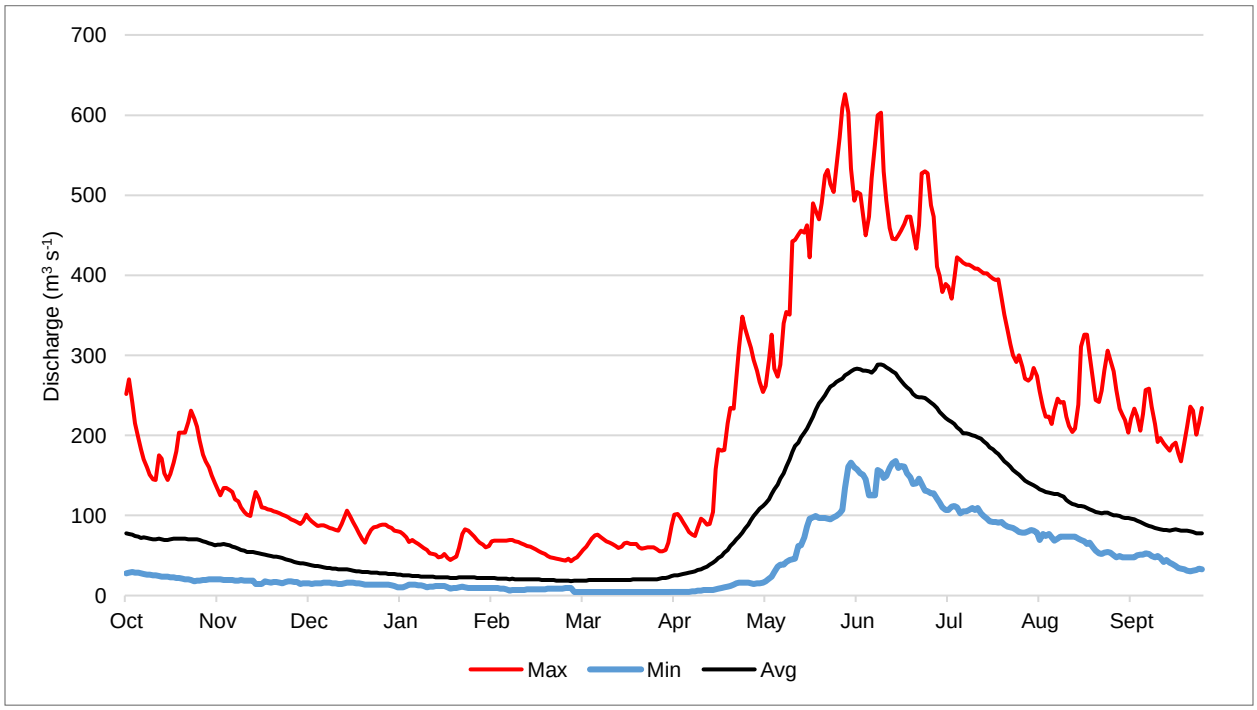

Figure 3.4: Cariboo River (08KH003, 1926 - 1994) gauging station, 23 km downstream of Cariboo Lake. Hydrograph of mean daily flows.

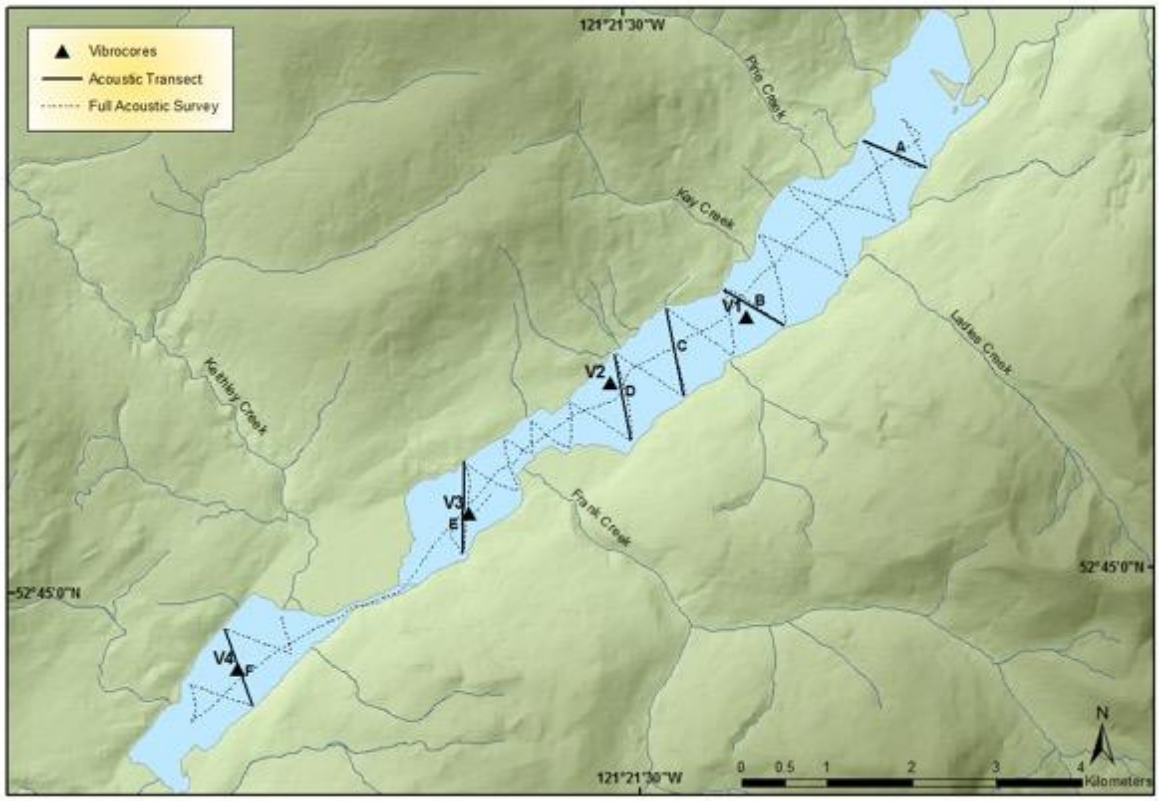

Figure 3.5: Map of Stratabox acoustic transects analyzed in detail and the full breadcrumb trail of the acoustic survey lines.

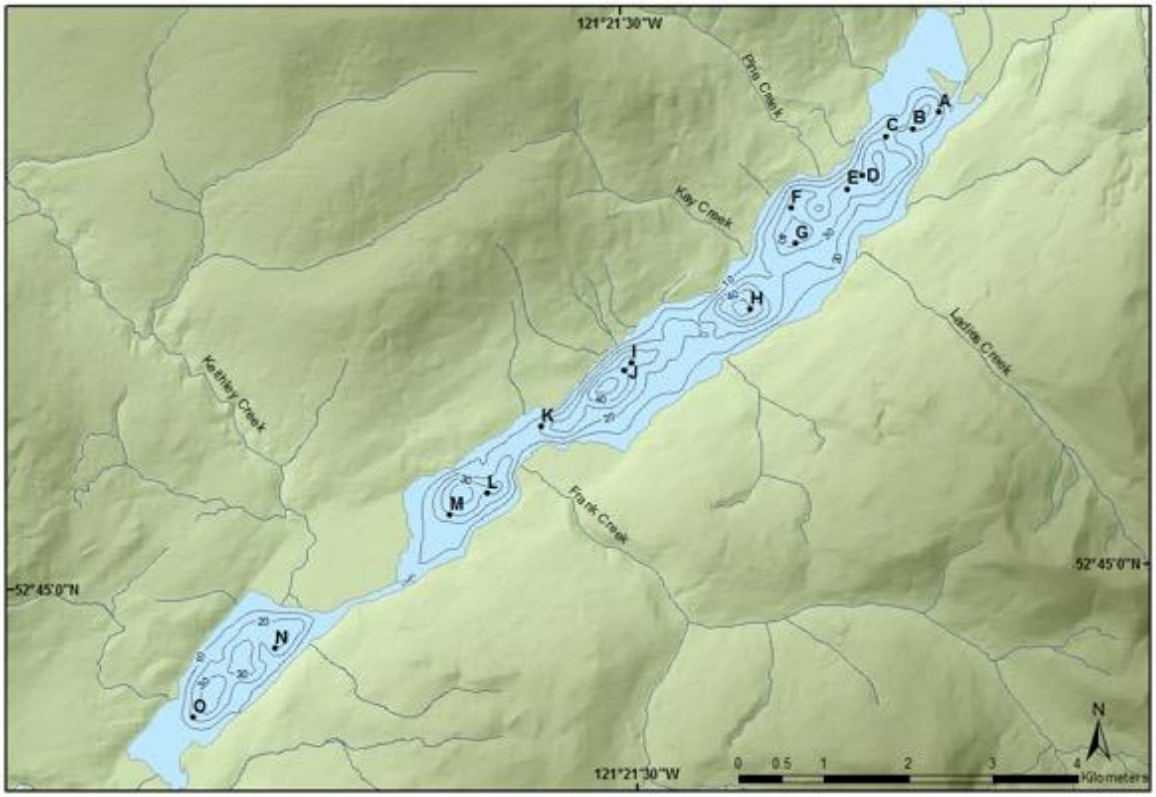

Figure 3.6: Map of Cariboo Lake CTD water column profile locations.

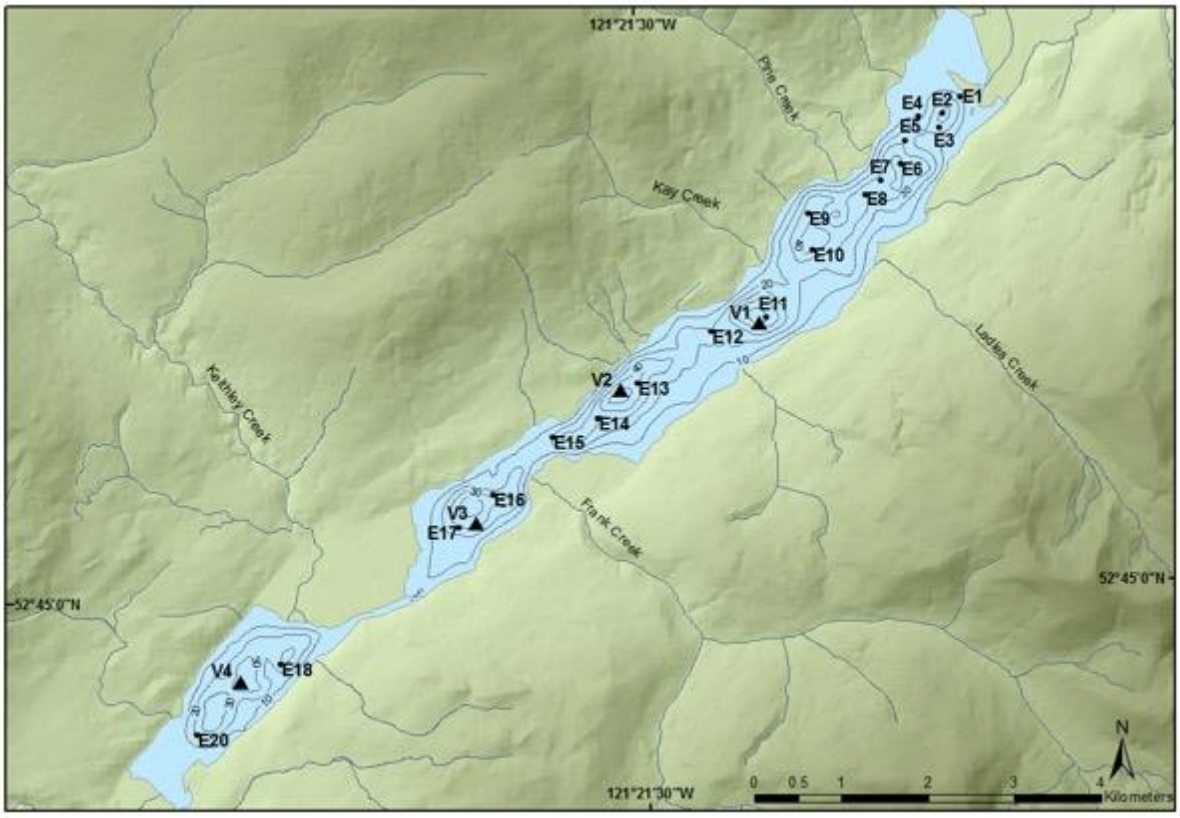

Figure 3.7: Map of core locations across Cariboo Lake. Surficial cores are denoted by black circles. Vibrocores (Long) are denoted by triangles.

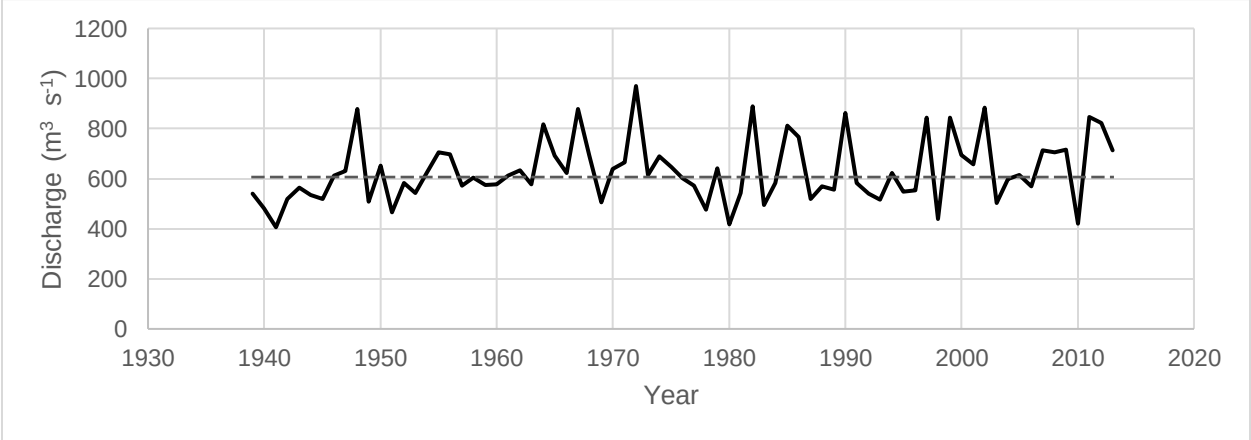

Figure 4.1: June peak daily discharge for Quesnel River gaging station (08KH006, 1939-2013) downstream of the Cariboo River confluence, 50 km downstream of the Cariboo River gaging station. Dashed line is average peak daily discharge.

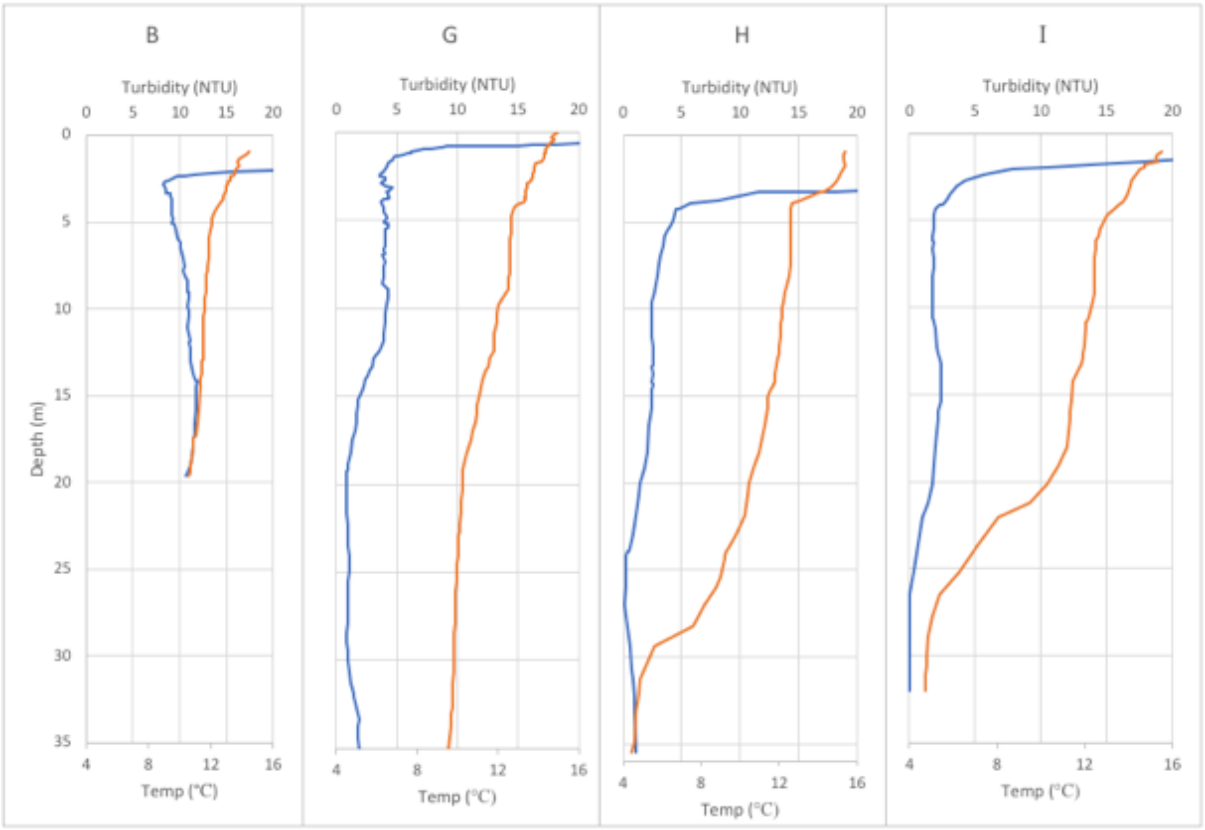

Figure 4.2: CTD water column profiles for the Cariboo River delta basin. Orange lines are temperature and blue lines are turbidity.

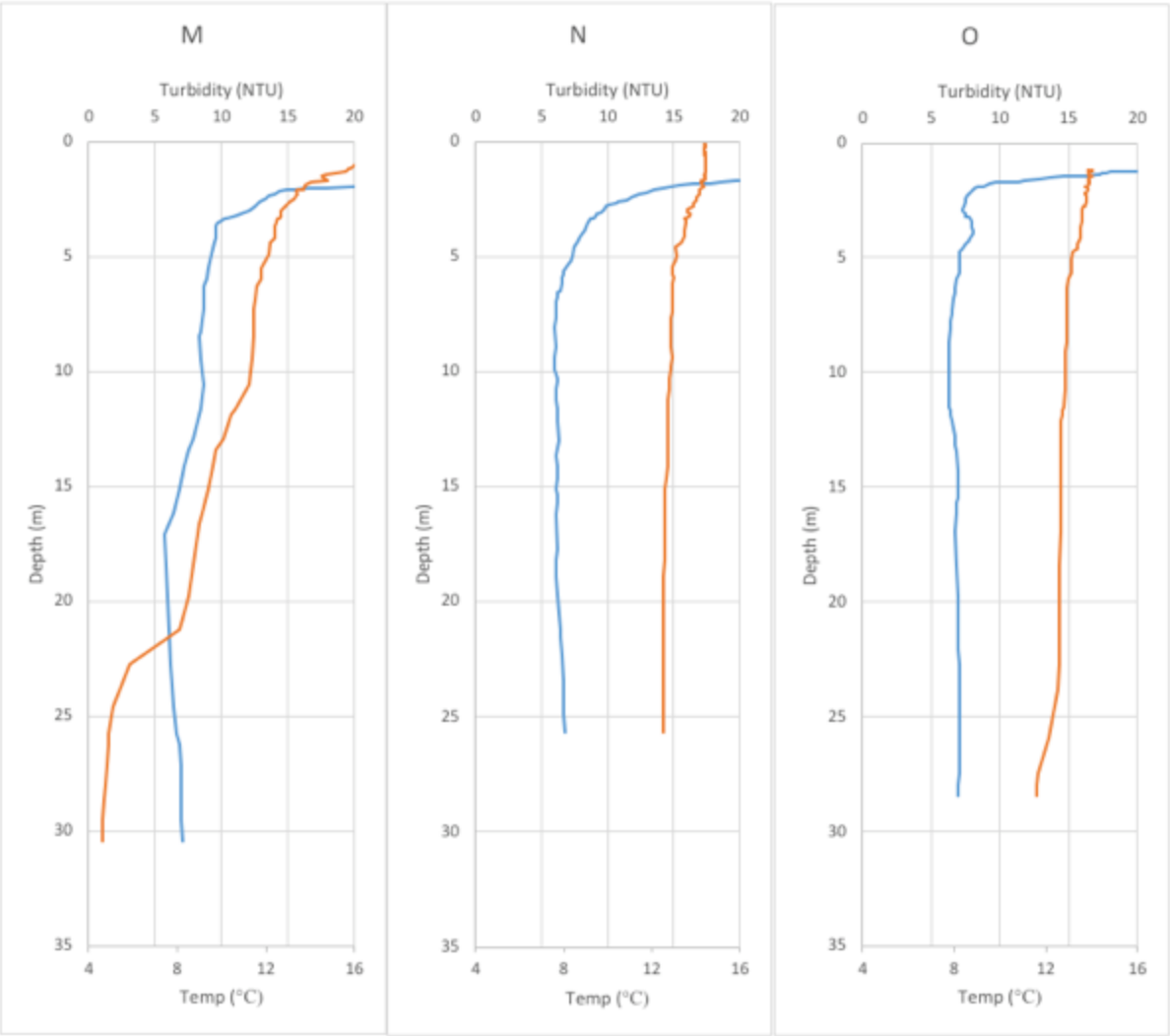

Figure 4.3: CTD water column profiles for the Frank Creek and Keithley Creek delta. Orange lines are temperature and blue lines are turbidity.

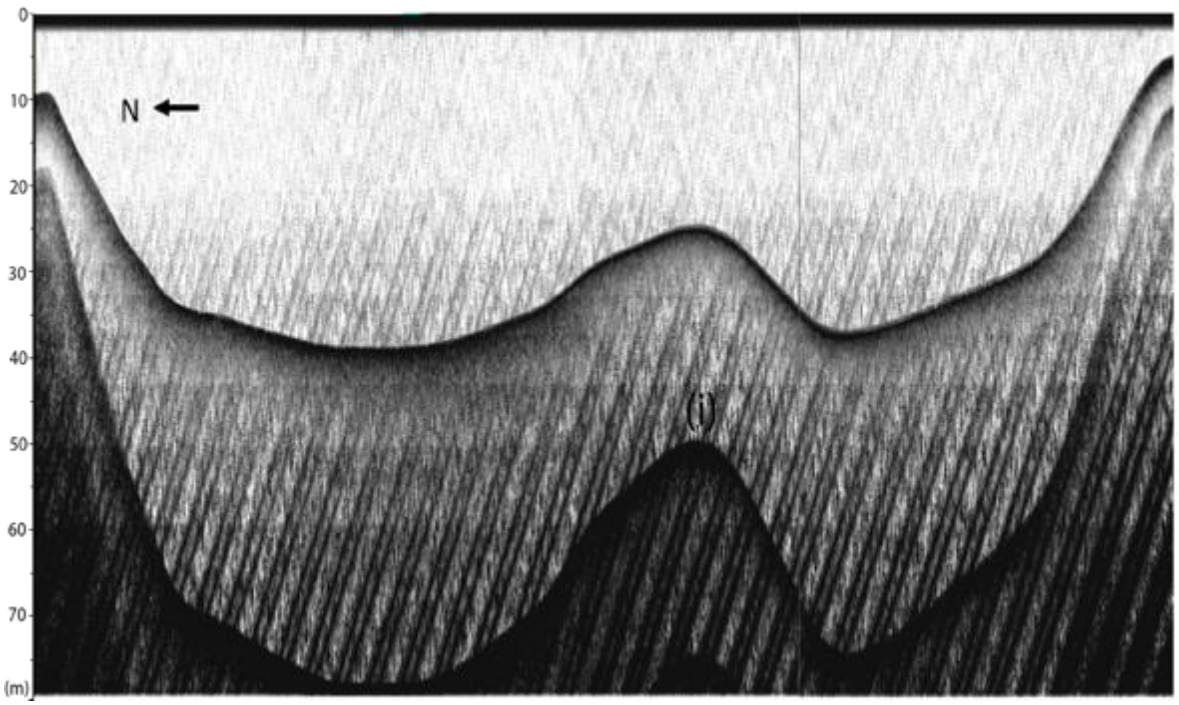

Figure 4.4: Stratabox acoustic transect A. Duplicate acoustic reflector is denoted by (i). Looking up-lake, see Fig. 3.5 for location.

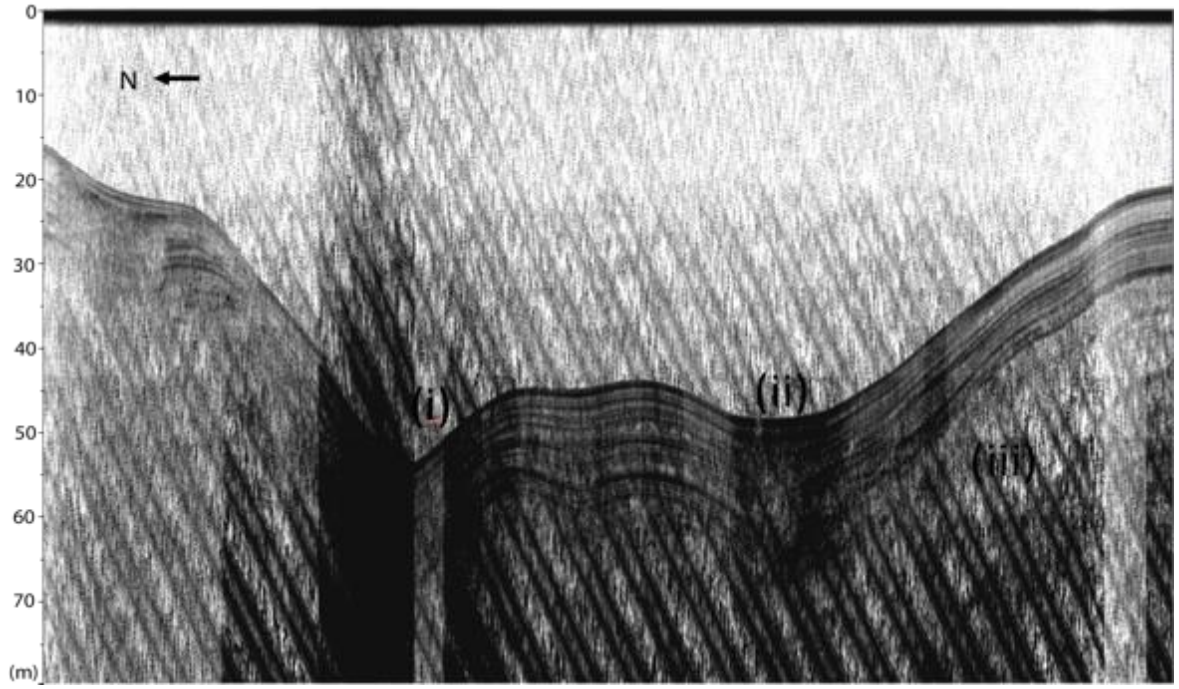

Figure 4.5: Stratabox acoustic transect B. Scour channels are denoted by (i) and (ii). Looking up-lake, see Fig. 3.5 for location.

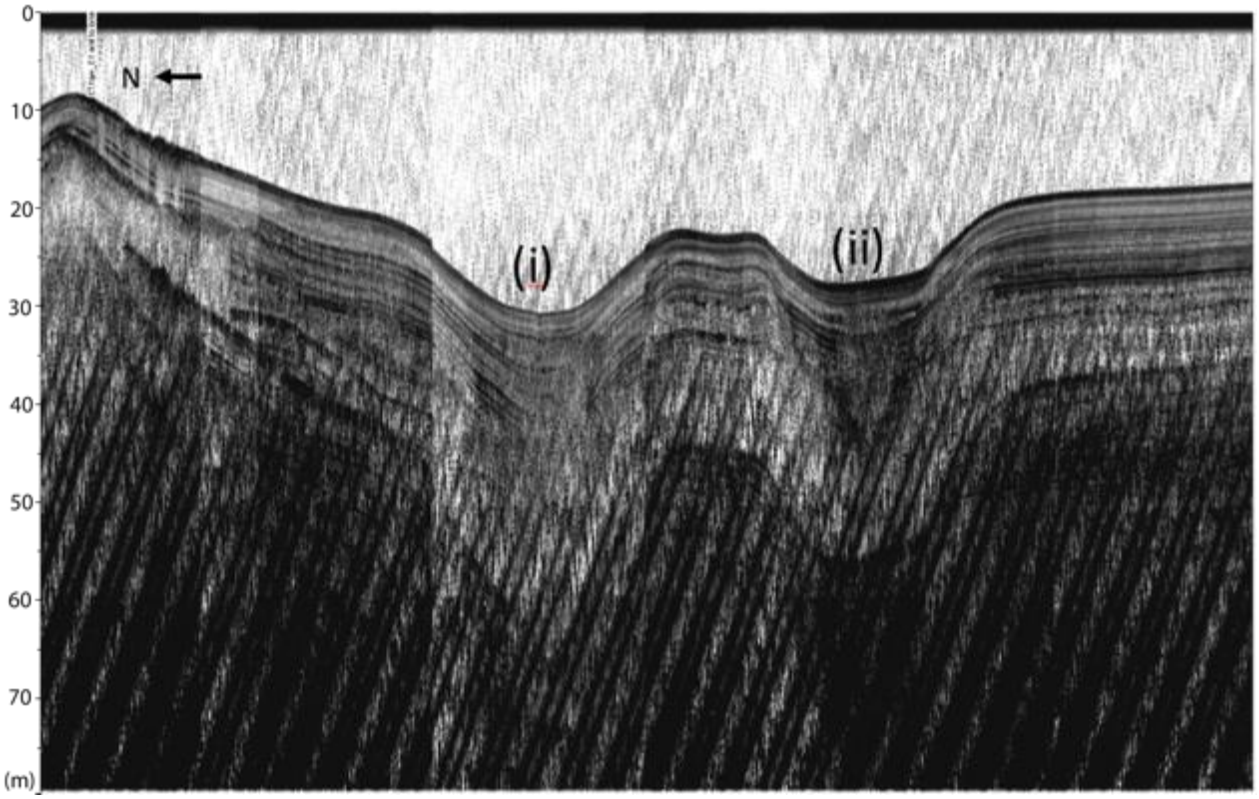

Figure 4.6: Stratabox acoustic transect C. Scour channels are denoted by (i) and (ii). Looking up-lake, see Fig. 3.5 for location.

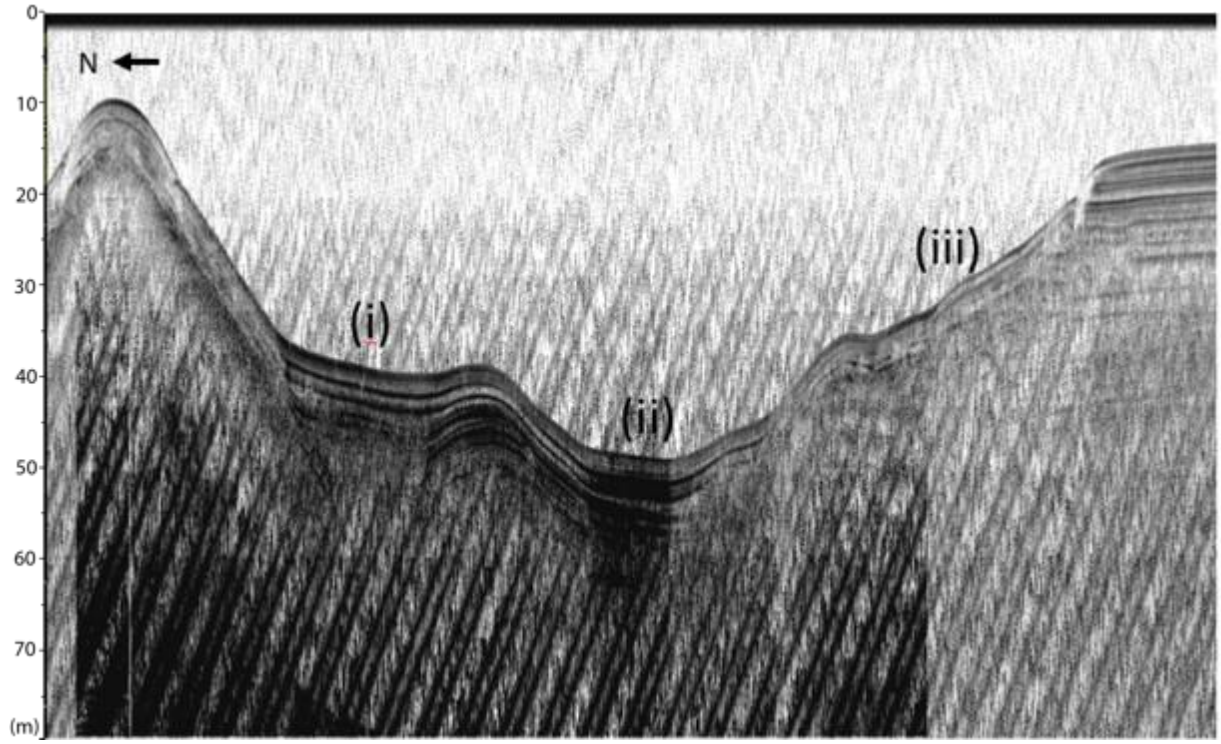

Figure 4.7: Stratabox acoustic transect D. Scour channels are denoted by (i) and (ii). Slumping is observed at (iii). Looking up-lake, see Fig. 3.5 for location.

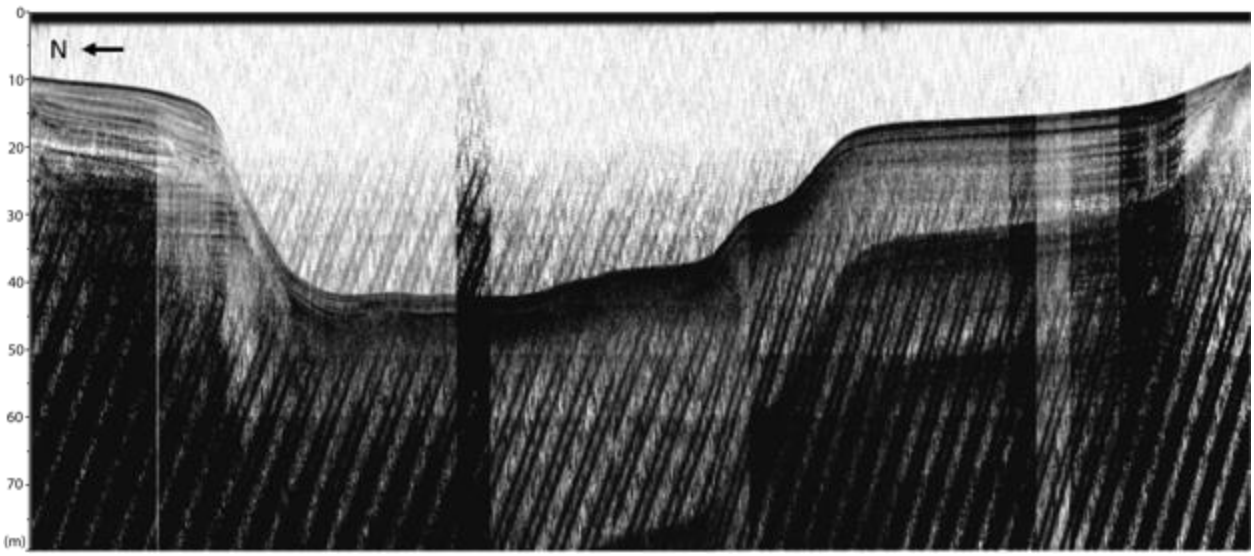

Figure 4.8: Stratabox acoustic transect E. Looking up-lake, see Fig. 3.5 for location.

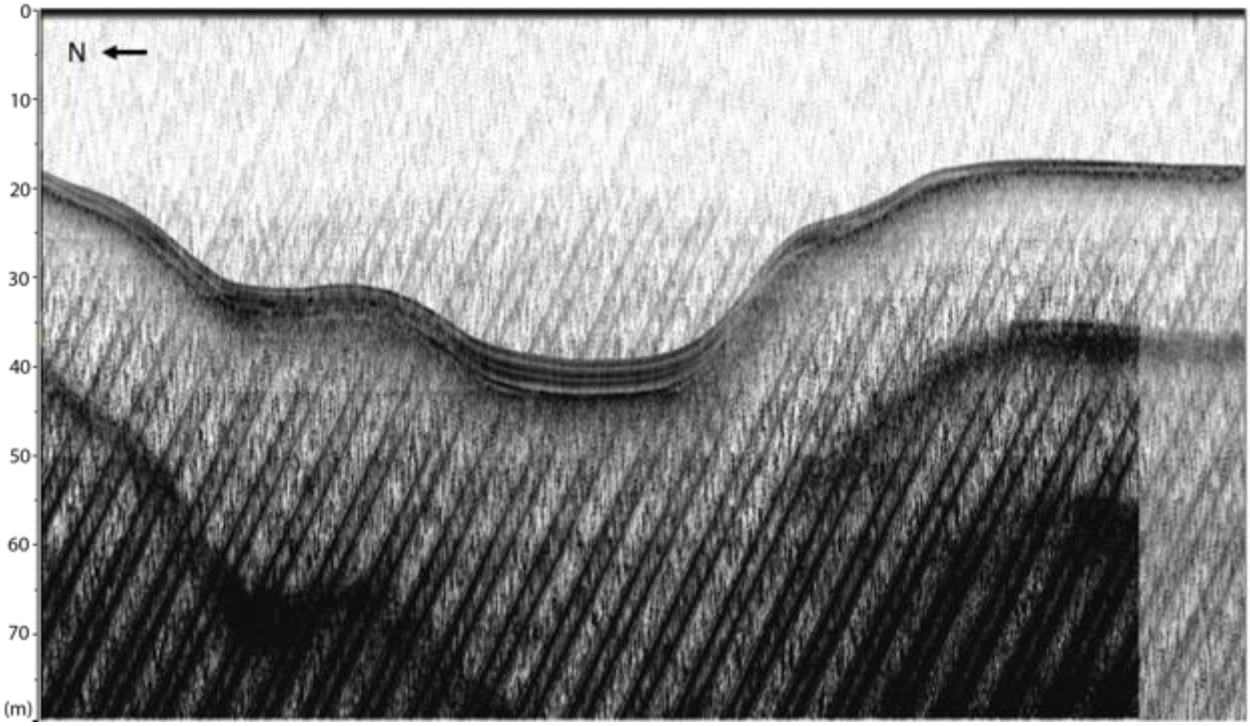

Figure 4.9: Stratabox acoustic transect F. See Fig. 3.5 for location.

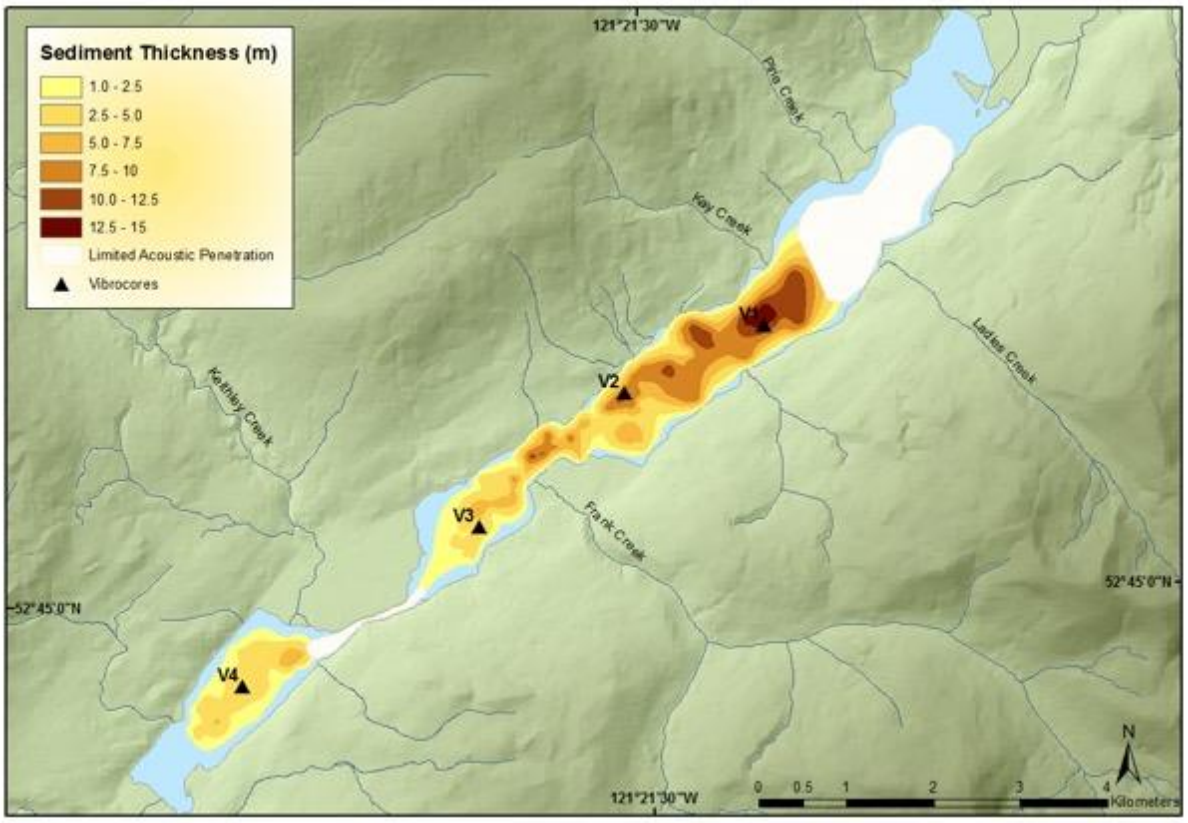

Figure 4.10: Cariboo Lake sediment thickness map.

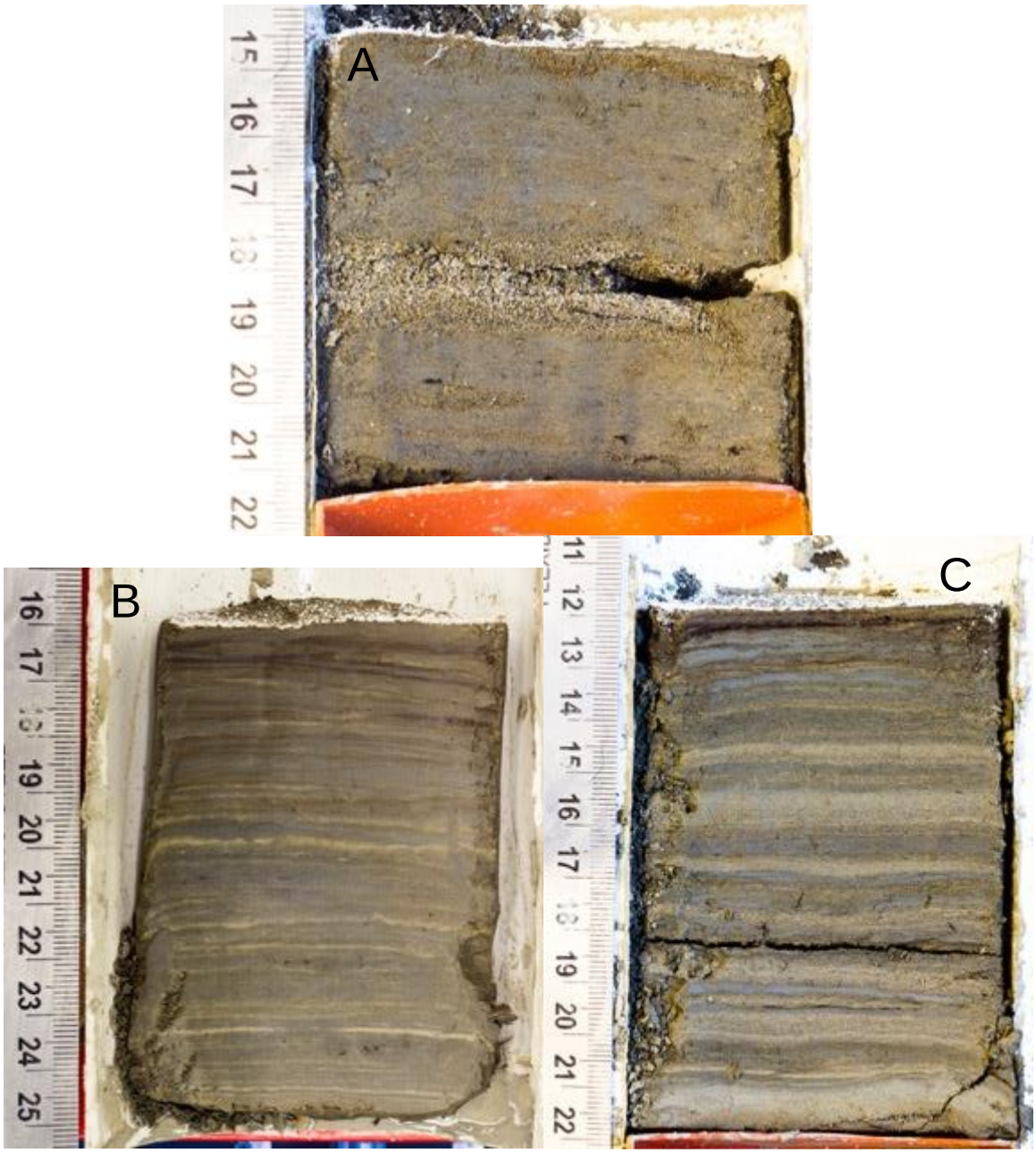

Figure 4.11: Surficial Ekman sediment core photographs. A (E1) is proximal to the Cariboo River delta. B (E13) was retrieved from the second deepest basin in the lake in the Cariboo River basin. C (E18) was retrieved from the Keithley Creek basin.

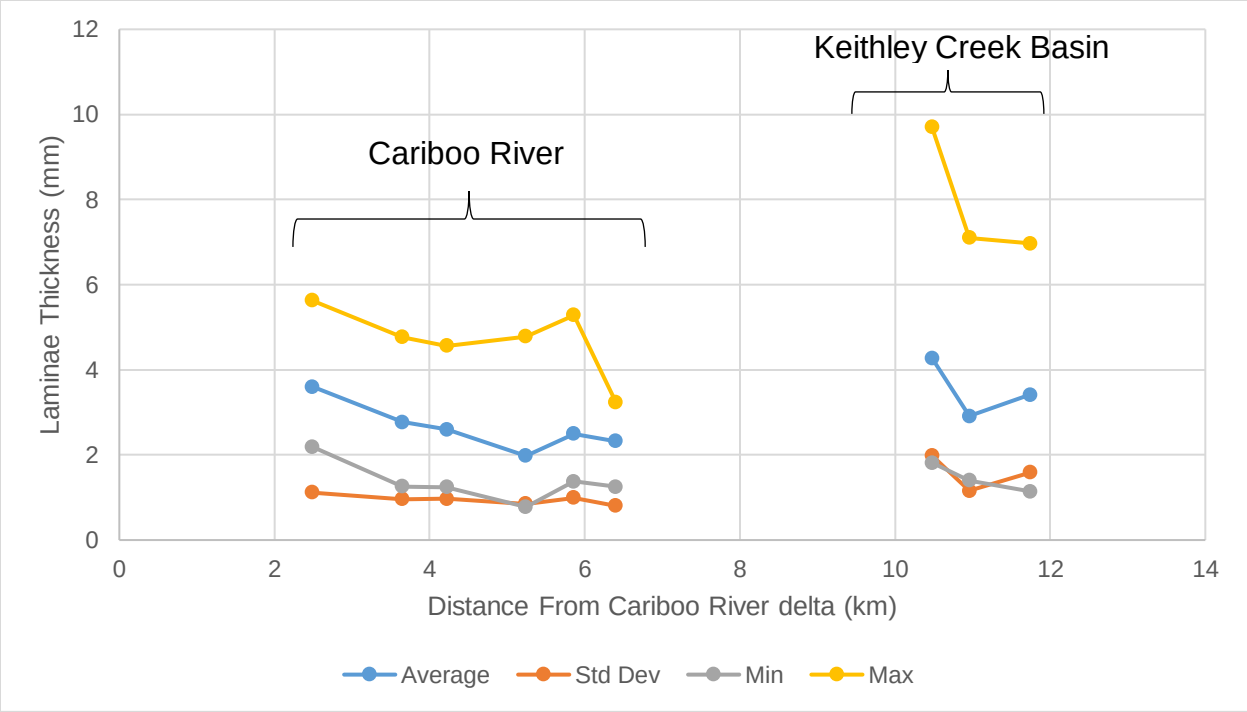

Figure 4.12: Laminae Statistics calculated on surficial Ekman cores E9-15 and E18-E20.

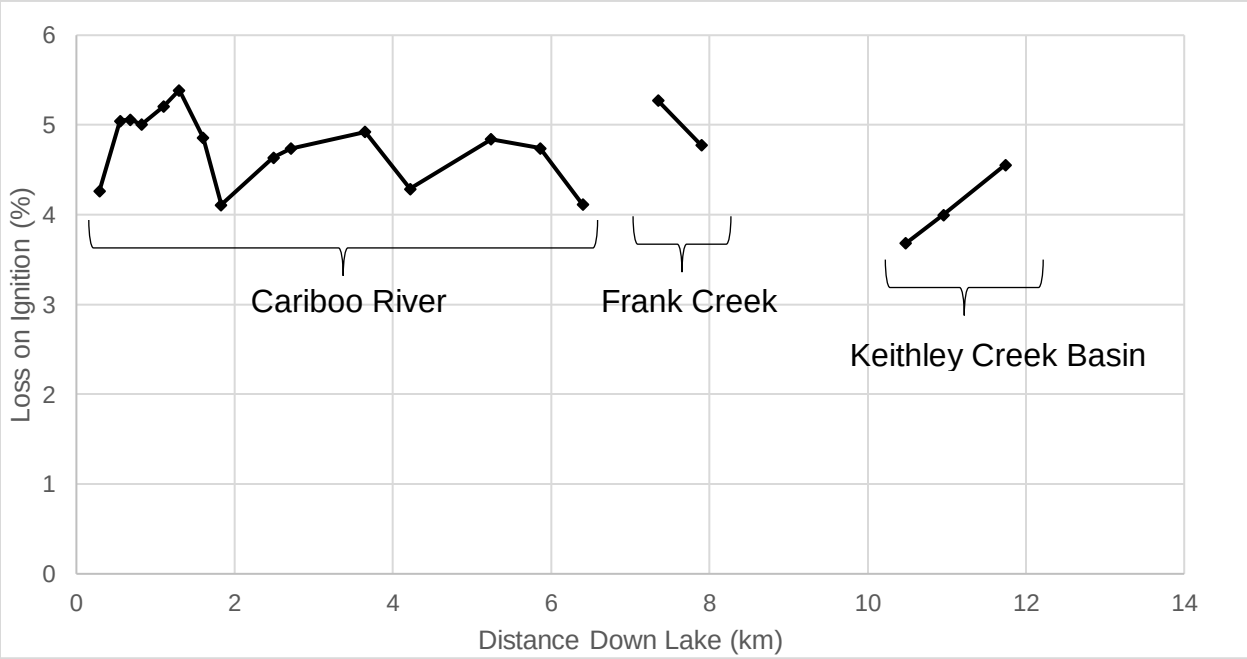

Figure 4.13: Ekman bulk sample percent organic versus distance from Cariboo delta (km).

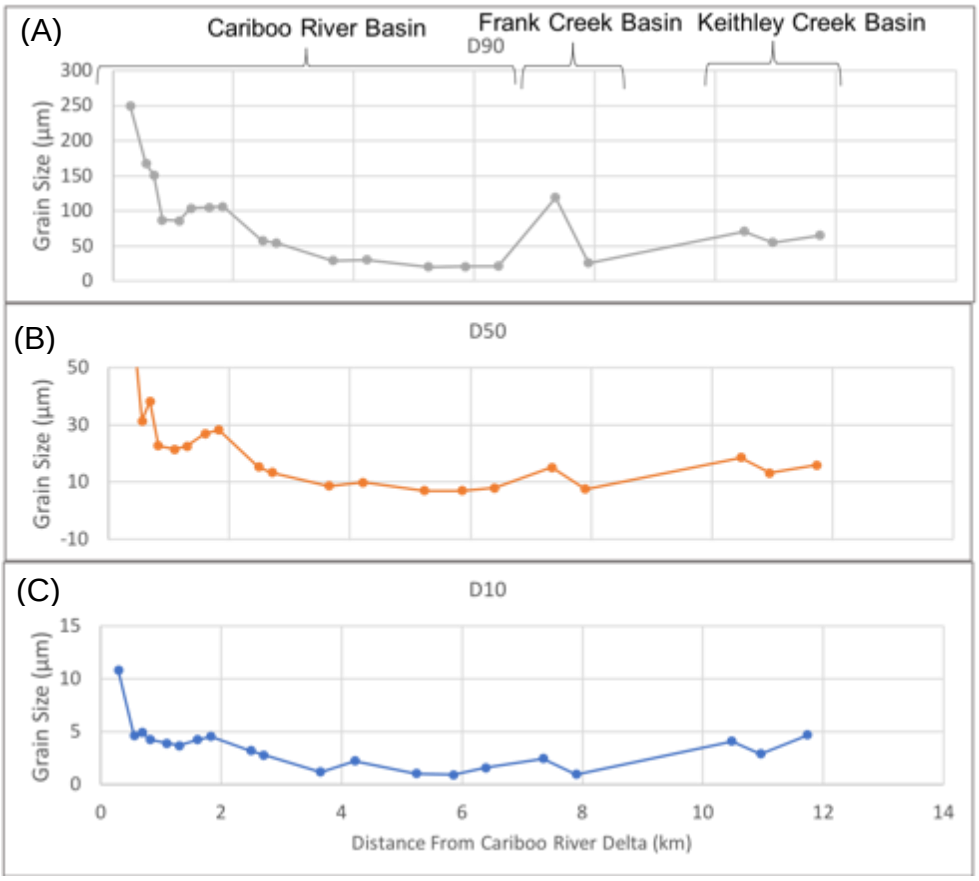

Figure 4.14: Ekman bulk sample grain size diameter versus distance from the Cariboo River delta. (A) D_{90}, (B) D_{50}, (C) D_{10}.

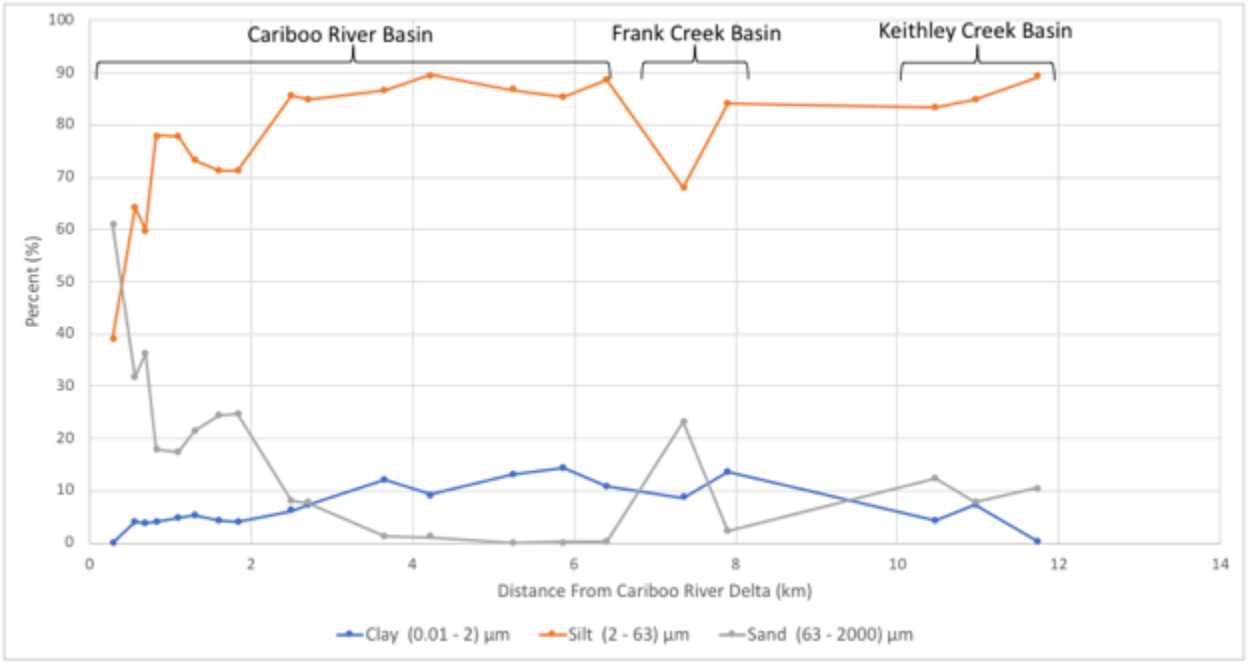

Figure 4.15: Ekman bulk sample percent composition of clay, silt, and sand sized particles versus distance from Cariboo River delta.

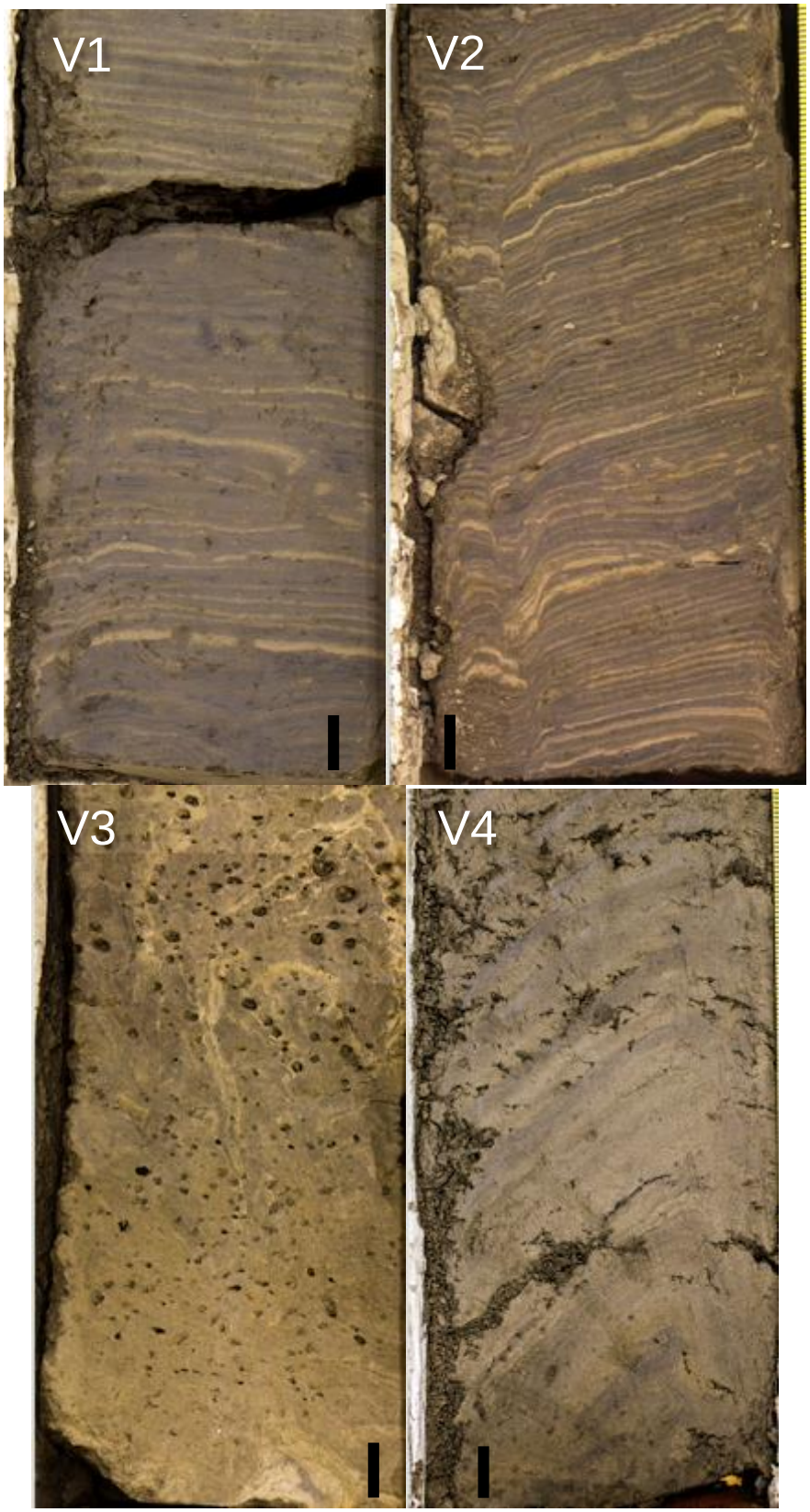

Figure 4.16: The bottom ~13 cm from vibrocores. V1 (277-290 cm), V2 (370-383 cm), V3 (182-195 cm), and V4 (402-415 cm). Black bars are 1 cm scale.

Turbidite #	Core	Year AD	Couplet Thickness (mm)	Core Depth (cm)
1	V1	1671	13.3	79.0
2	V1	1398	15.9	137.3
3	V1	1296	5.3	160.9
4	V1	1259	3.4	167.8
5	V1	1258	2.7	168.1
6	V1	1226	2.7	175.7
7	V1	1225	3.6	176.0
8	V1	1024	3.9	223.5
1	V2	1823	2.3	29.9
2	V2	1648	4.0	58.8
3	V2	1532	2.3	76.8
4	V2	1301	8.8	109.0
5	V2	1263	3.0	114.0
6	V2	789	5.1	180.0
7	V2	493	47.0	230.6
8	V2	490	4.7	231.5
9	V2	377	3.5	250.4

Figure 4.17: Timing and thickness of turbidite laminae in V1 and V2.

Figure 4.18: Event-based layers at V1 (left) and V2 (right) at depths of 137 cm and 230.5 cm respectively.

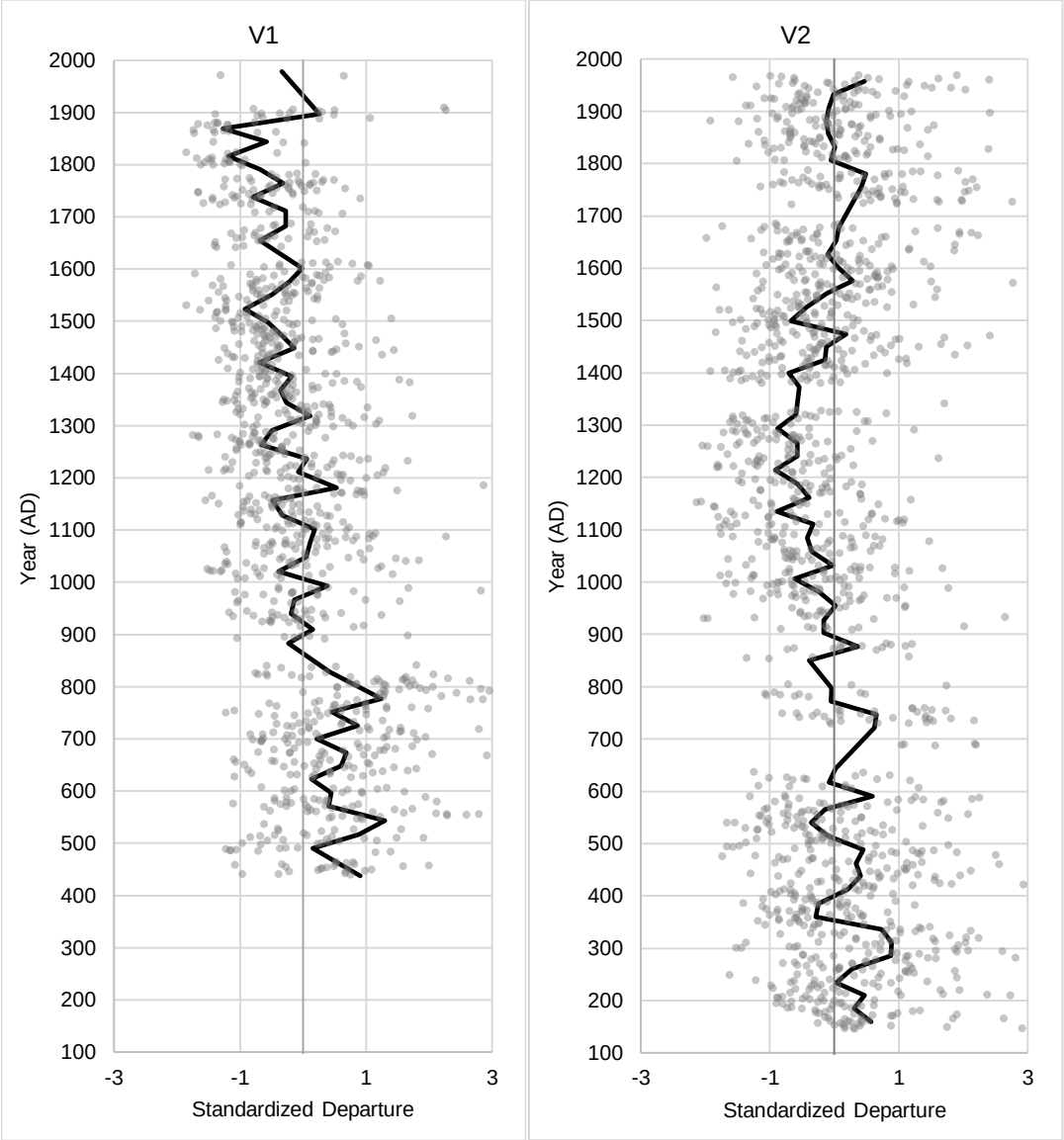

Figure 4.19: Black lines are V1 and V2 varve thickness 25-year moving average presented as standard deviations away from mean. Grey scatter plot is raw varve thickness plotted as standard deviations from the mean.

V1									
	Varve Thickness			**Grain Size**			**%LOI**		
	Std. Dept.	*p-value*	N	Std. Dept.	*p-value*	N	Std. Dept.	*p-value*	N
1951-2017	-	-	2	1.40	0.043	5	-1.59	0.000	5
1751-1950	-0.56	0.000	86	0.31	0.974	5	-0.05	1.000	8
1251-1750	-0.40	0.000	386	-0.33	0.821	19	-0.43	0.085	26
751-1250	0.22	0.023	343	-0.30	0.627	17	0.52	0.291	27
440-750	0.53	0.000	230	0.45	0.714	10	0.26	0.984	18

Figure 4.20: V1 standardized departures (number of standard deviations from the mean). P-values are from one-way ANOVA comparison between groups and the respective mean for the entire core.

V2									
	Varve Thickness			**Grain Size**			**%LOI**		
	Std. Dept.	*p-value*	N	Std. Dev.	*p-value*	N	Std. Dev.	*p-value*	N
1951-2017	0.43	0.674	20	0.83	0.487	5	-0.86	0.372	3
1751-1950	0.04	0.796	182	-0.29	0.995	4	0.16	1.000	10
1251-1750	-0.15	0.044	392	-0.18	1.000	15	-0.49	0.086	18
751-1250	-0.33	0.000	298	-0.84	0.840	11	0.17	0.999	17
150-750	0.29	0.000	479	0.48	0.537	13	0.45	0.521	25

Figure 4.21: V2 standardized departures (number of standard deviations from the mean). P-values are from one-way ANOVA comparison between groups and the respective mean for the entire core.

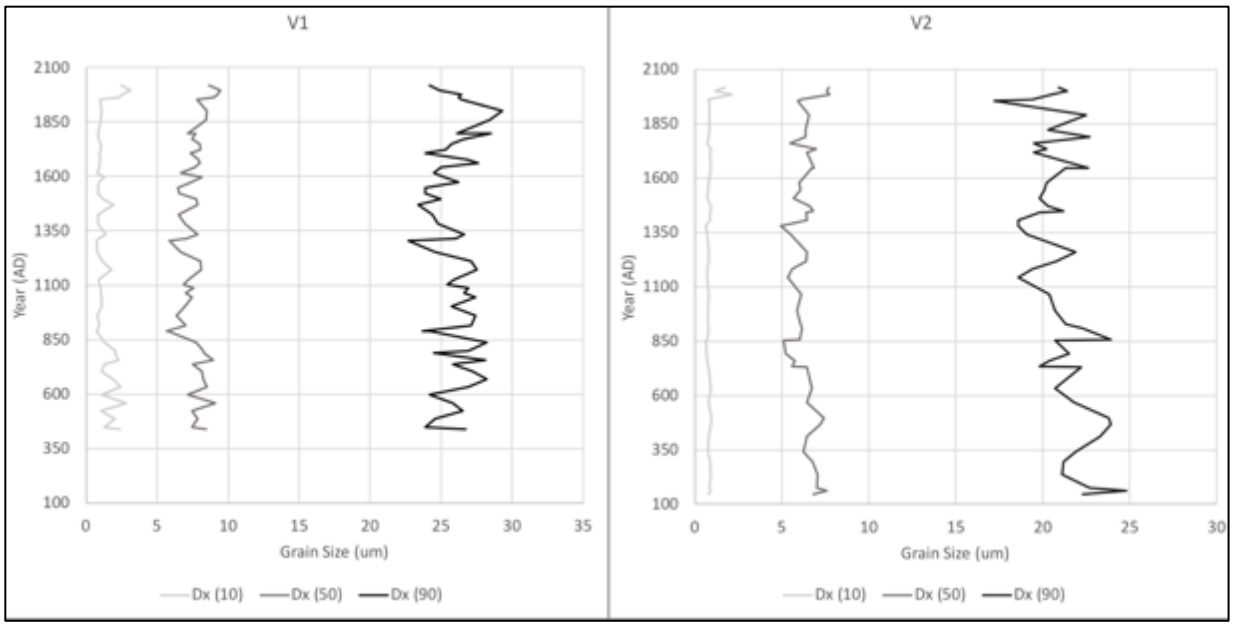

Figure 4.22: Raw grain size diameter at V1 and V2

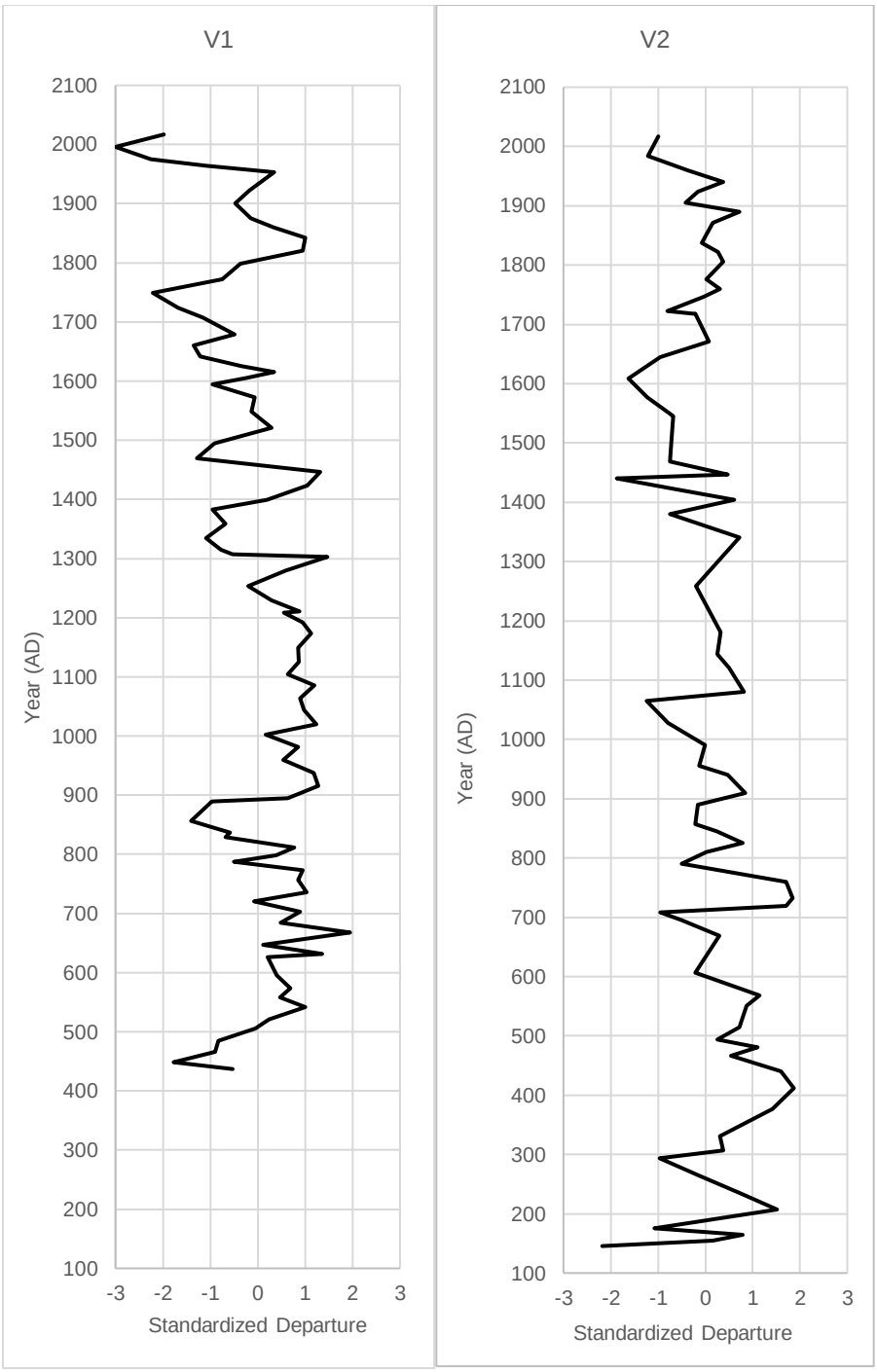

Figure 4.23: Percent Organics (% LOI) at V1 and V2 Number of standard deviations away from mean % LOI.

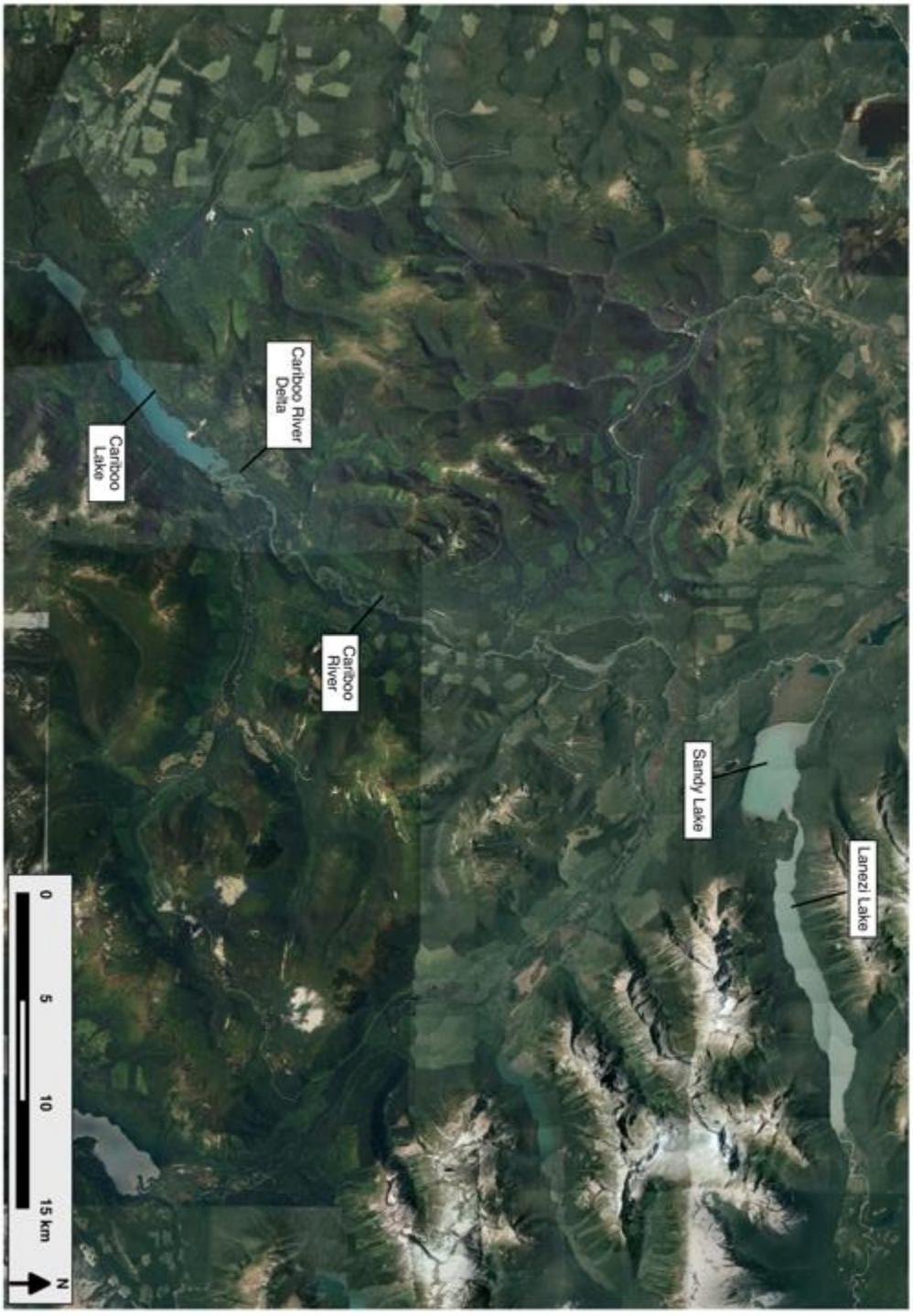

Figure 5.1: Satellite Imagery of Cariboo Lake watershed (Google Earth, Digital Globe, 2018)

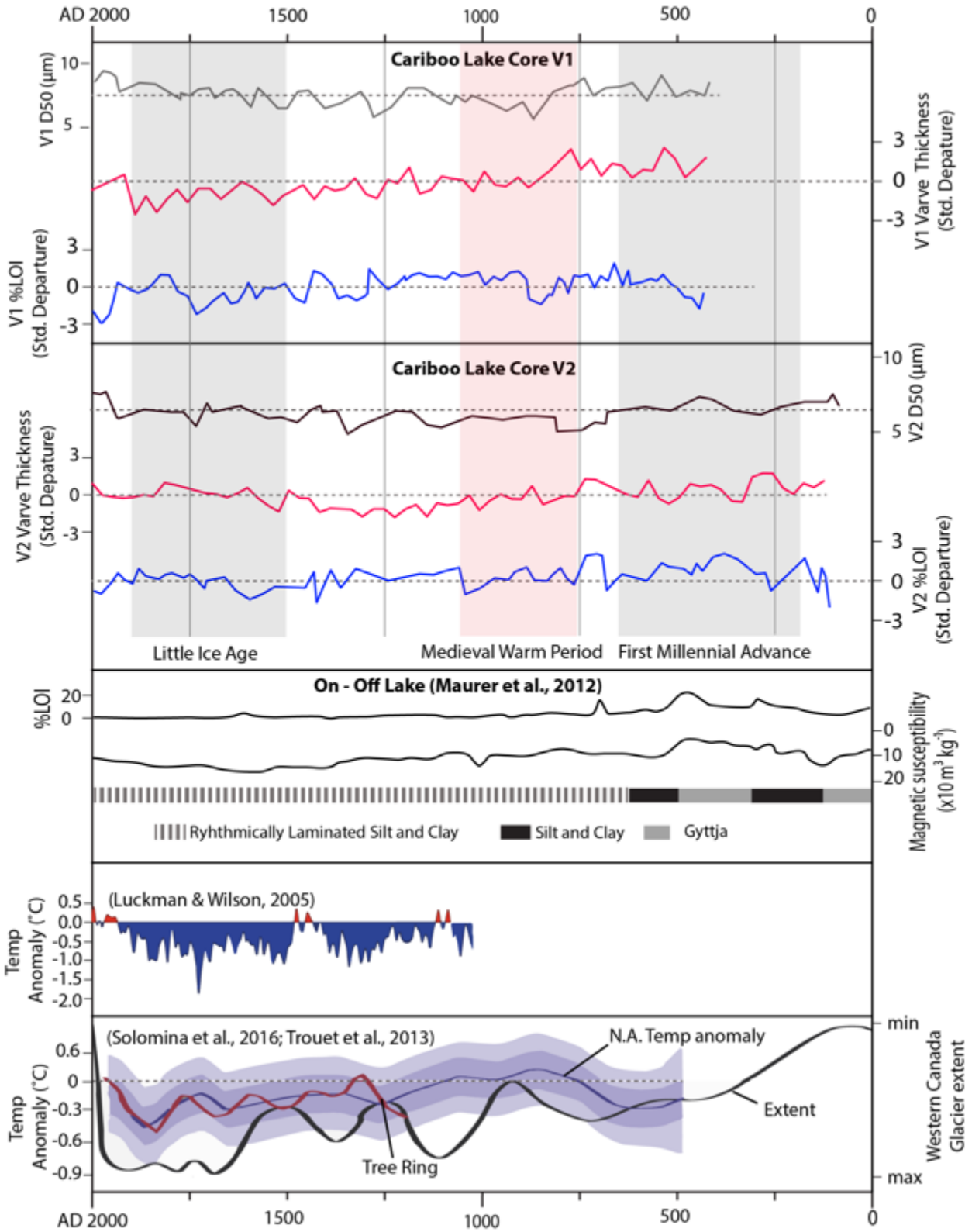

Figure 5.2: Comparison of the Cariboo Lake temporal sediment record with the Maurer et al., (2012) On-Off Lake sediment record and three paleoclimate records. ***Cariboo Lake Cores V1 & V2.*** *The black lines are D50 (µm) grain size. The red lines are 25-year average moving filters of varve thickness expressed as the number of standard deviations from the mean. The blue lines are 25-year average moving filters of percent organics (%LOI$_{550}$) expressed as the number of standard deviations from the mean. The vertical grey bars represent below average climate anomalies, the First Millennial Advance (AD 200-700) and Little Ice age*

(AD 1500-1900). Red vertical bar represents above average temperature, from AD 750-1100 during the Medieval Warm Period. ***On-Off Lake Maurer et al., (2012).*** *Top line is the percent organics (%LOI$_{550}$). Bottom line is the magnetic susceptibility (x10 m^3 kg^{-1}).* ***Luckman & Wilson, (2005).*** *Summer temperature reconstruction (1073-1983) using the regional curve standardization method (RCS2004) for tree-ring data from the Rocky Mountains.* ***Gavin et al., (2011).*** *Composite record of July temperature anomalies based on chironomid assemblages from southern British Columbia (Palmer et al., 2002; Rosenberg et al., 2004; Chase et al., 2008).* ***Menounos et al., (2009).*** *Glacier advance periods in the Interior and Rocky Mountains.* ***Olga et al., (2016) & Trouet et al., (2013).*** *Black line is glacier extent in western North America. Blue line is anomaly from average North American temperatures from 1904-1980 based on pollen data. Red line are anomalies based on tree-ring data.*

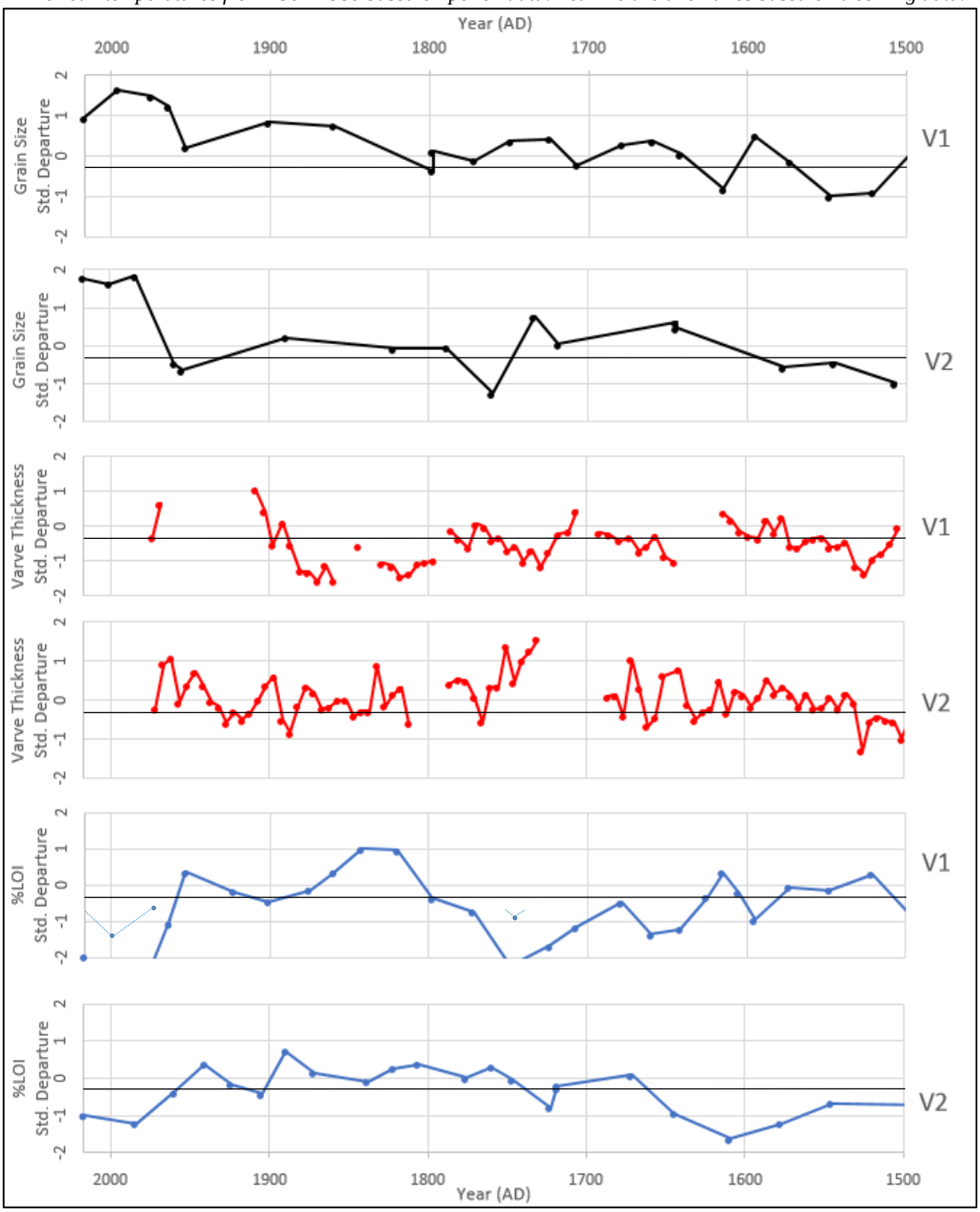

Figure 5.3: Standardized departures from the mean of grain size (black), varve thickness (Red), %LOI (Blue) from AD1500-2017 in Cariboo Lake. Varve thickness is represented as a 5-year moving average. Grain size and %LOI are represented as ~5-year average through the sampling of ~5 laminae layers at each data point.

Figure 5.4: Fractured tree stumps at 1-3 m provide evidence of a Landslide in the Pine Creek delta likely caused by hydraulic mining activity circa 1860.

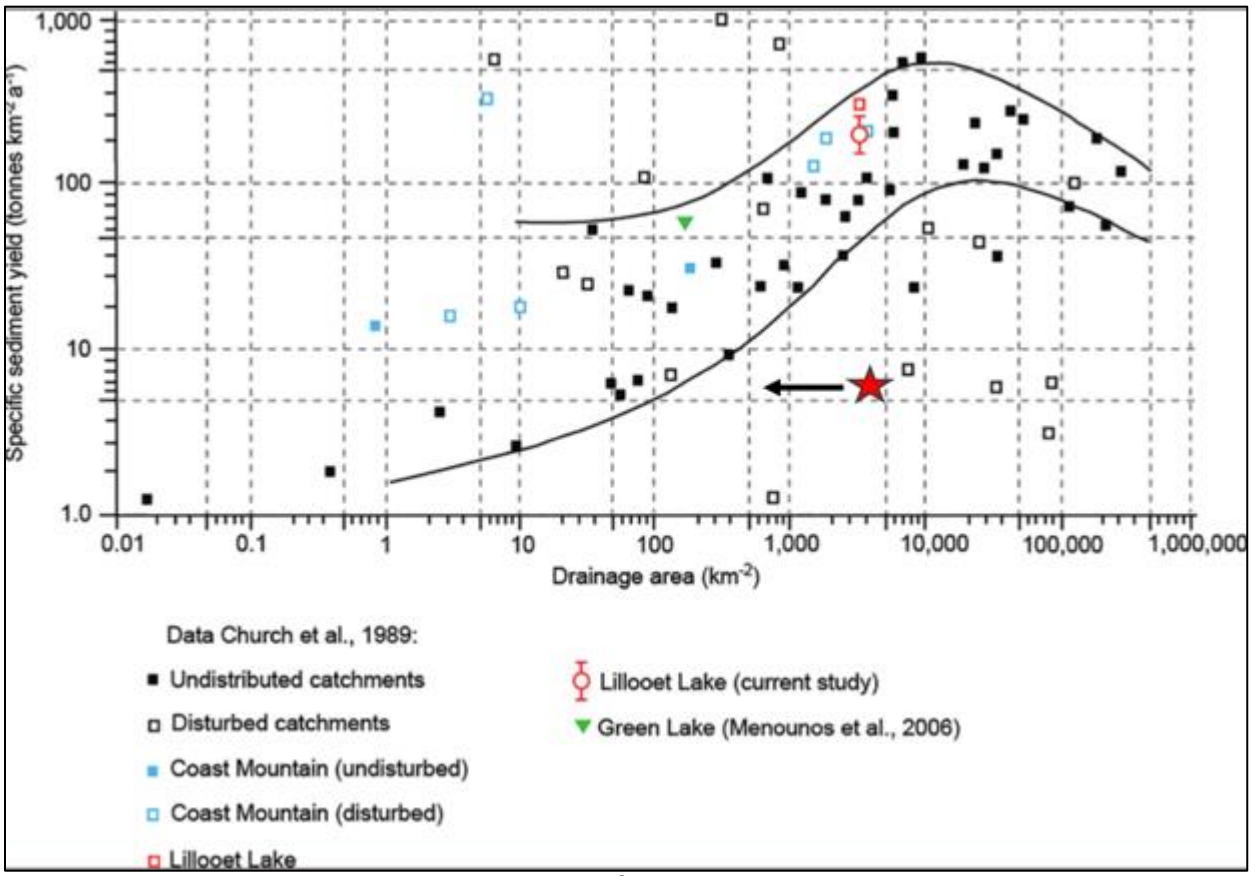

Figure 5.5: Suspended sediment yield versus drainage area (km^3). Heideman et al., 2017 is the red circle and this study is the red star. Plot is adapted from Heideman et al., (2017). Large black arrow left of the red start indicates that Cariboo Lake is estimated to retrieve sediment from a drainage area smaller than the actual catchment area due to filtering of up-valley lakes.

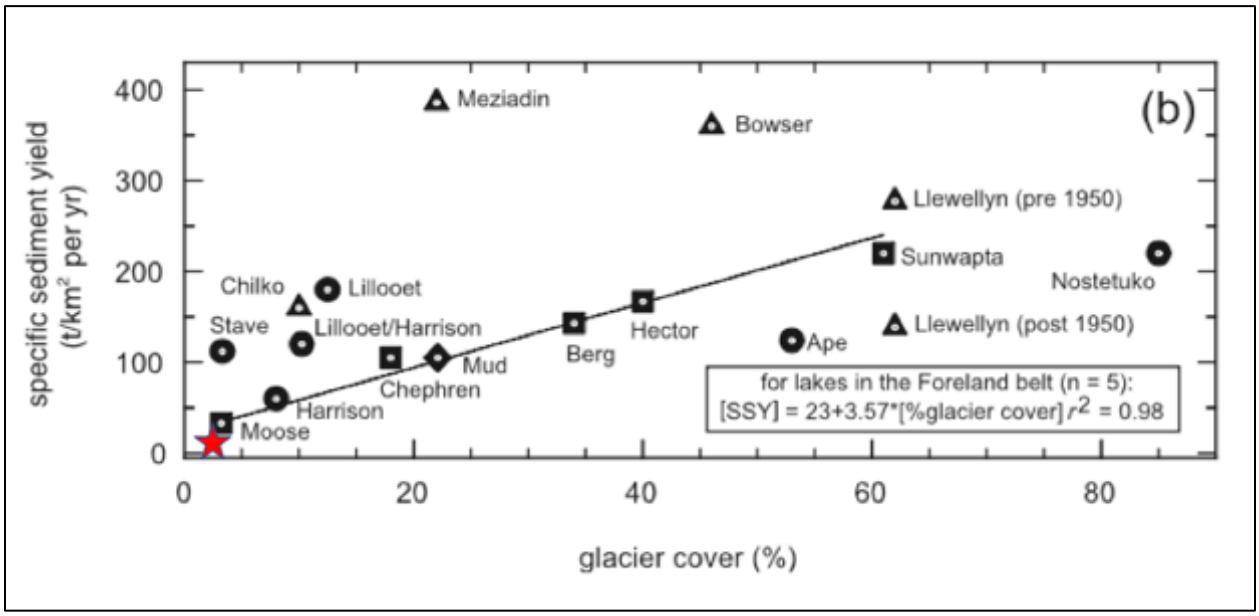

Figure 5.6: Specific sediment yield versus percent glacier cover between Coastal Belt (circles), Inter-montane Belt (triangles), Foreland Belt (Squares), and Omineca Belt (diamond) to suspended sediment yield in Cariboo Lake (red star). Plot is adapted from Hodder et al., (2006).

Appendix A: Statistical Results

Table A.1: V1 log transformed varve thickness log transformed ANOVA results.

Between-Subjects Factors

		N
Group	1251-1750	386
	1751-1950	86
	440-1950	1045
	440-750	230
	751-1250	343

Tests of Between-Subjects Effects

Dependent Variable: lnVarveThickness

Source	Type III Sum of Squares	df	Mean Square	F	Sig.
Corrected Model	25.094[a]	4	6.274	50.115	.000
Intercept	2578.596	1	2578.596	20598.536	.000
Group	25.094	4	6.274	50.115	.000
Error	261.008	2085	.125		
Total	4981.518	2090			
Corrected Total	286.102	2089			

a. R Squared = .088 (Adjusted R Squared = .086)

Multiple Comparisons

Dependent Variable: lnVarveThickness

Tukey HSD

(I) Group	(J) Group	Mean Difference (I-J)	Std. Error	Sig.	95% Confidence Interval	
					Lower Bound	Upper Bound
1251-1750	1751-1950	.12350539*	.042189233	.028	.008321854	.238688929
	440-1950	-.1380096*	.021073736	.000	-.19554434	-.08047482
	440-750	-.3394924*	.029471775	.000	-.41995524	-.25902966
	751-1250	-.2237849*	.026254065	.000	-.29546280	-.15210697
1751-1950	1251-1750	-.1235054*	.042189233	.028	-.23868893	-.00832185
	440-1950	-.2615150*	.039691493	.000	-.36987927	-.15315068
	440-750	-.4629978*	.044720217	.000	-.58509138	-.34090430
	751-1250	-.3472903*	.042668352	.000	-.46378189	-.23079867
440-1950	1251-1750	.13800958*	.021073736	.000	.080474823	.195544344
	1751-1950	.26151498*	.039691493	.000	.153150677	.369879274
	440-750	-.2014829*	.025769532	.000	-.27183792	-.13112781
	751-1250	-.0857753*	.022017248	.001	-.14588601	-.02566460
440-750	1251-1750	.33949245*	.029471775	.000	.259029661	.419955237
	1751-1950	.46299784*	.044720217	.000	.340904300	.585091381
	440-1950	.20148286*	.025769532	.000	.131127808	.271837922
	751-1250	.11570756*	.030153647	.001	.033383154	.198031973
751-1250	1251-1750	.22378489*	.026254065	.000	.152106974	.295462797
	1751-1950	.34729028*	.042668352	.000	.230798666	.463781888
	440-1950	.08577530*	.022017248	.001	.025664597	.145886006
	440-750	-.1157076*	.030153647	.001	-.19803197	-.03338315

Table A.2: V2 log transformed varve thickness ANOVA Results

Between-Subjects Factors

		N
Group	1251-1750	392
	150-2017	1371
	150-750	479
	1751-1950	182
	1951-2017	20
	751-1250	298

Tests of Between-Subjects Effects

Dependent Variable: lnVarveThickness

Source	Type III Sum of Squares	df	Mean Square	F	Sig.
Corrected Model	13.150[a]	5	2.630	19.144	.000
Intercept	2107.014	1	2107.014	15337.261	.000
Group	13.150	5	2.630	19.144	.000
Error	375.868	2736	.137		
Total	10839.837	2742			
Corrected Total	389.018	2741			

a. R Squared = .034 (Adjusted R Squared = .032)

Multiple Comparisons

Dependent Variable: lnVarveThickness

Tukey HSD

(I) Group	(J) Group	Mean Difference (I-J)	Std. Error	Sig.	95% Confidence Interval	
					Lower Bound	Upper Bound
1251-1750	150-2017	-.0614628*	.021228739	.044	-.12200145	-.00092417
	150-750	-.1736163*	.025243995	.000	-.24560541	-.10162728
	1751-1950	-.0988779*	.033245817	.035	-.19368597	-.00406976
	1951-2017	-.18537512	.084967017	.247	-.42767813	.056927897
	751-1250	.069127480	.028486112	.147	-.01210723	.150362188
150-2017	1251-1750	.06146281*	.021228739	.044	.000924175	.122001448
	150-750	-.1121535*	.019672483	.000	-.16825415	-.05605292
	1751-1950	-.03741506	.029240925	.796	-.12080229	.045972174
	1951-2017	-.12391231	.083481383	.674	-.36197869	.114154080
	751-1250	.13059029*	.023689784	.000	.063033417	.198147166
150-750	1251-1750	.17361634*	.025243995	.000	.101627280	.245605409
	150-2017	.11215353*	.019672483	.000	.056052918	.168254148
	1751-1950	.074738477	.032274318	.188	-.01729917	.166776127
	1951-2017	-.01175877	.084591614	1.000	-.25299124	.229473694
	751-1250	.24274382*	.027346038	.000	.164760300	.320727350
1751-1950	1251-1750	.09887787*	.033245817	.035	.004069764	.193685972
	150-2017	.037415056	.029240925	.796	-.04597217	.120802287
	150-750	-.07473848	.032274318	.188	-.16677613	.017299173
	1951-2017	-.08649725	.087314182	.921	-.33549375	.162499245
	751-1250	.16800535*	.034868767	.000	.068569030	.267441666
1951-2017	1251-1750	.185375119	.084967017	.247	-.05692790	.427678134
	150-2017	.123912307	.083481383	.674	-.11415408	.361978695
	150-750	.011758774	.084591614	1.000	-.22947369	.252991242
	1751-1950	.086497251	.087314182	.921	-.16249924	.335493747
	751-1250	.25450260*	.085615072	.035	.010351506	.498653692
751-1250	1251-1750	-.06912748	.028486112	.147	-.15036219	.012107228
	150-2017	-.1305903*	.023689784	.000	-.19814717	-.06303342
	150-750	-.2427438*	.027346038	.000	-.32072735	-.16476030
	1751-1950	-.1680053*	.034868767	.000	-.26744167	-.06856903
	1951-2017	-.2545026*	.085615072	.035	-.49865369	-.01035151

Table A.3: V1 log transformed D_{50} Grain size ANOVA results.

Between-Subjects Factors

		N
Group	1251-1750	19
	1751-1950	5
	1951-2017	5
	450-2017	56
	450-750	10
	751-1250	17

Tests of Between-Subjects Effects

Dependent Variable: lnD50

Source	Type III Sum of Squares	df	Mean Square	F	Sig.
Corrected Model	.225[a]	5	.045	3.546	.005
Intercept	240.054	1	240.054	18939.771	.000
Group	.225	5	.045	3.546	.005
Error	1.344	106	.013		
Total	459.049	112			
Corrected Total	1.568	111			

a. R Squared = .143 (Adjusted R Squared = .103)

Multiple Comparisons

Dependent Variable: lnD50
Tukey HSD

(I) Group	(J) Group	Mean Difference (I-J)	Std. Error	Sig.	95% Confidence Interval	
					Lower Bound	Upper Bound
1251-1750	1751-1950	-.07651682	.056586210	.755	-.24075947	.087725826
	1951-2017	-.1921899*	.056586210	.012	-.35643258	-.02794729
	450-2017	-.03679380	.029890048	.821	-.12355028	.049962683
	450-750	-.09175009	.043983419	.303	-.21941287	.035912697
	751-1250	.011798935	.037585192	1.000	-.09729286	.120890735
1751-1950	1251-1750	.076516821	.056586210	.755	-.08772583	.240759467
	1951-2017	-.11567312	.071202753	.584	-.32234058	.090994347
	450-2017	.039723021	.052547576	.974	-.11279741	.192243450
	450-750	-.01523327	.061663393	1.000	-.19421254	.163746007
	751-1250	.088315756	.057275471	.638	-.07792748	.254558995
1951-2017	1251-1750	.19218994*	.056586210	.012	.027947292	.356432584
	1751-1950	.115673118	.071202753	.584	-.09099435	.322340582
	450-2017	.15539614*	.052547576	.043	.002875710	.307916567
	450-750	.100439851	.061663393	.582	-.07853942	.279419125
	751-1250	.20398887*	.057275471	.007	.037745634	.370232113
450-2017	1251-1750	.036793799	.029890048	.821	-.04996268	.123550281
	1751-1950	-.03972302	.052547576	.974	-.19224345	.112797407
	1951-2017	-.1553961*	.052547576	.043	-.30791657	-.00287571
	450-750	-.05495629	.038649577	.714	-.16713748	.057224909
	751-1250	.048592735	.031175236	.627	-.04189403	.139079502
450-750	1251-1750	.091750087	.043983419	.303	-.03591270	.219412872
	1751-1950	.015233267	.061663393	1.000	-.16374601	.194212541
	1951-2017	-.10043985	.061663393	.582	-.27941913	.078539423
	450-2017	.054956288	.038649577	.714	-.05722491	.167137485
	751-1250	.103549023	.044866709	.200	-.02667753	.233775573
751-1250	1251-1750	-.01179894	.037585192	1.000	-.12089073	.097292864
	1751-1950	-.08831576	.057275471	.638	-.25455900	.077927483
	1951-2017	-.2039889*	.057275471	.007	-.37023211	-.03774563
	450-2017	-.04859273	.031175236	.627	-.13907950	.041894032
	450-750	-.10354902	.044866709	.200	-.23377557	.026677528

Table A.4: V2 log transformed D_{50} Grain size ANOVA results.

Between-Subjects Factors

		N
Group	1251-1750	15
	150-2017	48
	150-750	13
	1751-1950	4
	1951-2017	5
	751-1250	11

Tests of Between-Subjects Effects

Dependent Variable: lnD50

Source	Type III Sum of Squares	df	Mean Square	F	Sig.
Corrected Model	.187[a]	5	.037	3.293	.009
Intercept	175.174	1	175.174	15455.162	.000
Group	.187	5	.037	3.293	.009
Error	1.020	90	.011		
Total	329.544	96			
Corrected Total	1.207	95			

a. R Squared = .155 (Adjusted R Squared = .108)

Multiple Comparisons

Dependent Variable: lnD50

Tukey HSD

(I) Group	(J) Group	Mean Difference (I-J)	Std. Error	Sig.	95% Confidence Interval	
					Lower Bound	Upper Bound
1251-1750	150-2017	.000006080	.031492126	1.000	-.09169997	.091712132
	150-750	-.05649079	.040342208	.727	-.17396856	.060986976
	1751-1950	.029615017	.059909973	.996	-.14484469	.204074726
	1951-2017	-.08881677	.054977162	.591	-.24891198	.071278436
	751-1250	.096390538	.042261281	.213	-.02667563	.219456704
150-2017	1251-1750	-.00000608	.031492126	1.000	-.09171213	.091699971
	150-750	-.05649687	.033286687	.537	-.15342874	.040435000
	1751-1950	.029608936	.055405006	.995	-.13173217	.190950041
	1951-2017	-.08882285	.050029973	.487	-.23451169	.056865986
	751-1250	.096384458	.035588280	.084	-.00724972	.200018637
150-750	1251-1750	.056490790	.040342208	.727	-.06098698	.173968556
	150-2017	.056496870	.033286687	.537	-.04043500	.153428740
	1751-1950	.086105807	.060872444	.718	-.09115665	.263368261
	1951-2017	-.03232598	.056024440	.992	-.19547090	.130818933
	751-1250	.15288133*	.043614967	.009	.025873184	.279889472
1751-1950	1251-1750	-.02961502	.059909973	.996	-.20407473	.144844692
	150-2017	-.02960894	.055405006	.995	-.19095004	.131732168
	150-750	-.08610581	.060872444	.718	-.26336826	.091156647
	1951-2017	-.11843179	.071417428	.563	-.32640157	.089537987
	751-1250	.066775521	.062160893	.890	-.11423893	.247789977
1951-2017	1251-1750	.088816773	.054977162	.591	-.07127844	.248911981
	150-2017	.088822853	.050029973	.487	-.05686599	.234511692
	150-750	.032325983	.056024440	.992	-.13081893	.195470898
	1751-1950	.118431789	.071417428	.563	-.08953799	.326401566
	751-1250	.18520731*	.057421773	.021	.017993319	.352421302
751-1250	1251-1750	-.09639054	.042261281	.213	-.21945670	.026675628
	150-2017	-.09638446	.035588280	.084	-.20001864	.007249722
	150-750	-.1528813*	.043614967	.009	-.27988947	-.02587318
	1751-1950	-.06677552	.062160893	.890	-.24778998	.114238935
	1951-2017	-.1852073*	.057421773	.021	-.35242130	-.01799332

Table A.5: V1 log transformed %LOI ANOVA results.

Between-Subjects Factors

		N
group	1251-1750	26
	1751-1950	8
	1951-2017	5
	450-1950	80
	450-750	18
	751-1250	27

Tests of Between-Subjects Effects

Dependent Variable: lnLOI

Source	Type III Sum of Squares	df	Mean Square	F	Sig.
Corrected Model	.091[a]	5	.018	7.226	.000
Intercept	184.006	1	184.006	73344.298	.000
group	.091	5	.018	7.226	.000
Error	.396	158	.003		
Total	400.339	164			
Corrected Total	.487	163			

a. R Squared = .186 (Adjusted R Squared = .160)

Multiple Comparisons

Dependent Variable: lnLOI

Tukey HSD

(I) group	(J) group	Mean Difference (I-J)	Std. Error	Sig.	95% Confidence Interval	
					Lower Bound	Upper Bound
1251-1750	1751-1950	-.02777743	.020250716	.744	-.08620098	.030646109
	1951-2017	.07185810*	.024459172	.043	.001293108	.142423085
	450-1950	-.03028437	.011307168	.085	-.06290568	.002336934
	450-750	-.03913520	.015358047	.117	-.08344334	.005172937
	751-1250	-.0537389*	.013762647	.002	-.09344432	-.01403353
1751-1950	1251-1750	.027777435	.020250716	.744	-.03064611	.086200978
	1951-2017	.09963553*	.028554481	.008	.017255532	.182015530
	450-1950	-.00250694	.018573080	1.000	-.05609049	.051076607
	450-750	-.01135777	.021283253	.995	-.07276019	.050044658
	751-1250	-.02596149	.020162284	.791	-.08412991	.032206929
1951-2017	1251-1750	-.0718581*	.024459172	.043	-.14242308	-.00129311
	1751-1950	-.0996355*	.028554481	.008	-.18201553	-.01725553
	450-1950	-.1021425*	.023089368	.000	-.16875556	-.03552938
	450-750	-.1109933*	.025320673	.000	-.18404373	-.03794287
	751-1250	-.1255970*	.024386007	.000	-.19595093	-.05524312
450-2017	1251-1750	.030284374	.011307168	.085	-.00233693	.062905681
	1751-1950	.002506939	.018573080	1.000	-.05107661	.056090485
	1951-2017	.10214247*	.023089368	.000	.035529382	.168755559
	450-750	-.00885083	.013066654	.984	-.04654827	.028846614
	751-1250	-.02345455	.011148016	.291	-.05561670	.008707603
450-750	1251-1750	.039135203	.015358047	.117	-.00517294	.083443343
	1751-1950	.011357768	.021283253	.995	-.05004466	.072760195
	1951-2017	.11099330*	.025320673	.000	.037942871	.184043728
	450-1950	.008850829	.013066654	.984	-.02884661	.046548272
	751-1250	-.01460372	.015241254	.930	-.05857491	.029367470
751-1250	1251-1750	.05373892*	.013762647	.002	.014033532	.093444315
	1751-1950	.025961489	.020162284	.791	-.03220693	.084129907
	1951-2017	.12559702*	.024386007	.000	.055243115	.195950925
	450-1950	.023454550	.011148016	.291	-.00870760	.055616703
	450-750	.014603721	.015241254	.930	-.02936747	.058574911

Table A.6: V2 log transformed LOI ANOVA results.

Between-Subjects Factors

		N
Group	1251-1750	18
	150-1950	70
	150-750	25
	1751-1950	10
	1951-2017	3
	751-1250	17

Tests of Between-Subjects Effects

Dependent Variable: lnLOI

Source	Type III Sum of Squares	df	Mean Square	F	Sig.
Corrected Model	.061[a]	5	.012	3.443	.006
Intercept	146.172	1	146.172	40933.552	.000
Group	.061	5	.012	3.443	.006
Error	.489	137	.004		
Total	355.073	143			
Corrected Total	.551	142			

a. R Squared = .112 (Adjusted R Squared = .079)

Multiple Comparisons

Dependent Variable: lnLOI
Tukey HSD

(I) Group	(J) Group	Mean Difference (I-J)	Std. Error	Sig.	95% Confidence Interval	
					Lower Bound	Upper Bound
1251-1750	150-2017	-.04228479	.015792426	.086	-.08793231	.003362723
	150-750	-.0662289*	.018472291	.006	-.11962247	-.01283530
	1751-1950	-.04815692	.023568696	.324	-.11628150	.019967669
	1951-2017	.026693847	.037265381	.980	-.08102058	.134408272
	751-1250	-.04839085	.020209990	.165	-.10680720	.010025502
150-2017	1251-1750	.042284794	.015792426	.086	-.00336272	.087932311
	150-750	-.02394409	.013923088	.521	-.06418834	.016300166
	1751-1950	-.00587212	.020201740	1.000	-.06426462	.052520379
	1951-2017	.068978641	.035232591	.372	-.03286007	.170817349
	751-1250	-.00610605	.016157678	.999	-.05280932	.040597212
150-750	1251-1750	.06622888*	.018472291	.006	.012835298	.119622465
	150-2017	.023944088	.013923088	.521	-.01630017	.064188341
	1751-1950	.018071967	.022359229	.966	-.04655669	.082700621
	1951-2017	.092922729	.036512468	.119	-.01261542	.198460880
	751-1250	.017838035	.018785510	.933	-.03646090	.072136966
1751-1950	1251-1750	.048156915	.023568696	.324	-.01996767	.116281499
	150-2017	.005872121	.020201740	1.000	-.05252038	.064264621
	150-750	-.01807197	.022359229	.966	-.08270062	.046556688
	1951-2017	.074850762	.039337237	.405	-.03885230	.188553821
	751-1250	-.00023393	.023814980	1.000	-.06907039	.068602527
1951-2017	1251-1750	-.02669385	.037265381	.980	-.13440827	.081020577
	150-2017	-.06897864	.035232591	.372	-.17081735	.032860067
	150-750	-.09292273	.036512468	.119	-.19846088	.012615422
	1751-1950	-.07485076	.039337237	.405	-.18855382	.038852296
	751-1250	-.07508469	.037421631	.344	-.18325075	.033081365
751-1250	1251-1750	.048390847	.020209990	.165	-.01002550	.106807195
	150-2017	.006106053	.016157678	.999	-.04059721	.052809318
	150-750	-.01783803	.018785510	.933	-.07213697	.036460896
	1751-1950	.000233932	.023814980	1.000	-.06860253	.069070390
	1951-2017	.075084694	.037421631	.344	-.03308137	.183250753

References

Allen, J. R. L. (1982). Sedimentary Structures: Their Character and Physical Basis. *Developments in Sedimentology*, *30*, 169–185.

Atkinson, J. F., Lin, G., & Joshi, M. (1994). Physical Model of Niagara River Discharge. *Journal of Great Lakes Research*, *20*(3), 583–589.

Beedle, M. J., Menounos, B. P., & Wheate, R. (2015). Glacier change in the Cariboo Mountains, British Columbia, Canada (1952-2005). *Cryosphere*, *9*(1), 65–80.

Benn, D. I., & Evans, D. J. A. (2010). *Glaciers & Glaciation*. *Hodder Education* (Vol. 1).

Berthier, E., Schiefer, E., Clarke, G. K. C., Menounos, B. P., & Rémy, F. (2010). Contribution of Alaskan glaciers to sea-level rise derived from satellite imagery. *Nature Geoscience*, *3*(2), 92–95.

Brune, G. M. (1953). Trap efficiency of reservoirs. *T Am Geophys Union 22:649-655*.

Carrivick, J. L., & Heckmann, T. (2017). Short-term geomorphological evolution of proglacial systems. *Geomorphology*, *287*, 3–28.

Carrivick, J. L., & Tweed, F. S. (2013). Proglacial Lakes: Character, behaviour and geological importance. *Quaternary Science Reviews*, *78*, 34–52.

Cashman, B. H., Clark, D. E., Clague, J. J., & Bilderback, E. I. (2002). New constraints on Holocene glaciation in Garibaldi Provincial Park, British Columbia, Canada. *Geological Society of America Bulletin*, *34*(A-78).

Cavalli, M., Trevisani, S., Comiti, F., & Marchi, L. (2013). Geomorphometric assessment of spatial sediment connectivity in small Alpine catchments. *Geomorphology*, *188*(April), 31–41.

Clague, J. J. (2000). Recognizing order in chaotic sequences of Quaternary sediments in the Canadian Cordillera. *Quaternary International*, *68–71*, 29–38.

Clarke, G. K. C., Jarosch, A. H., Anslow, F. S., Radić, V., & Menounos, B. (2015). Projected deglaciation of western Canada in the twenty-first century. *Nature Geoscience*, *8*(5), 372–377.

Cockburn, J. M. H., & Lamoureux, S. F. (2008). Inflow and lake controls on short-term mass accumulation and sedimentary particle size in a High Arctic lake: Implications for interpreting varved lacustrine sedimentary records. *Journal of Paleolimnology*, *40*(3), 923–942.

Csanady, G. T. (1978). Water Circulation and Dispersal Mechanisms. In *Lakes* (pp. 21–64). New York, NY: Springer New York.

Desloges, J. R. (1999). Geomorphic and climatic interpretations of abrupt changes in glaciolacustrine deposition at Moose Lake, British Columbia, Canada. *Gff*, *121*(3), 202–207.

Desloges, J. R., & Gilbert, R. (1991). Sedimentary record of Harrison Lake: implications for deglaciation in southwestern British Columbia. *Canadian Journal of Earth Sciences*, *28*(5), 800–815.

Desloges, J. R., & Gilbert, R. (1994a). Sediment source and hydroclimatic inferences from glacial lake sediments: the postglacial sedimentary record of Lillooet Lake, British Columbia. *Journal of Hydrology*, *159*(1–4), 375–393.

Desloges, J. R., & Gilbert, R. (1994b). The record of extreme hydrological and

geomorphological events inferred from glaciolacustrine sediments, (224).

Desloges, J. R., & Gilbert, R. (1995). The sedimentary record of Moose Lake: implications for glacier activity in the Mount Robson area, British Columbia. *Canadian Journal of Earth Sciences*, *32*, 65–78.

Dirszowsky, R. W. (2004). Bed sediment sources and mixing in the glacierized upper Fraser River watershed, east-central British Columbia. *Earth Surface Processes and Landforms*, *29*(5), 533–552.

Dirszowsky, R. W., & Desloges, J. R. (1997). Glaciolacustrine sediments and neoglacial history of the Chephren lake basin, Banff National Park, Alberta. *Geographie Physique Et Quaternaire*, *51*(1), 41–53.

Environment Canada. (2014). Canadian Climate Normals 1981-2010 Station Data. *Climate Normals and Averages*, 1–4.

Evans, M., & Church, M. (2000). A method for error analysis of sediment yields derived from estimates of lacustrine sediment accumulation. *Earth Surface Processes and Landforms*, *25*(11), 1257–1267.

Fulton, R. J., Ryder, J. M., & Tsang, S. (2004). The Quaternary glacial record of British Columbia, Canada. *Developments in Quaternary Sciences*, *2*, 39–50.

Gardner, J. S. (1972). Recent glacial history and some associated landforms in the Canadian Rocky Mountains. *Mountain Geomorphology*, 55–62.

Gilbert, R. (1975). Sedimentation in Lillooet Lake, British Columbia. *Canadian Journal of Earth Sciences*, *12*(10), 1697–1711.

Gilbert, R., Crookshanks, S., Hodder, K. R., Spagnol, J., & Stull, R. B. (2006). The Record of an Extreme Flood in the Sediments of Montane Lillooet Lake, British Columbia: Implications for Paleoenvironmental Assessment. *Journal of Paleolimnology*, *35*(4), 737–745.

Gilbert, R., & Desloges, J. R. (2012). Late glacial and Holocene sedimentary environments of Quesnel Lake, British Columbia. *Geomorphology*, *179*, 186–196.

Gloor, M., Wüest, A., & Münnich, M. (1994). Benthic boundary mixing and resuspension induced by internal seiches. *Hydrobiologia*, *284*(1), 59–68.

Glur, L., Stalder, N. F., Wirth, S. B., Gilli, A., & Anselmetti, F. S. (2015). Alpine lacustrine varved record reveals summer temperature as main control of glacier fluctuations over the past 2250 years. *The Holocene*, *25*(2), 280–287.

Gray, A. B., Pasternack, G. B., & Watson, E. B. (2010). Hydrogen peroxide treatment effects on the particle size distribution of alluvial and marsh sediments. *The Holocene*, *20*(2), 293–301.

Green, T. (1987). The importance of double diffusion to the settling of suspended material. *Sedimentology*, *34*(2), 319–331.

Gurnell, A. M. (1982). The dynamics of suspended sediment concentration in an Alpine pro-glacial stream network, (138).

Håkanson, L., & Jansson, M. (1983). *Principles of Lake Sedimentology*. Berlin, Heidelberg: Springer Berlin Heidelberg.

Harbor, J. M. (1993). Glacial geomorphology: modeling processes and landforms. *Geomorphology*, *7*(1–3), 129–140.

Heideman, M., Menounos, B. P., & Clague, J. J. (2015). An 825-year long varve record from Lillooet Lake, British Columbia, and its potential as a flood proxy. *Quaternary Science*

Reviews, *126*, 158–174.

Heideman, M., Menounos, B. P., & Clague, J. J. (2017). A multi-century estimate of suspended sediment yield from Lake, Lillooet Mountains, Coast, *32*(September 2017), 18–32.

Hiemstra, J. F., & Rijsdijk, K. F. (2003). Observing artificially induced strain: implications for subglacial deformation. *Journal of Quaternary Science*, *18*(5), 373–383.

Hodder, K. R., Desloges, J. R., & Gilbert, R. (2006). Pattern and timing of sediment infill at glacier-fed Mud Lake: Implications for lateglacial and Holocene environments in the Monashee Mountain region of British Columbia, Canada. *Holocene*, *16*(5), 705–716.

Hodder, K. R., & Gilbert, R. (2007). Evidence for flocculation in glacier-fed Lillooet Lake, British Columbia.

Hodder, K. R., Gilbert, R., & Desloges, J. R. (2007). Glaciolacustrine varved sediment as an alpine hydroclimatic proxy. *Journal of Paleolimnology*, *38*(3), 365–394.

Hooke, R. L., & Elverhøi, A. (1996). Sediment flux from a fjord during glacial periods, Isfjorden, Spitsbergen. *Global and Planetary Change*, *12*(1–4), 237–249.

Imboden, D. M., & Wüest, A. (1995). Mixing Mechanisms in Lakes. In *Physics and Chemistry of Lakes* (pp. 83–138). Berlin, Heidelberg: Springer Berlin Heidelberg.

IPCC. (2014). *Summary for Policymakers*. *Climate Change 2014: Synthesis Report. Contribution of Working Groups I, II and III to the Fifth Assessment Report of the Intergovernmental Panel on Climate Change*.

Karlen, W. (1981). Lacustrine Sediment Studies. A Technique to Obtain a Continous Record of Holocene Glacier Variations. *Geografiska Annaler. Series A, Physical Geography*, *63*(3/4), 273.

Koch, J., Osborn, G. D., & Clague, J. J. (2007). Pre-`Little Ice Age' glacier fluctuations in Garibaldi Provincial Park, Coast Mountains, British Columbia, Canada. *The Holocene*, *17*(8), 1069–1078.

Koi, T., Hotta, N., Ishigaki, I., Matuzaki, N., Uchiyama, Y., & Suzuki, M. (2008). Prolonged impact of earthquake-induced landslides on sediment yield in a mountain watershed: The Tanzawa region, Japan. *Geomorphology*, *101*(4), 692–702.

Lamoureux, S. F. (2002). Temporal patterns of suspended sediment yield following moderate to extreme hydrological events recorded in varved lacustrine sediments. *Earth Surface Processes and Landforms*, *27*(10), 1107–1124.

LeBlanc, L. R., Mayer, L., Rufino, M., Schock, S. G., & King, J. (1992). Marine sediment classification using the chirp sonar. *The Journal of the Acoustical Society of America*, *91*(1), 107–115.

Leeder, M. R. (2009). On the Interactions between Turbulent Flow, Sediment Transport and Bedform Mechanics in Channelized Flows. In *Modern and Ancient Fluvial Systems* (pp. 5–18).

Leonard, E. M. (1986). Use of lacustrine sedimentary sequences as indicators of Holocene glacial history, Banff National Park, Alberta, Canada. *Quaternary Research*, *26*(2), 218–231.

Leonard, E. M., & Reasoner, M. A. (1999). A continuous holocene glacial record inferred from proglacial lake sediments in Banff National Park, Alberta, Canada. *Quaternary Research*, *51*(1), 1–13.

Luckman, B. H. (1988). 8000 year old wood from the Athabasca Glacier, Alberta. *Canadian*

Journal of Earth Sciences, *25*(1), 148–151.

Luckman, B. H. (1995). Calendar-dated, early "Little Ice Age" glacier advance at Robson Glacier, British Columbia, Canada. *The Holocene*, *5*(2), 149–159.

Luckman, B. H. (2000). The Little Ice Age in the Canadian Rockies. *Geomorphology*.

Luckman, B. H., Holdsworth, G., & Osborn, G. D. (1993). Neoglacial glacier fluctuations in the canadian rockies. *Quaternary Research*, *39*(2), 144–153.

Luckman, B. H., & Kavanagh, T. (2000). Impact of climate fluctuations on mountain environments in the Canadian Rockies. *Ambio*, *29*(7), 371–380.

Luckman, B. H., & Wilson, R. J. S. (2005). Summer temperatures in the Canadian Rockies during the last millennium: A revised record. *Climate Dynamics*, *24*(2–3), 131–144.

Matthews, J. A., Olaf Dahl, S., Nesje, A., Berrisford, M. S., & Andersson, C. (2000). Holocene glacier variations in central Jotunheimen, southern Norway based on distal glaciolacustrine sediment cores. *Quaternary Science Reviews*, *19*(16), 1625–1647.

Maurer, M. K., Menounos, B. P., Luckman, B. H., Osborn, G. D., Clague, J. J., Beedle, M. J., … Atkinson, N. (2012). Late Holocene glacier expansion in the Cariboo and northern Rocky Mountains, British Columbia, Canada. *Quaternary Science Reviews*, *51*, 71–80.

Menounos, B. P. (1997). The water content of lake sediments and its relationship to other physical parameters: an alpine case study. *The Holocene*, *7*(2), 207–212.

Menounos, B. P. (2002). Climate, Fine-Sediment Transport Linkages, Coast Mountains, British Columbia, *1996*.

Menounos, B. P. (2006a). Anomalous early 20th century sedimentation in proglacial Green Lake, British Columbia, Canada. *Canadian Journal of Earth Sciences*, *43*(6), 671–678.

Menounos, B. P. (2006b). Anomalous early 20th century sedimentation in proglacial Green Lake, British Columbia, Canada. *Canadian Journal of Earth Sciences*, *43*(6), 671–678.

Menounos, B. P., & Clague, J. J. (2008). Reconstructing hydro-climatic events and glacier fluctuations over the past millennium from annually laminated sediments of Cheakamus Lake, southern Coast Mountains, British Columbia, Canada. *Quaternary Science Reviews*, *27*(7–8), 701–713.

Menounos, B. P., Clague, J. J., Gilbert, R., & Slaymaker, O. (2005). Environmental reconstruction from a varve network in the southern Coast Mountains, British Columbia, Canada. *The Holocene*, *15*(8), 1163–1171.

Menounos, B. P., Koch, J., Osborn, G. D., Clague, J. J., & Mazzucchi, D. (2004). Early Holocene glacier advance, southern Coast Mountains, British Columbia, Canada. *Quaternary Science Reviews*, *23*(14–15), 1543–1550.

Menounos, B. P., Osborn, G. D., Clague, J. J., & Luckman, B. H. (2009). Latest Pleistocene and Holocene glacier fluctuations in western Canada. *Quaternary Science Reviews*, *28*(21–22), 2049–2074.

Minkus, R. (2006). *Evidence of latest Pleistocene glacier advance in the southern Coast Mountains, British Columbia, CanadaNo Title*. University of Calgary, Calgary Alberta.

Mood, B. J., & Smith, D. J. (2015). Holocene glacier activity in the British Columbia Coast Mountains, Canada. *Quaternary Science Reviews*, *128*, 14–36.

Morehead, M. D., & Syvitski, J. P. (1999). River-plume sedimentation modeling for sequence stratigraphy: application to the Eel margin, northern California. *Marine Geology*, *154*(1–4), 29–41.

Nasmith, H. (1962). Late glacial history and surficial deposits of the Okanagan Valley, British Columbia. *Dept. of Mines and Petroleum Resources*.

O'Hara, S. L., Street-Perrott, F. A., & Burt, T. P. (1993). Accelerated soil erosion around a Mexican highland lake caused by prehispanic agriculture. *Nature*, *362*(6415), 48–51.

O'Sullivan, P. E. (1983). Annually-laminated lake sediments and the study of Quaternary environmental changes - a review. *Quaternary Science Reviews*, *1*(4), 245–313.

Onstad, C. (1984). Sediment yield modelling. In Erosion and sediment yield: Some methods of measurement and modelling. *Geo Books*, 71–89.

Osborn, G. D., & Luckman, B. H. (1988). Holocene glacier fluctuations in the Canadian Cordillera (Alberta and British Columbia). *Quaternary Science Reviews*, *7*(2), 115–128.

Osborn, G. D., Menounos, B. P., Koch, J., Clague, J. J., & Vallis, V. (2007). Multi-proxy record of Holocene glacial history of the Spearhead and Fitzsimmons ranges, southern Coast Mountains, British Columbia. *Quaternary Science Reviews*, *26*(3–4), 479–493.

Petticrew, E. L., Albers, S. J., Baldwin, S. A., Carmack, E. C., Déry, S. J., Gantner, N., … Vagle, S. (2015). The impact of a catastrophic mine tailings impoundment spill into one of North America's largest fjord lakes: Quesnel Lake, British Columbia, Canada. *Geophysical Research Letters*, *42*(9), 3347–3355.

Porter, S. C., & Denton, G. H. (1967). Chronology of neoglaciation in the North American Cordillera. *American Journal of Science*, *265*(3), 177–210.

Reyes, A. D. V, Wiles, G. C., Smith, D. J., Barclay, D. J., Allen Scott Jackson Sonya Larocque Sarah Laxton Dave Lewis, S., Calkin, P. E., & Clague, J. J. (2006). Expansion of alpine glaciers in Pacific North America in the first millennium A. *Geology*, *341*(3).

Ryder, J. M., & Thomson, B. (1986). Neoglaciation in the southern Coast Mountains of British Columbia: chronology prior to the late Neoglacial maximum. *Canadian Journal of Earth Sciences*, *23*(3), 273–287.

Schiefer, E., Hassan, M. A., Menounos, B. P., Pelpola, C. P., & Slaymaker, O. (2010). Interdecadal patterns of total sediment yield from a montane catchment, southern Coast Mountains, British Columbia, Canada. *Geomorphology*, *118*(1–2), 207–212.

Schiefer, E., Kaufman, D., McKay, N., Retelle, M., Werner, A., & Roof, S. (2018). Fluvial suspended sediment yields over hours to millennia in the High Arctic at proglacial Lake Linnévatnet, Svalbard. *Earth Surface Processes and Landforms*, *43*(2), 482–498.

Smith, D. J., & Desloges, J. R. (2000). Little Ice Age history of Tzeetsaytsul Glacier, Tweedsmuir Provincial Park, British Columbia. *Géographie Physique et Quaternaire*, *54*(2), 135.

Smith, J. G. (2003). Aspects of the loss-on-ignition (loi) technique in the context of clay-rich, glaciolacustrine sediments. *Geografiska Annaler: Series A, Physical Geography*, *85*(1), 91–97.

Smith, N. D. (1978). Sedimentation processes and patterns in a glacier-fed lake with low sediment input. *Canadian Journal of Earth Sciences*, *15*(5), 741–756.

Smith, N. D., & Ashley, G. M. (1985). Proglacial lacustrine environment. In *Glacial Sedimentary Environments*.

Smith, N. D., Venol, M. A., & Kennedy, S. K. (1982). Comparison of sedimentation regimes in four glacier-fed lakes of western Alberta. *Research in Glacial, Glacio-Fluvial, and Glacio-Lacustrine Systems.*, 203–238.

Smol, J. (2009). Pollution of lakes and rivers: a paleoenvironmental perspective. *Book*, 383.

Souch, C. (1994). A Methodology to Interpret Downvalley Lake Sediments as Records of Neoglacial Activity: Coast Mountains, British Columbia, Canada. *Geografiska Annaler: Series A, Physical Geography*, *76*(3), 169–185.

Striberger, J., Björck, S., Holmgren, S., & Hamerlík, L. (2012). The sediments of Lake Lögurinn - A unique proxy record of Holocene glacial meltwater variability in eastern Iceland. *Quaternary Science Reviews*, *38*, 76–88.

Sugden, D. E. (1978). Glacial geomorphology. *Progress in Physical Geography: Earth and Environment*, *2*(2), 309–320.

Terzhagi, K. (1955). Evaluation of Coefficient of Subgrade Reaction. *Geotech.*, *5*, 297–326.

Thomas, E. K., & Briner, J. P. (2009). Climate of the past millennium inferred from varved proglacial lake sediments on northeast Baffin Island, Arctic Canada. *Journal of Paleolimnology*, *41*(1), 209–224.

Trouet, V., Diaz, H. F., Wahl, E. R., Viau, A. E., Graham, R., Graham, N., & Cook, E. R. (2013). A 1500-year reconstruction of annual mean temperature for temperate North America on decadal-to-multidecadal time scales. *Environmental Research Letters*, *8*(2).

van Rensbergen, P., de Batist, M., Beck, C., & Chapron, E. (1999). High-resolution seismic stratigraphy of glacial to interglacial fill of a deep glacigenic lake: Lake Le Bourget, Northwestern Alps, France. *Sedimentary Geology*, *128*(1–2), 99–129.

Viau, A. E., Ladd, M., & Gajewski, K. (2012). The climate of North America during the past 2000years reconstructed from pollen data. *Global and Planetary Change*, *84–85*, 75–83.

Wells, M. G. (2009). How Coriolis forces can limit the spatial extent of sediment deposition of a large-scale turbidity current. *Sedimentary Geology*, *218*(1–4), 1–5.

Wohl, E. E. (2014). *Rivers in the landscape: Science and Management*. (W. S. The Atrium, Southern Gate, Chichester, Ed.). John Wiley & Sons, Ltd.

Wohl, E. E., Magilligan, F. J., & Rathburn, S. L. (2017). Introduction to the special issue: Connectivity in Geomorphology. *Geomorphology*, *277*, 1–5.

Wood, C., & Smith, D. J. (2004). Dendroglaciological Evidence For A Neoglacial Advance Of the Saskatchewan Glacier, Banff National Park, Canadian Rocky Mountains. *Tree-Ring Research*, *60*(1), 59–65.

Wood, L. J., & Smith, D. J. (2013). Climate and glacier mass balance trends from ad 1780 to present in the Columbia Mountains, British Columbia, Canada. *Holocene*, *23*(5), 739–748.

Wright, L. D. (1977). Sediment transport and deposition at river mouths: A synthesis. *Geological Society of America Bulletin*, *88*(6), 857.

Zolitschka, B. (1998). A 14,000 year sediment yield record from western Germany based on annually laminated lake sediments. *Geomorphology*, *22*(1), 1–17.

Zolitschka, B., Francus, P., Ojala, A. E. K., & Schimmelmann, A. (2015). Varves in lake sediments - a review. *Quaternary Science Reviews*, *117*, 1–41.